



# Jangheung Cu-Pb-Zn-Ag Project South Korea

Compiled by Christopher M. Sennitt

*B.App.Sci (Applied Geology), MSc (Economic Geology), FAIG, FSEG*

13<sup>th</sup> August 2021

**Senlac Geological Services Pty Ltd**

21 Pandian Crescent

Bellbowrie

QLD. 4070.

Australia.

Tel: +61-7-32027144

Fax: +61-7-32027745

Email: [senlac@senlac.com.au](mailto:senlac@senlac.com.au)



THIS PAGE IS LEFT INTENTIONALLY BLANK FOR PRINTING PURPOSES & NOTES

# TABLE OF CONTENTS

Page No.

<b>1.0</b>	<b>EXECUTIVE SUMMARY</b>	<b>5</b>
<b>2.0</b>	<b>INTRODUCTION</b>	<b>7</b>
2.1	Location & Access	7
2.2	Physiography	11
2.3	Vegetation	11
2.4	Climate	15
2.5	Local Economy	16
2.6	Existing Infrastructure	18
<b>3.0</b>	<b>TENURE</b>	<b>19</b>
3.1	Mining Rights	19
3.2	Surface Rights	19
3.3	Korean Mining Act – Mining Rights	19
3.4	Mine Development Permit Process	22
3.5	Environmental Social Impact Assessment (ESIA) Process	23
<b>4.0</b>	<b>DATABASE</b>	<b>24</b>
<b>5.0</b>	<b>PREVIOUS INVESTIGATIONS</b>	<b>28</b>
<b>6.0</b>	<b>REGIONAL GEOLOGY OF KOREA</b>	<b>29</b>
<b>7.0</b>	<b>STREAM SEDIMENT GEOCHEMICAL SURVEYS</b>	<b>34</b>
<b>8.0</b>	<b>AIRBORNE GEOPHYSICAL SURVEYS</b>	<b>39</b>
<b>9.0</b>	<b>PROSPECT GEOLOGY</b>	<b>43</b>
9.1	Prospect Geology	43
9.2	Mineralization	53
9.3	Rock Chip Geochemistry	54
9.4	Alteration	60
9.5	Soil Geochemical Surveys	63
9.6	Ground Geophysical Surveys	68
9.7	Drilling Program	74
<b>10.0</b>	<b>CONCEPTUAL EXPLORATION MODEL</b>	<b>83</b>
<b>11.0</b>	<b>PROPOSED EXPLORATION PROGRAM</b>	<b>92</b>
<b>12.0</b>	<b>METALLURGY</b>	<b>110</b>
<b>13.0</b>	<b>CONCEPTUAL MINING &amp; MILLING OPERATION</b>	<b>111</b>
<b>14.0</b>	<b>REFERENCES</b>	<b>117</b>

## APPENDICES

**Appendix I    Digital Drill Logs**  
**Appendix II    Rock Chip Sample Register**

PAGE NO.

### LIST OF TABLES

<b>Table 1</b>	Climate Data for Jangheung (1981-2010)	15
<b>Table 2</b>	Tenement Schedule – Mining Rights	19
<b>Table 3</b>	Anomalous Levels for Selected Elements Stream Geochemistry	34
<b>Table 4</b>	Summary of Soil Geochemical Anomalies	63
<b>Table 5</b>	Drill Hole Collar Survey Data	74
<b>Table 6</b>	Significant Mineralized Drill Intersections	77
<b>Table 7</b>	Drill Hole Assays	78-82
<b>Table 8</b>	Recommended Exploration Budget	104

### LIST OF FIGURES

<b>Figure 1</b>	Location Map Jangheung Project, South Korea	6
<b>Figure 2</b>	Cities and Provincial Map of South Korea	8
<b>Figure 3</b>	County Location Map	9
<b>Figure 4</b>	Physiographic Relief Map	12
<b>Figure 5</b>	Drainage Pattern Map	13
<b>Figure 6</b>	Tenure and Topographic Map	20
<b>Figure 7</b>	Flow Diagram of the Mining Right Reporting Process	22
<b>Figure 8</b>	Digital Elevation Model	25
<b>Figure 9</b>	SPOT Satellite Image	26
<b>Figure 10</b>	Satellite Image (1m Resolution)	27
<b>Figure 11</b>	Tectonic Elements Map of South Korea	32
<b>Figure 12</b>	Regional Geology Map of South Korea	33
<b>Figure 13a-p</b>	Stream Sediment Geochemistry – Element Colour Plots	35-38
<b>Figure 14</b>	Regional Magnetic Anomaly Map	40
<b>Figure 15</b>	Radiometric Channel Response Maps	42
<b>Figure 16</b>	Regional Geology Map of Jangheung project	45
<b>Figure 17</b>	Geology Map of Jangheung project	46
<b>Figure 18</b>	Rock Chip Sample Location Map	55
<b>Figure 19</b>	Copper Soil Geochemistry Map	64
<b>Figure 20</b>	Lead Soil Geochemistry Map	65
<b>Figure 21</b>	Zinc Soil Geochemistry Map	66
<b>Figure 22</b>	Soil Geochemistry Compilation Map	67
<b>Figure 23</b>	VLF-EM East Direction Colour Plot	69
<b>Figure 24</b>	VLF-EM North Direction Colour Plot	70
<b>Figure 25</b>	Line 0 East VLF-EM Pseudo-Section	71
<b>Figure 26a-b</b>	Line 0 North VLF-EM Pseudo-Section	71
<b>Figure 27</b>	Total Magnetic Intensity Image	72
<b>Figure 28</b>	Colour Conductivity Plot IP Dipole-Dipole Geophysical Survey	73

<b>Figure 29</b>	Drill Hole Location Map	75
<b>Figure 30</b>	Drill Hole Columnar Visual Geological Log	76
<b>Figure 31</b>	Examples of Time Domain EM Geophysical Surveys in Exploration	91
<b>Figure 32a-j</b>	Drill Plans & Sections, Anomalies A-P	93-101
<b>Figure 33</b>	SPOT Satellite Image	102
<b>Figure 34</b>	Satellite Image	103
<b>Figure 35</b>	Conceptual Pile Top RCD Mining Operation	111
<b>Figure 36</b>	Continuous Vat Leach “Turn-Key” Plant	114

### LIST OF PHOTOGRAPHS

<b>Photograph 1</b>	Jangheung Bus Terminal	10
<b>Photograph 2</b>	Small fishing port of Sumumpo	10
<b>Photograph 3</b>	View of jeamsan peak	14
<b>Photograph 4</b>	View of Sajasan peak	14
<b>Photograph 5</b>	View looking towards Jeamsan	16
<b>Photograph 6</b>	Feedlot agricultural facility at Eunheung-ri	17
<b>Photograph 7</b>	Terraced rice paddy fields at Haksong-ri	17
<b>Photograph 8</b>	View of rockwall freshwater dam	18
<b>Photograph 9</b>	Outcrop of granite gneiss	44
<b>Photograph 10</b>	Cut slab of granite gneiss	44
<b>Photograph 11</b>	Cut slab of granite gneiss	45
<b>Photograph 12</b>	View of Sajasan peak	47
<b>Photograph 13</b>	Cut slab of diorite porphyry	48
<b>Photograph 14</b>	Outcrop of andesite tuff at Jeamsan	49
<b>Photograph 15</b>	Cut slab of andesite tuff	49
<b>Photograph 16</b>	View looking NE of Jangheung project	50
<b>Photograph 17</b>	View looking NW of Jangheung project	51
<b>Photograph 18</b>	View looking E of Anomaly I	51
<b>Photograph 19</b>	Outcrop of gossanous breccia at Anomaly I	52
<b>Photograph 20</b>	Outcrop of gossanous breccia at Anomaly I	52
<b>Photograph 21</b>	Prismatic quartz and uraltite crystals infilling vughs in breccia	53
<b>Photograph 22</b>	Cut slab of Breccia	54
<b>Photograph 23</b>	Cut slab of mineralized breccia from Anomaly B	56
<b>Photograph 24</b>	Cut slab of brecciated granite gneiss from Anomaly B	56
<b>Photograph 25</b>	Cut slab of gossanous stockwork in diorite porphyry (Anomaly I)	57
<b>Photograph 26</b>	Cut slab of gossanous breccia with granite gneiss clasts (Anomaly I)	57
<b>Photograph 27</b>	Cut slab of gossanous breccia with granite gneiss clasts (Anomaly B)	58
<b>Photograph 28</b>	Cut slab of brecciated diorite porphyry (Anomaly I)	58
<b>Photograph 29</b>	Cut slab of brecciated granite gneiss (Anomaly B)	59
<b>Photograph 30</b>	Cut slab of brecciated diorite porphyry (Anomaly F)	59
<b>Photograph 31</b>	Intense leached altered diorite porphyry	61
<b>Photograph 32</b>	Outcrop of granite gneiss	61
<b>Photograph 33</b>	Cut slab of granite gneiss (anomaly F)	62
<b>Photograph 34</b>	Cut slab of granite gneiss (anomaly F)	62

## 1.0 EXECUTIVE SUMMARY

The Jangheung project is situated 320km south of Seoul, in Boseong-Gun County of Chollanam-Do province, in the southwestern coastal region of South Korea. Mineralization at Jangheung consists of a cluster of 16 Cu-Ag-Zn-Pb-mineralized subvertical breccia pipes, developed around the margin of a Cretaceous diorite porphyry intrusion into basement granite gneiss. Jangheung has the potential to aggregate into a significant Cu-Ag-Zn-Pb polymetallic base metal deposit.

Previous exploration at Jangheung was conducted by the *Korean Institute of Energy & Resources* (“KIER”) during 1971-1982. Follow up of regional stream geochemical anomalies located 16 breccia pipes, using a combination of float prospecting, soil geochemical surveys and VLF-EM geophysical surveys. Five (5) of these breccia pipes were tested with 12 diamond drill holes (total 1,524m of BQ core). Three (3) of these 5 breccia pipes (I, E and B) recorded highly significant mineralized intersections, including:

Intersection	CuEq (%)	Hole ID	Interval	Anomaly ID	Cu (%)	Pb (%)	Zn (%)
146m	2.45	JD-10	0-146m	Anomaly B	0.44	0.26	4.87
69m	1.71	JD-11	33-102m	Anomaly B	0.21	0.09	3.73
34m	1.71	JD-12	71-105m	Anomaly B	0.28	0.19	3.47
8m	5.32	JD-7	16-24m	Anomaly E	1.27	6.03	4.80
9m	2.42	JD-7	53-62m	Anomaly E	1.10	1.27	2.20
6m	4.10	JD-1	23-29m	Anomaly I	0.16	2.85	7.40

**NOTE:** CuEq was calculated using April 2016 metal prices of Cu = US\$2.18/lb, Pb = US\$0.78/lb & Zn = US\$0.86/lb.

Based on the drill results, KIER reported a historical inferred mineral resource<sup>1</sup> of 1Mt @ combined 5% Cu-Pb-Zn & 64g/t Ag, at Anomalies E and B. There has been no exploration conducted since 1982.

The following conclusions are made for the Jangheung Zn-Ag-Pb-Cu project:

- ❖ Silver was not analyzed by KIER in drill core, but a bulk metallurgical sample indicated significant silver grades (>100g/t Ag) accompanies the mineralization, confirmed by KME rock chip sampling.
- ❖ The breccia pipes are subvertical, display an “inverted cone” or “carrot-shaped” morphology. At least 16 breccia pipes have been identified, occurring as a “cluster”. More ‘blind’ pipes can be expected at depth. The conceptual geological model is degassing and de-volatilized hyperbyssal breccia pipes related to the intrusion of mineralized diorite porphyry.
- ❖ Stockwork vein and disseminated mineralized, carbonate altered diorite porphyry was intersected in Anomalies E and I and offers a potentially larger exploration target than the breccia pipes (unlikely to be a porphyry copper intrusion).
- ❖ Thermal oxidized supergene leaching/overprinting may have occurred in the upper levels of the breccia pipes, resulting in depletion of zinc (in particular) at or near surface.
- ❖ Most of the breccia pipes have yet to be drill-tested. Only 5 of the geochemical anomalies and 3 of the hydrothermal breccia pipes have been drill-tested. Geochemical Anomalies A, D, F, H, J, K, L, M, N, O and P and conductive geophysical Anomalies H, I, K & L remain untested.
- ❖ A close-spaced (50m grid line spacing) UAV drone VLF/EM geophysical survey is considered to be the best geophysical exploration tool to locate ‘blind’ mineralized breccia pipes in the area.

Check diamond drilling of the breccias at Anomalies B, E, F and I is recommended to confirm grades, followed by resource definition drilling. Drill core should be collected for detailed geotechnical and metallurgical investigations.

<sup>1</sup> Cautionary Statement: This resource was classified based upon the *Korean Institute of Energy Resources* resource estimation classification scheme and reporting nomenclature (1982). The resource estimate is historical and does not comply with current NI43-101 or 2012 JORC Code reporting requirements.

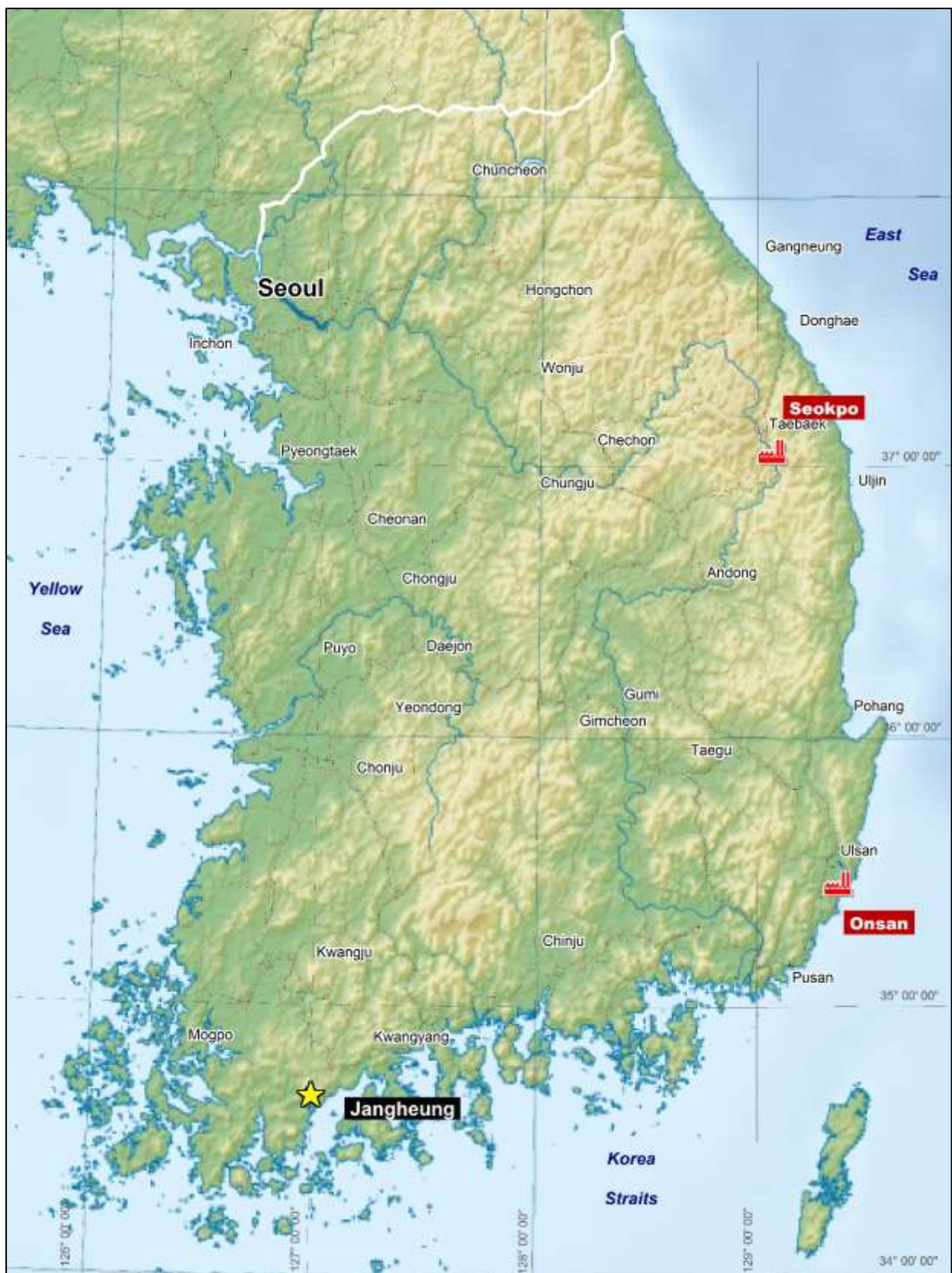


Figure 1. Location Map of the Jangheung Cu-Ag-Zn-Pb Project, Republic of Korea. The location of the main base metal refineries is shown.

## 2.0 INTRODUCTION

The Jangheung copper-silver-zinc-lead project is situated in the southwestern coastal region of South Korea.

This Technical Report on the Jangheung Cu-Ag-Zn-Pb Project was compiled with the following objectives:

- a) Review the geology and tenor of Cu-Ag-Zn-Pb mineralization.
- b) Identify Exploration Targets for resource definition drilling.
- c) Prepare an exploration program and budget.

This report has been prepared in compliance with the *JORC Code 2012 Edition of Reporting of Mineral Resources and Ore Reserves* guidelines.

### 2.1 LOCATION & ACCESS

#### Location

The Jangheung project is located about 320km south of Seoul, and 7km southeast of the coastal town of Jangheung, mainly situated within Boseong-Gun County, Chollanam-Do Province. The area lies adjacent to the secluded inlet of Boseong Bay.

Jangheung town and surrounding district has a population of 53,392 (2001 Census). Reasonable accommodation and restaurants are available in Jangheung. Accommodation is available closer to the project area at a beach resort style hotel at Sumunpo, but meal facilities are more limited.

Boseong town is located about 7km to the northeast of the project area and has a population of 61,329 (2001 census). The region has a long history of green tea production, with several tea plantations established near Boseong. The Boseong Fragrance Tea Festival is held in May each year and attracts domestic tourists.

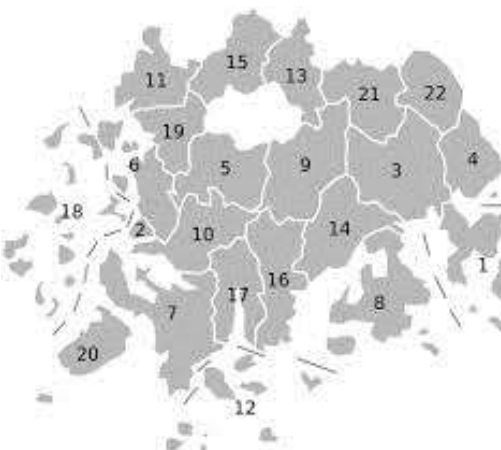
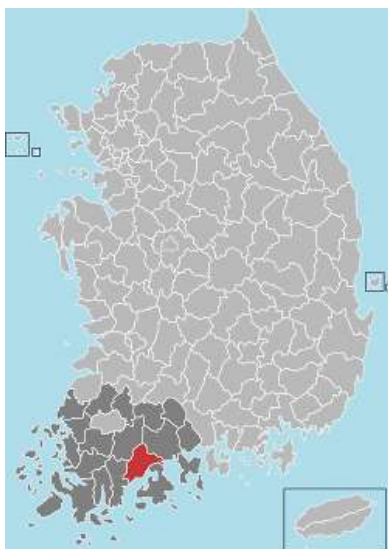
#### Access

Travel time from Seoul to Jangheung is approximately 4.5hrs, sequentially using the *Gyeonggbu, Nonsan-Cheonan, and Jeonju-Suncheon Expressways* to Suncheon, then by taking the *Yongam Expressway* to Jangheung.

Access to the prospect area is via *Route 18* to the village of Eunheung-ri. Unsealed roads and forestry logging tracks from Eunheung-ri afford access to the western and southern sectors of the project area. Alternative access is from the north via hiking trails from the *Jeamsan Forest Resort*, with roads enabling access from the north via Boseong.

The area is serviced by the *Gyeongjeon Railway Line* that passes through Boseong town.

South Korea is well serviced by international flights into Incheon Airport, near the capital Seoul. There are also international connections with some Asian destinations into Busan and Taegu. The major shipping container ports are Incheon in the northwest, near Seoul, Pyeongtaek further to the south and Busan in the southeast of the Korean Peninsula.



- 1 = Yeosu City
- 2 = Mokpo
- 3 = Suncheon
- 4 = Gwangyang
- 5 = Naju
- 6 = Muan County
- 7 = Haenam County
- 8 = Goheung County
- 9 = Hwasun County
- 10 = Yeongnam County
- 11 = Yeonggwang County
- 12 = Wando County
- 13 = Damyang County
- 14 = Boseong County**
- 15 = Jangseong County
- 16 = Jangheung County
- 17 = Gangjin County
- 18 = Sinan County
- 19 = Hampyeong County
- 20 = Jindo County
- 21 = Gokseong County
- 22 = Gurye County

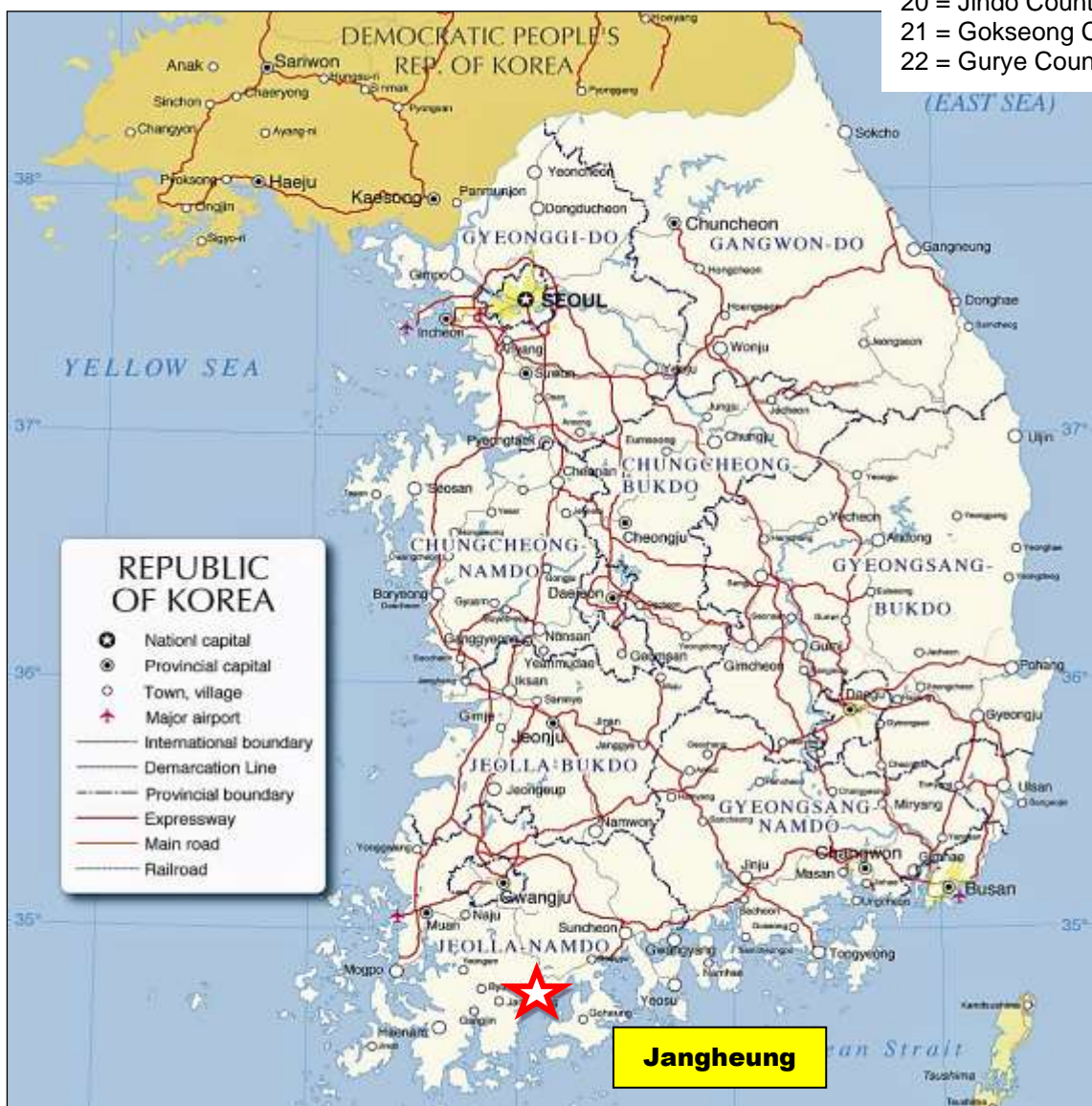


Figure 2. Cities and Provincial Map of the Republic of South Korea. The location of the Jangheung Project in Chollanam-Do Province is highlighted.

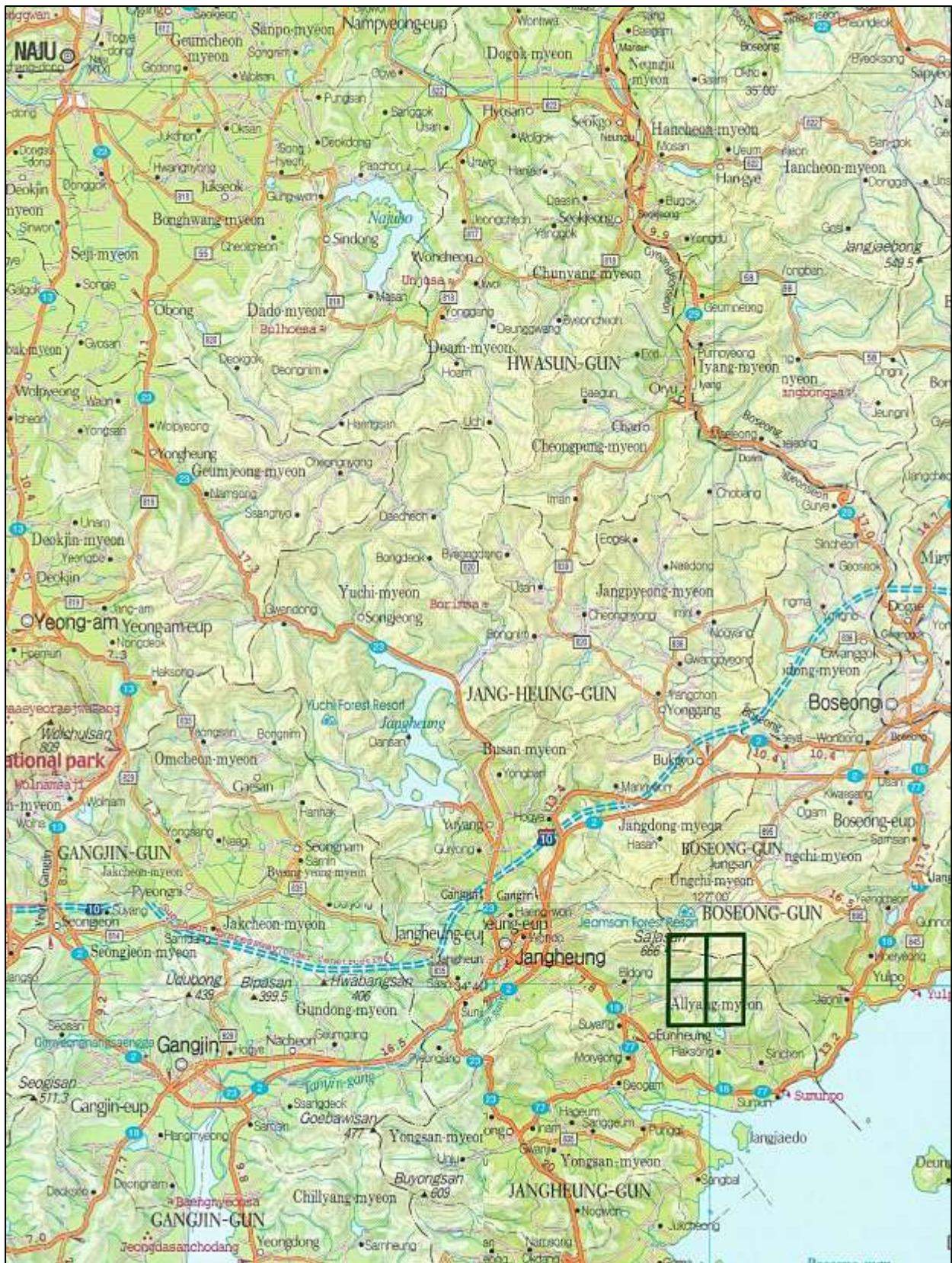
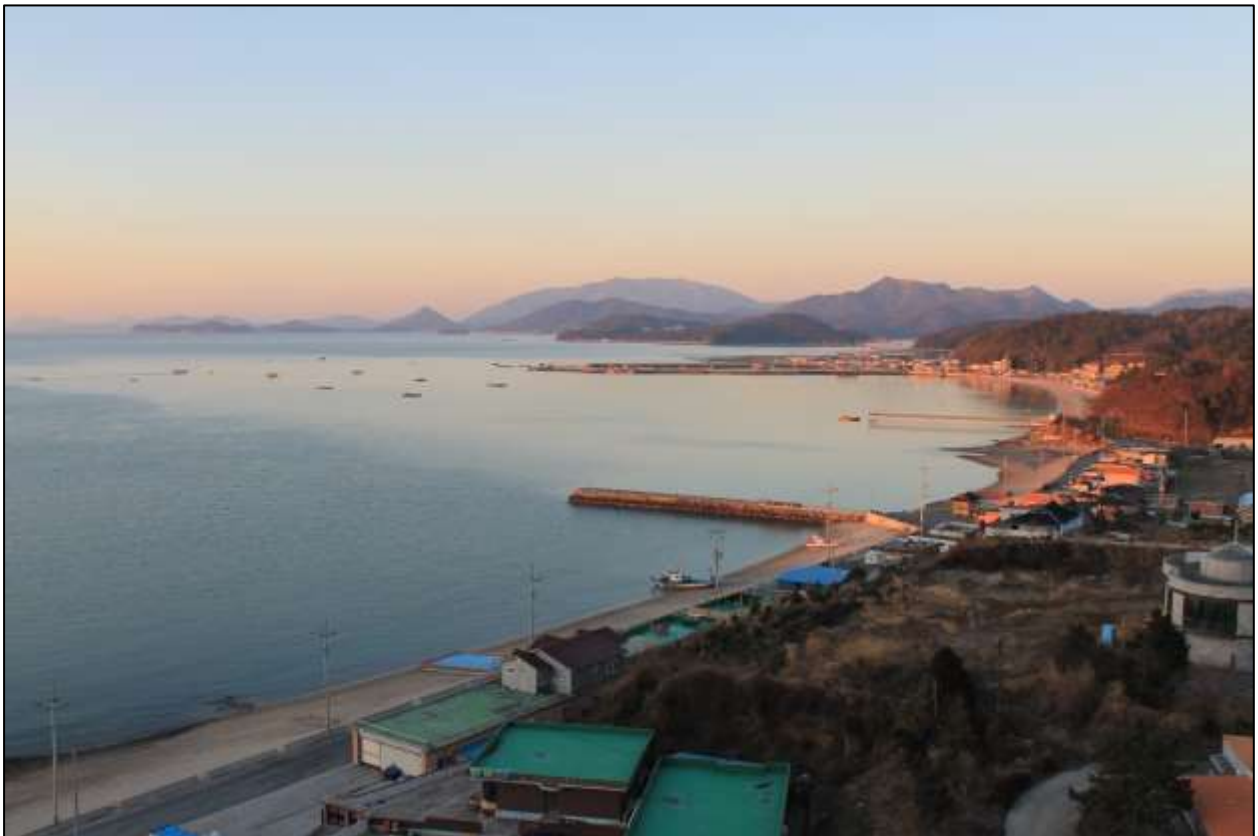


Figure 3. District Location Map of the Jangheung Cu-Ag-Zn-Pb Project. The main road network and villages are shown, along with the borders of each county (“Gun”). The Mining Rights are indicated.



Photograph 1. Jangheung bus terminal.



Photograph 2. Small fishing port of Sumunpo. The hotel-resort at Sumunpo is the closest accommodation to the Jangheung project, although meal options are limited.

## 2.2 PHYSIOGRAPHY

The Jangheung project lies in the southern coastal region of Chollanam-Do Province, situated within Boseong-Gun county.

The district is characterized by rugged, steep hilly terrain in an attractive coastal setting adjacent to the secluded and sheltered inlet of Boseong Bay. Elevations within the project area reach 668masl at Sajasan peak, then rise along a connected ridgeline up to 778masl at Jeamsan, located about 1,300m further to the north.

Most of the creeks are perennial, fed by summer rains, winter snows and mountain springs. The creeks form a radial drainage pattern, flowing away from the ridgeline hosting the breccia pipe outcrops.

Jeamsan and Sajasan are both popular hiking attractions throughout the year, with several mountain trails along the ridgeline affording scenic views of the coast. The *Jeamsan Mountain Resort* is located just to the north of the project area, with road access from the north.

## 2.3 VEGETATION

Vegetation in South Korea is typical of a temperate climate. The hilly terrain of the Haman Project area is relatively well forested (Figure 8) and consists of widespread pine needle coniferous alpine vegetation, with an admixture of fir, pine and Korean cedar. Bamboo is found in the lower parts of the area.

Thick dense undergrowth, consisting of scrubby thorny vegetation (“gashin”) develops quickly in June after the first heavy rains, making access very difficult off walking tracks. The scrubby undergrowth browns and dies out rapidly during October-November at the onset of winter.

The hill slopes of the project area are generally well forested, but the mountain ridges are characterized by conifer pine forest, a thick understory of secondary regrowth and sparsely-vegetated rocky bluffs with talus scree slopes and limited soil cover. The soils are primarily brown forest soils and mountain brown forest soils.

Cherry blossoms bloom for a brief period, marking the beginning of spring in April. Flowers typically bloom in summer.

The surrounding climate and soil provide good conditions for growing a unique green tea that has a distinct taste and aroma. Almost one third of all tea farmland in Korea is located near Boseong and nearly half of all green tea production in Korea comes from this area.

The Jangheung district is noted for its production of shiitake mushrooms and barley crops, as well as eco-friendly farming practices.

Cheonkwansan near Jangheung town is famous for its beautiful scenery featuring eulalias. The plants reach full height around mid-September and until October.

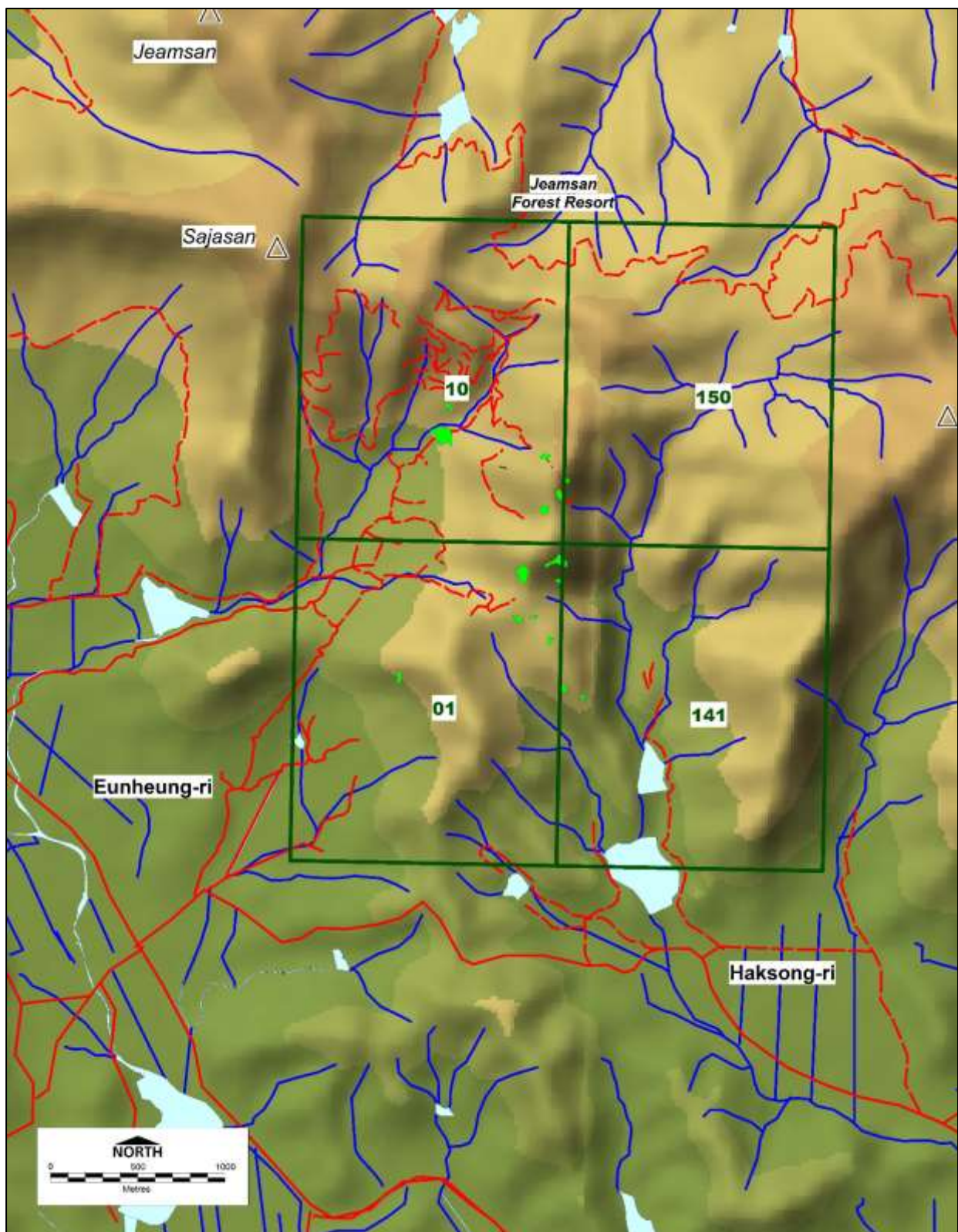


Figure 4. Physiographic Relief Map of the Jangheung Project. The mapped breccia pipe outcrops are highlighted in green.

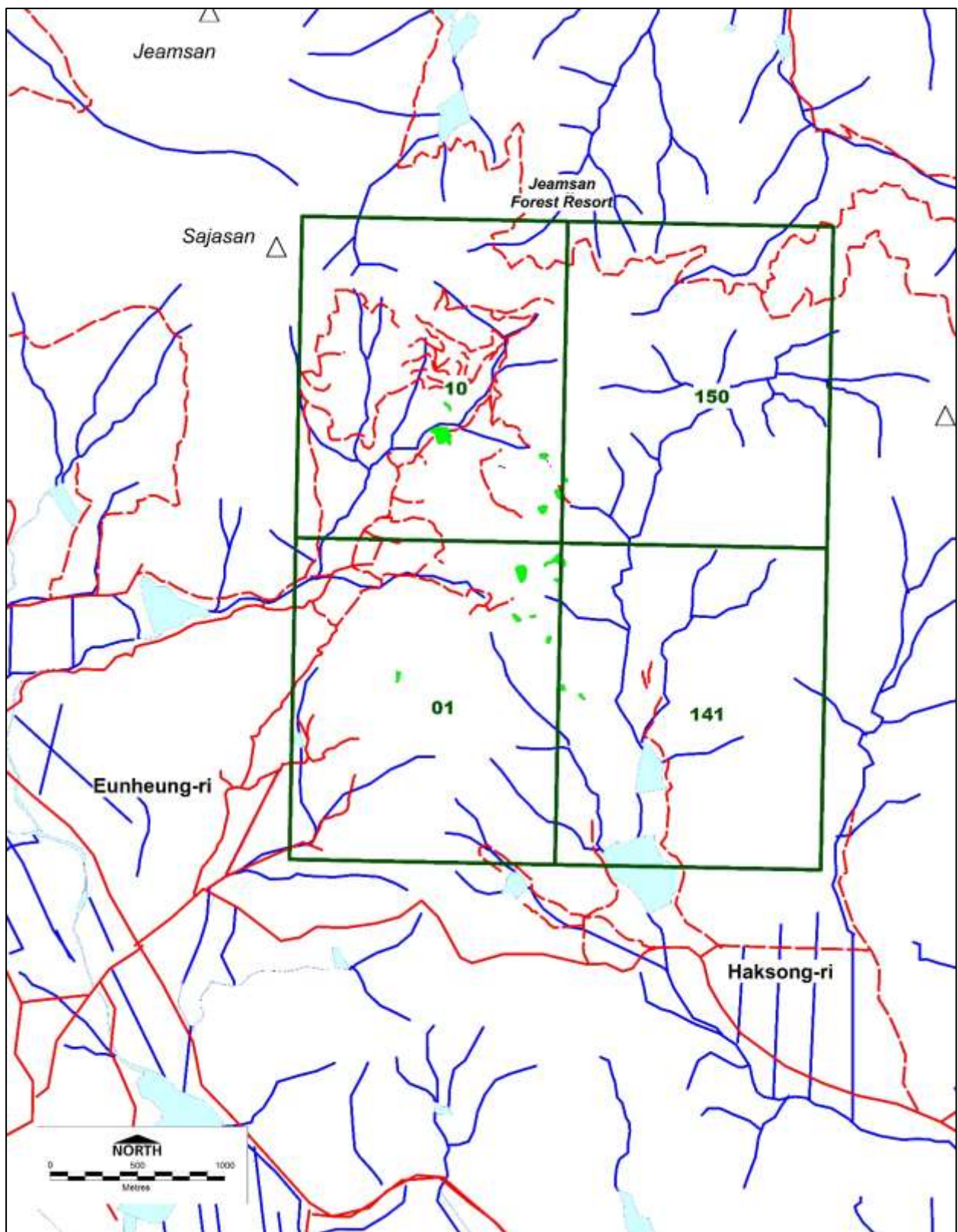


Figure 5. Drainage Pattern Map of the Jangheung Project. The mapped breccia pipe outcrops are highlighted in green. The creeks display a radial pattern draining away from the ridge hosting the breccia pipes.



**Photograph 3. View looking northeast of the rugged, steep terrain of Jeamsan peak (778masl), with well forested hill slopes, but exposed bare rocky bluffs on the main ridgeline.**



**Photograph 4. View looking northeast of Sajasan peak (668masl), The Jangheung project area is located behind, on the reverse slopes of Sajasan. The peak is composed of bare rocky bluffs of andesite tuff that cap diorite porphyry.**

## 2.4 CLIMATE

South Korea lies within the East Asian Monsoon region and experiences a typical temperate zone climate, with four distinct seasons (comprising winter, spring, summer and autumn). The movement of air masses from the Asian continent exerts greater influence on South Korea's weather than does air movement from the Pacific Ocean.

Because of its location near the southwest coast, Chollanamdo-Do Province has a relatively milder climate compared to other parts of Korea, being less humid and cooler in summer, slightly wetter and warmer in winter. Although average temperature in January is 1.2°C and freezing temperatures can occur during December-March, snowfalls are relatively uncommon and minor.

Spring and autumn are pleasant, but normally short in duration. Milder temperatures in the spring produce slush, muddy conditions on unsealed roads in March-April. Blossoming of some fruit trees produces spectacular proliferation of colours for a brief period.

Summers are short, hot, and humid in the “wet season” (“Jangma”), rainfall being concentrated in the June-August period, when daily temperatures average 26°C. Daily thunderstorms are common in August. Typically, 2-3 “typhoons” occur annually in coastal areas, although South Korea is less prone to typhoons than Japan, Taiwan, the east coast of China, or the Philippines. During the autumn months of September and October, the climate becomes noticeably cooler, daily temperatures reaching 20°C.

The region's annual rainfall is about 1505mm which sustains the local agricultural industry of the district. The average annual temperature is 13.0°C.

The prevailing winds are southeasterly and southwesterly in summer and northwesterly in winter. During spring, “Hwangsa” yellow sand dust is blown easterly into Korea from Mongolia and China, producing a dust haze which reduces visibility.

Climate data accumulated over a 30-year period (1981 – 2010) for the Jangheung Project area is indicated in Table 1 below, using meteorological data recorded in Jangheung, situated about 7km west of the project area.

**Table 1. Climate Data for Jangheung (1981-2010).**

MONTH	Jan	Feb	Mar	Apr	May	Jun	Jul	Aug	Sep	Oct	Nov	Dec	Year
Average High (°C)	6.2	8.4	12.9	18.9	23.3	26.3	28.8	30.2	26.9	22.3	15.3	9.0	19.0
Daily Mean (°C)	0.6	2.3	6.4	12.0	17.0	21.1	24.6	25.4	20.9	14.7	8.2	2.7	13.0
Average Low (°C)	-4.2	-3.1	0.4	5.2	11.0	16.7	21.4	21.6	16.2	8.5	2.3	-2.7	7.8
Precipitation (mm)	29.6	45.0	73.0	101.4	125.2	219.0	290.9	306.5	191.7	44.5	52.6	26.2	1,505.6
Av. Precipitation Days (≥ 0.1 mm)	8.5	7.3	8.8	8.3	9.0	10.2	13.9	12.5	9.0	5.4	7.2	7.5	107.6
Humidity (%)	68.2	66.7	66.6	66.7	71.0	75.8	82.1	80.2	77.3	71.9	70.5	70.0	72.2
Mean Monthly Sunshine Hours	152.7	159.5	188.1	208.7	217.3	169.5	145.6	179.0	166.7	197.2	161.1	150.4	2,095.9

Source: Korea Meteorological Administration



Photograph 5. View looking north towards Jeamsan. The photograph was taken in January 2016 after a snowfall.

## 2.5 LOCAL ECONOMY

The local land use is dominated by agriculture, as well as minor forestry logging activities on Sajasan and Jeamsan.

A cattle feedlot agricultural facility is present immediately to the west of the project area. To the southeast, paddy fields.

To the north of the project area is the *Jeamsan Natural Recreational Forest*, with hiking trails for domestic tourists.

Along the coastline to the south, the small fishing ports of Sumunpo and Yulpo support a local fishing industry.

The *Daehan Dawon* Tea Plantation is located about 7km NE of the project area, close to Boseong. This is the main region of Korea's green tea production, some of which is also exported. The tea plantation and is a popular domestic tourist attraction, with traditional *Pension* style accommodation nearby in a forest setting.



**Photograph 6. View of the feedlot agricultural facility on the western side of the ridge hosting the mineralized breccia pipes of the Jangheung project. This facility is an important employer in the local economy of Eunheung-ri.**



**Photograph 7. View of the terraced rice paddy fields and small village of Haksong-ri, located southeast of the Jangheung project.**

## 2.6 EXISTING INFRASTRUCTURE

### Road, Bus & Rail Transportation

Vehicle travel time from Seoul to Jangheung is approximately 4.5hrs, sequentially using the *Gyeonggbu, Nonsan-Cheonan, and Jeonju-Suncheon Expressways* to Suncheon, then by taking the *Yongam Expressway* to Jangheung. Access to the prospect area is via *Route 18* to the village of Eunheung-ri.

Unsealed roads and forestry logging tracks from Eunheung-ri afford access to the western and southern sectors of the project area. Alternative access is from the north via hiking trails from the *Jeamsan Forest Resort*, with roads from the north.

Regular bus services are available into Jangheung and Boseong Bus Terminals from the Dong Seoul Bus Terminal in Seoul (4.5 hours). The area is serviced by the *Gyeongjeon Railway Line* that passes through Boseong.

### Accommodation

Accommodation facilities are available in Jangheung and Boseong towns. The towns have convenient accommodation and restaurant facilities nearby. Internet services are usually available in the motel rooms. A comfortable beach resort hotel at Sumunpo is located much closer to the project area, but meal facilities are very limited.

### Communications

The Jangheung Project area is covered by the national cellular phone communications network.

### Power Supply

The national electricity grid, with large pylons supporting three-phase electrical power supply, is located to the south of the project area.

### Water Supply

There are several dams located on watercourses draining to the west and south of the ridge hosting the breccia pipe bodies at Jangheung. The dams are mainly used for water supply for agricultural purposes.



Photograph 8. View of two-tier rockwall freshwater dam on the catchment draining the eastern flank of the Jangheung prospect. The water is used for local agricultural purposes. The photograph was taken in January 2016 when water levels tend to be at lowest levels. The dam is full in August after the summer rains.

## 3.0 TENURE

### 3.1 MINING RIGHTS

#### Tenure Status

The Jangheung project area is covered by 4 Mining Right blocks, Jangheung-10, Gangjin-01, Sorokdo-141 and Boseong-150, as presented in the Figure and Table below.

**Table 2. Tenement Schedule - Mining Rights.**

Land Register	Registered Number	Area (ha)	Registered Holder	Minerals	Registration Date	Expiry Date
Jangheung-10	Application	282	<i>Shin Han Mine Inc</i>	Cu, Pb, Zn, Ag	6 August 2021	
Gangjin-01	Open	282				
Boseong-150	Open	282				
Sorokdo-141	Open	282				

### 3.2 SURFACE RIGHTS

The Jangheung Project area is covered by Surface Rights held by several landowners. The owners of the cattle feedlot west of the project area are likely to be the main landowners.

The local communities at the small villages of Eunheung (southwest) and Haksong (south) could be potentially affected by any proposed mining and processing operation at Jangheung.

### 3.3 KOREAN MINING ACT – MINING RIGHTS

The Korean Mining Act is administered by the *Ministry of Trade, Industry & Energy* (“MOTIE”). The Korean Mining Act was promulgated and wholly updated on 29 January 1981. The Mining Act has subsequently been revised and updated several times. The last recorded update was made on 23 July 2010.

A Mining Right is the only form of mining title in Korea. A Mining Right covers a 1 minute x 1 minute square Block (approximately 277 ha, or 2.8 km<sup>2</sup> in area).

Applications for Mining Rights are made in the Central Mining Registry office in Seoul, or with the local County office of the *Ministry of Trade, Industry & Energy* department.

No Royalty is payable. Mining Rights are Transferable.

A Mining Right permits the holder to conduct exploration and within the Mining Right.

A “Permit to Mine” is required by the holder of a Mining Right to engage in mining development and mining activities.

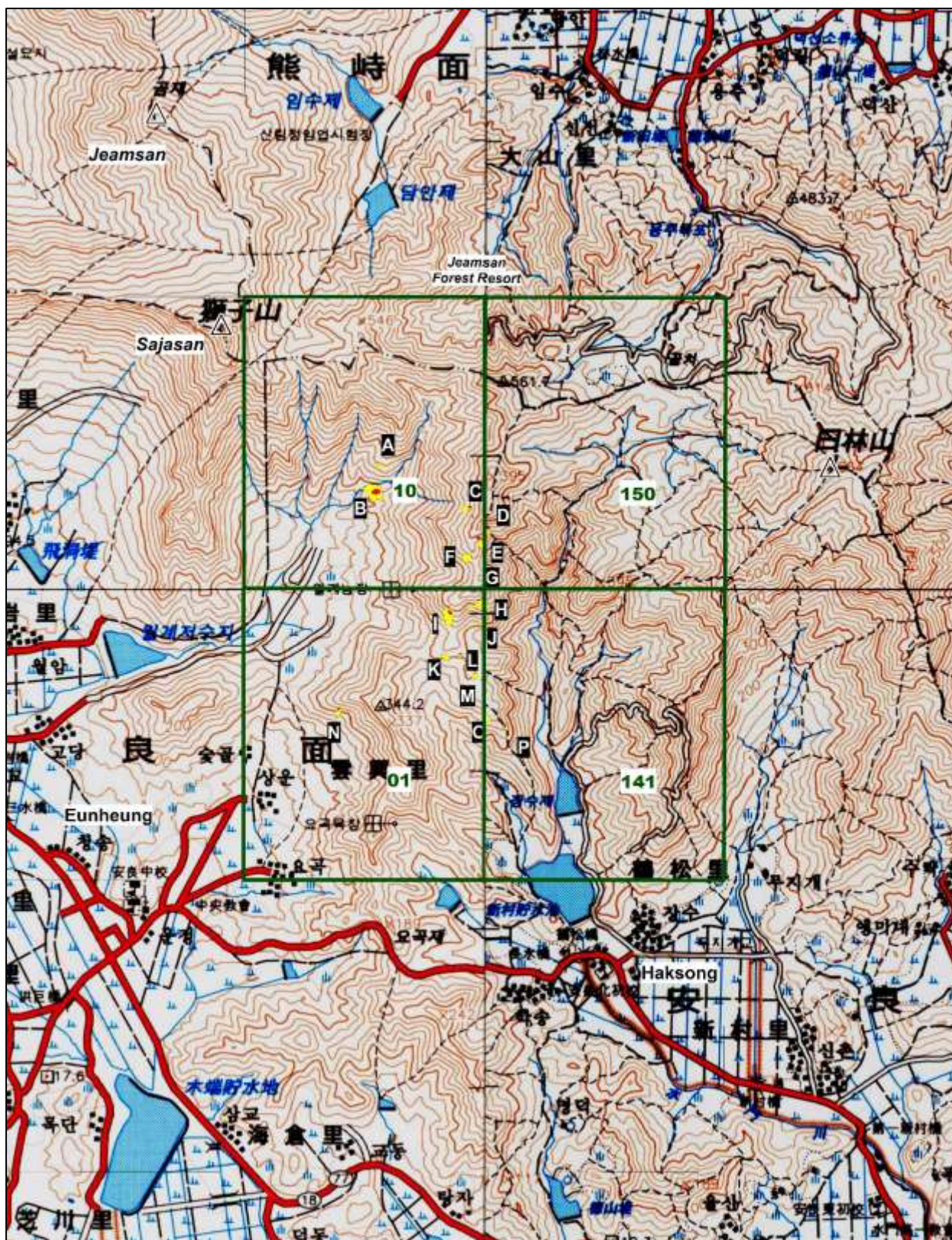


Figure 6. Tenure and Topographic Map of the Jangheung Project area, illustrating the Mining Rights of the area. The location of the breccia pipe structures (labelled A-P) are indicated, along with neighboring villages of Haksong-ri and Eunheung-ri and the prominent mountain peak at Sajasan.

### **Mining Right Application Process**

Under the Korean Mining Act, a Mineral Deposit Survey Report must be lodged with Central Mining Registry office in Seoul, or with the local County office of the *Ministry of Trade, Industry & Energy* department, within 6 months after submission of an Application for Mining Rights.

The Mineral Deposit Survey Report must be prepared by a Registered Geologist, classified as a “Competent Person”. The Mineral Deposit Survey Report must describe and indicate the following items:

- ❖ Area Map at 1:50,000 scale (Topographic Map Series).
- ❖ Mineralization description. Provide evidence of mineralization by sample analysis.
- ❖ Geology description.
- ❖ Physiography, geography, location, access.
- ❖ Proposed Work Program 3-Years:
  - Geophysics.
  - Geochemistry.
  - Drilling. Must have at least 3 drill sites for a minimum total of 450 metres.
  - Tunnelling.

The Korean Mining Act stipulates that certain “threshold values” for each element applied for must be met in order for a Mining Right to be granted.

### **Approval Process**

Approval of Mining Title is issued after completion of field investigation by local MOTIE officers. The area is reviewed by a combined 5-member panel of MOTIE and KORES officers to determine if tenure is contrary to the public interest.

Once Mining Title is approved and documentation completed, Registration Tax is payable within 30 days of the Approval Notice. Registration Tax is currently KRW 113,000 per mining right (about US\$100ea). Mining Title is officially recorded upon receipt of monies.

A Mining Right is granted for a period of 7 Years. After Registration, a 2 year “Decision” period is granted, after which the mining Right holder is required to make a decision to go to the Mining or Exploration Stage. The Mining Right is renewable for another 20 years if the mine is still in production and the reporting requirements have been met.

### **Work Requirements**

The Holder of a Mining Right is required to drill 3 holes of 150m depth (for a total metreage of 450m) as a requirement of meeting the work requirement conditions of the “Exploration Stage” of the Korean Mining Act.

### **KORES Technical Assistance**

The holder of a Mining Right is entitled to apply for technical assistance from the *Korean Resources Corporation* (“KORES”) after holding the Mining Right for at least 12 months. KORES is a wholly government-owned enterprise mandated to support the Korean domestic mining sector. Independent domestic resource developments are one of the key tasks of KORES.

KORES is able to provide technical assistance to the mining right holder, including diamond drilling, geological and geophysical surveys and laboratory analysis. KORES usually reviews requests for technical assistance in October of each year, as it prepares its budgets for the following year. However, it should be noted that the applicant is unable to direct KORES where the holes are drilled within the Mining Right.

### **Reporting Requirements**

Work Program Reports are required to be submitted 6-months before expiry to the Central Mining Registry office in Seoul, or with the local County office of the *Ministry of Trade, Industry & Energy* department. The report should describe the work completed on the Mining Right during the 3-year reporting period.

A Proposed Work Program is also required to be lodged for the subsequent 3-Year period.

If the “Exploration Stage” is selected, then every 2.5 Years, the Mining Right holder is required to submit a report on the Work Completed.

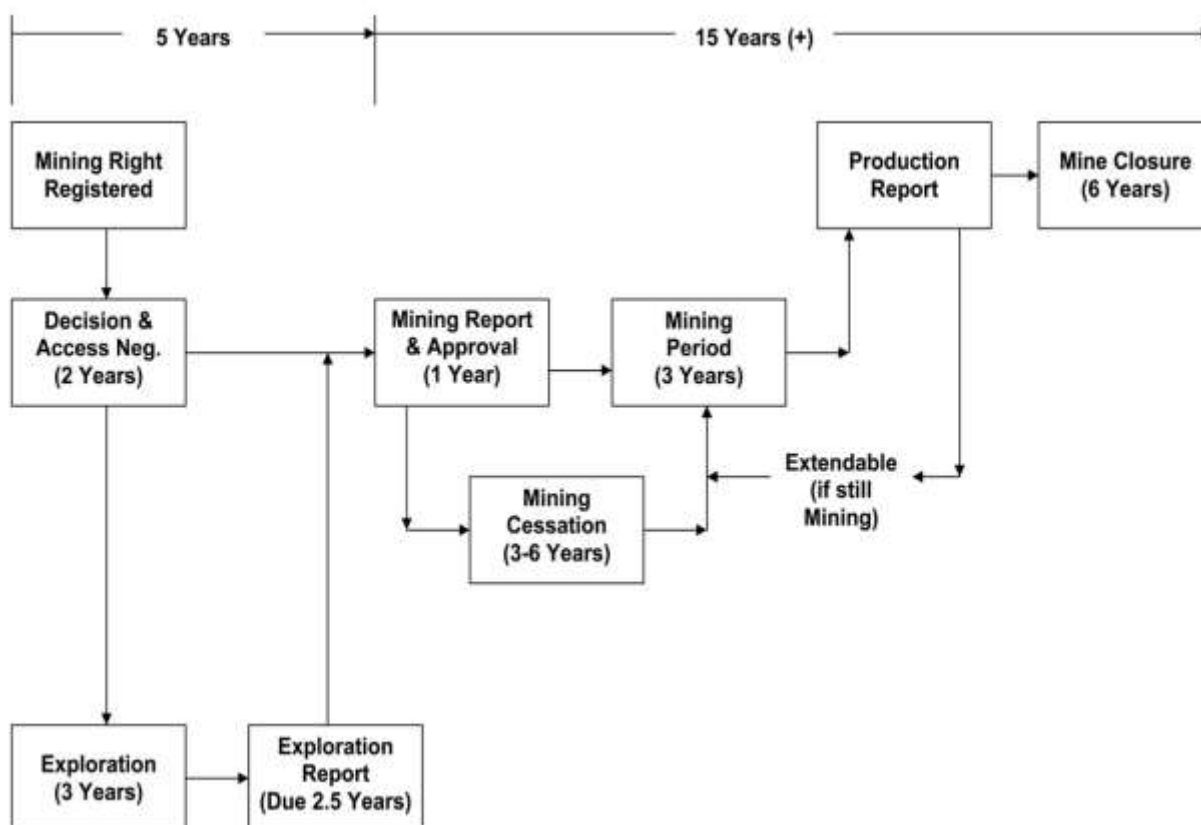


Figure 7. Flow Diagram of the Mining Right Reporting Process.

### 3.4 MINE DEVELOPMENT PERMIT PROCESS

#### Permit To Mine

After preparation of an Exploration Report, the Mining Right holder must elect to continue with the “Exploration Stage” or proceed to the “Mining Stage”, or abandon. If the Mining Right holder decides to progress to the “Mining Stage”, then an Application for “Mine Development Permit” is lodged.

The Mine Development Permit process requires submittal of a mine plan, financial studies, an Environmental Social Impact Assessment (“ESIA”) management plan that takes into account environmental disturbance, air quality (dust) and hydrological (surface and ground water impacts) aspects and community social impact studies (noise, disruption, employment issues, etc). The typical ESIA process is attached.

In order for mining to commence, negotiations and agreements are required with the owners of Surface Rights over the area affected by mining activities. This could entail either outright Acquisition or Long-Term Leasing arrangements with the owner of the Surface Rights.

#### Mine Closure

Rehabilitation is required after completion of mining activities. Visual issues mainly apply to restoration of the mine area. Approximate estimated cost of rehabilitation after mining is considered to be about US\$200,000 per Ha disturbed.

### 3.5 ENVIRONMENTAL SOCIAL IMPACT ASSESSMENT (ESIA) PROCESS

The Mine Development Permit process requires submittal of an **Environmental Social Impact Assessment** (“ESIA”) management plan, involving baseline environmental studies conducted over 4 seasons (12 month period), together with engagement of the local community and stakeholders. The ESIA process is summarised below.

#### **Project Description**

- Database Establishment.
- Project Characterization.
- Scoping Study Report.
- Develop Project Background Information Document.

#### **Draft Assessment Plan (DAR)**

- ESIA Committee established.
- Identify Stakeholders, including Landowners, Local Community, Local Government, Provincial Government & Regulatory Agencies involved in ESIA process.
- Key Project Issues.
  - Regulatory Responsibilities, including Stakeholder engagement and Develop Regulatory Review & Tracking Mechanisms.
- Additional Technical Issues to meet International Best Practice.
  - Identification of Local Restrictions, including Habitat Conservation & Protection Zones and Cultural Heritage.
- Development of Management Plan.
- Prevention & Mitigation Measures.
- Preparation of Draft Assessment Report (DAR).
- Submission of DAR to Stakeholders.

#### **Baseline Studies**

- Baseline Studies designed
- Baseline data collected over 4 seasons (12 Months) required for ESIA Report.
- Baseline Study Analysis.
- Environmental & Social Impact Evaluation.
  - Surface Hydrology.
  - Groundwater.
  - Dust
  - Noise.
  - Fauna.
  - Flora.
  - Local Community.

#### **Stakeholder Engagement, Group Discussion & Public Consultation**

- Regulatory Agencies involved in ESIA process.
- Project Background Information Document distributed to local community.
- Community Liason Office.
- Group Discussion Meeting.
- 30-day Public Notification Awareness Campaign.

#### **Public Hearing**

- Comments from Stakeholders.
- Comments from Local Community.

#### **Revision of the DAR & Finalisation of the ESIA**

- Collection of Opinion on DAR.
- Collect opinion from Public Hearing.
- Recommendations from EIA Committee.

## 4.0 DATABASE

A comprehensive geological database on Korea has been systematically acquired and built up over 18 years by *Senlac Geological Services Pty Ltd* since 1994. The database is in a Geographic Information System (GIS) format using *MAPINFO™* software. The map projection used for the GIS is WGS-84, zone 52 North UTM, although South Korea uses Tokyo Grid. The mineral occurrence database includes 800 gold deposits and 125 base metal deposits.

### Literature Review

A literature search for any relevant information pertaining to the Jangheung-Boseong mining district was undertaken of the libraries and database of the *Korean Resources Corporation* (“KORES”) in Seoul and the *Korea Institute of Geoscience and Mineral Resources* (“KIGAM”) in Daejeon.

The Atlas of Mineral Resources – Republic of Korea, compiled by the United Nations (ESCAP, 1987) lists the Jangheung deposit as Cu mineral occurrence No 1 and Pb-Zn mineral occurrence No 40.

An important source is David Gallagher (1963), a *United States Overseas Mines* (USOM) assistance engineer who inspected most of the major mines and historical mining archives of South Korea after the Korean War, including those of the Haman district. There is no recorded production from the Jangheung prospect area.

The journals of the *Geological Society of Korea* and the *Korean Institute of Mining Geology*, together with *Economic Environmental Geology*, publish most of the geological research papers in Korea.

### Geological Maps

South Korea has been mapped geologically at 1:50,000 scale by Korean and Japanese geologists in several phases. Digital and paper 1:250,000 and 1:50,000 scale maps are available for the entire country from the *Korean Institute of Geology Minerals and Mining* (“KIGAMM”) in Daejeon City. Each map sheet is accompanied by explanatory notes. The Jangheung Cu-Zn-Pb-Ag project is covered by the Jangheung and Boseong 1:50,000 scale Geological Map sheets.

### Remote Sensing

Satellite imagery for the database was acquired from free open INTERNET sources of *Google Earth™*. Remote sensing imagery is available over the Jangheung Project area, including:

- ❖ SPOT satellite imagery with 1.0m resolution (*Maxar Technologies & Centre National d'Etude Spatiales*, 2021) downloaded from *Google Earth*.
- ❖ SPOT satellite imagery with 2.5m resolution (*SK Energy & Centre National d'Etude Spatiales*, 2014) downloaded from *Google Earth*.

### Topographic Base Maps

Topographic maps are available in raster and vector digital file and paper form for all of South Korea in 1:50,000, 1:20,000 and 1:5,000 scales. These maps can be purchased through retail map shops of the *Korean National Mapping Service*. The Jangheung project is covered by the Jangheung NI52-05-16 and Hoecheon NI52-06-08 1:50,000 scale topographic map sheets and is further subdivided into 1:5,000 scale topographic map sheets.

A topographic base map for the Jangheung Project was compiled as a series of individual layers in the *MAPINFO™* GIS database. The layers include rivers, creeks, roads, buildings and elevation contours at 10m levels.

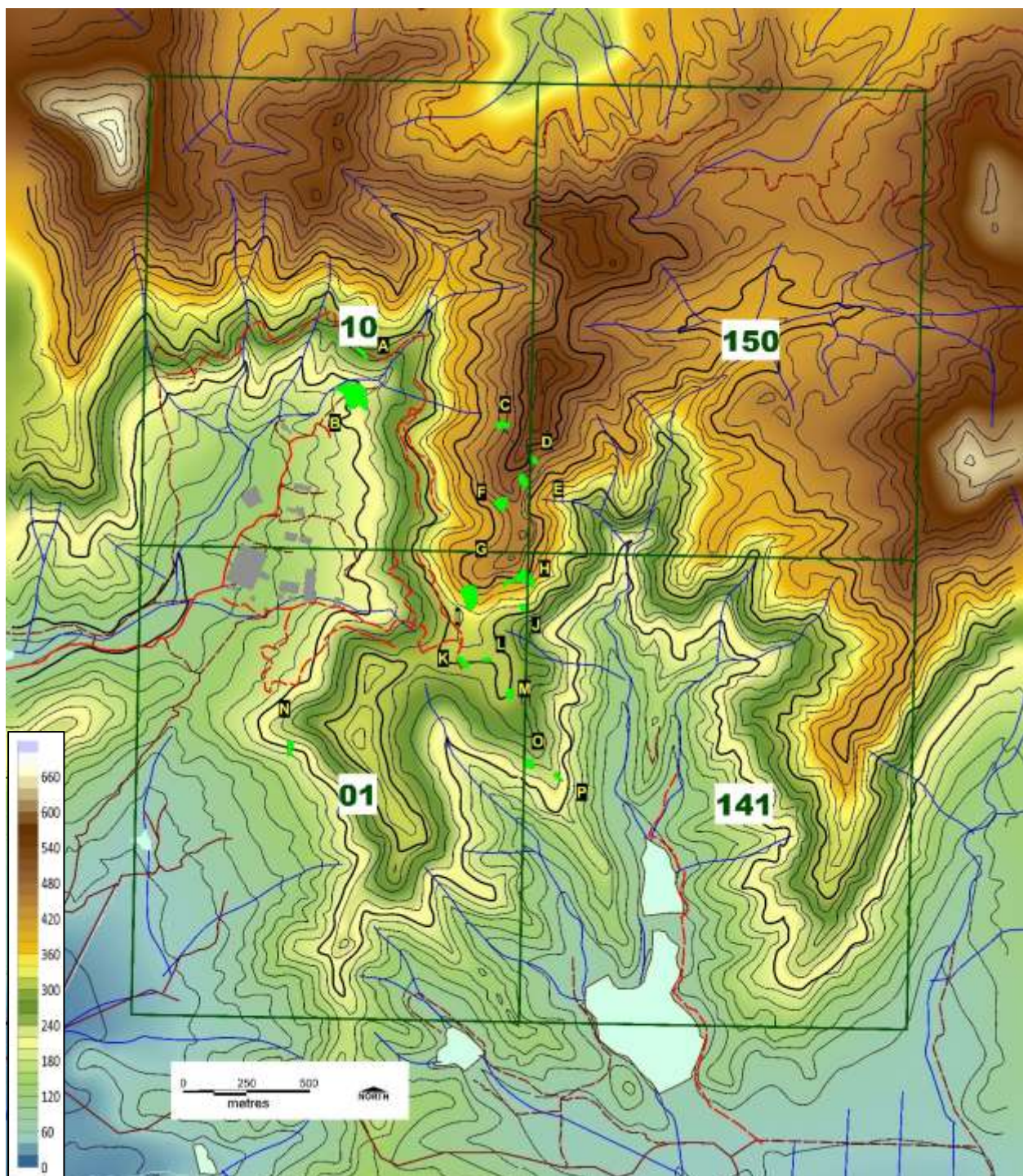


Figure 8. Digital Elevation Model of the Jangheung Project. The DEM was constructed by digitizing contours from the 1:50,000 scale topographic map sheets. The outcrops of the 16 breccia pipe/soil geochemical anomalies are shown in green and correspondingly labelled A, B, C, ...P.

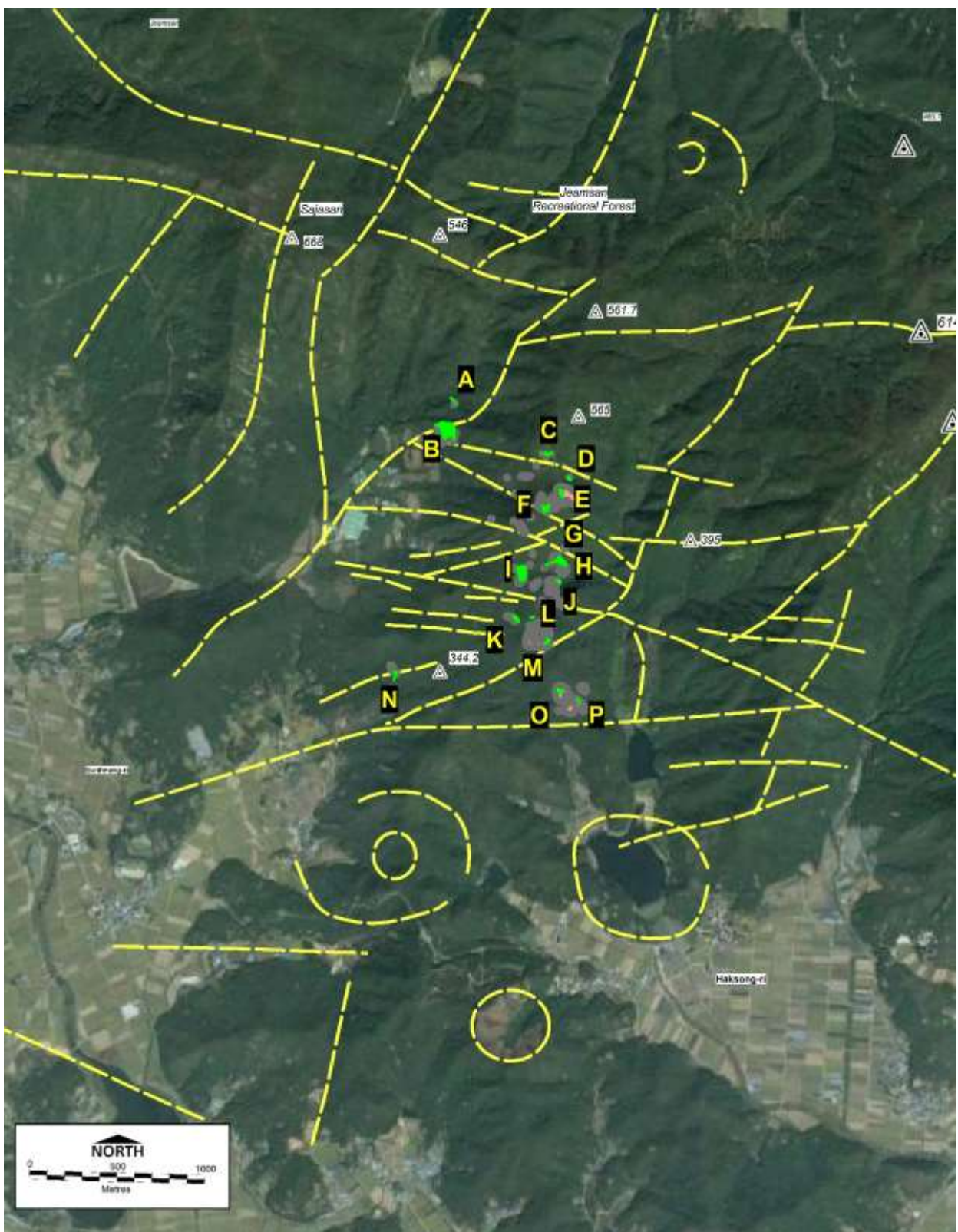


Figure 9. SPOT Satellite Image (2.5m resolution) of the Jangheung Project (SK Energy & Centre National d'Etude Spatiales, 2014) downloaded from *Google Earth*. The outcropping breccia pipes are shown and labelled A-P. Structures interpreted from the image are shown as yellow dashed lines, including faults, circular ring dyke/fractures and recessive zones.

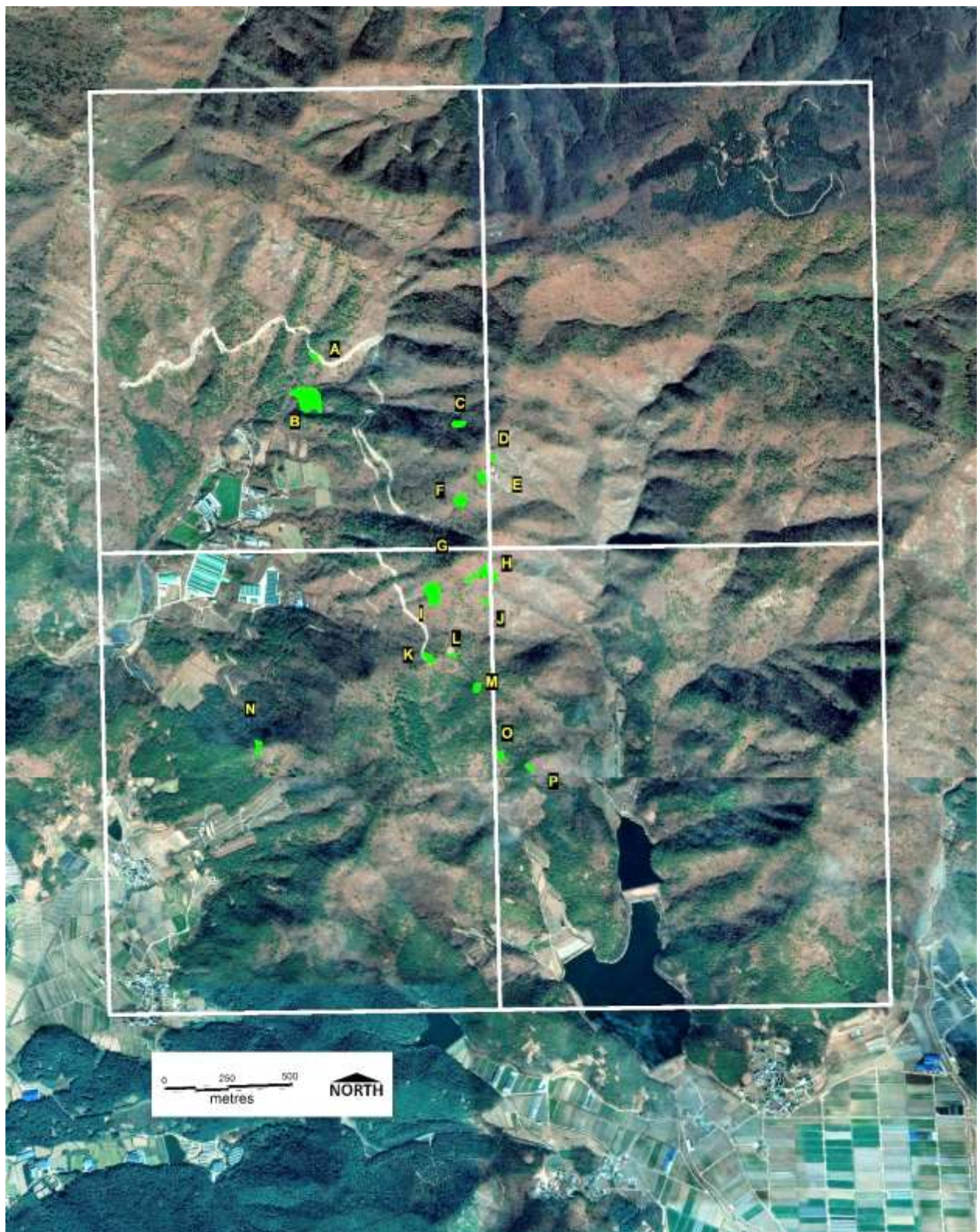


Figure 10. Satellite Image (1.0m resolution) of the Jangheung Project (*Maxer Technologies & Centre National d'Etude Spatiales, 2021*) downloaded from *Google Earth*. The outcrops of the breccia pipes are shown in green and labelled A-P.

## 5.0 PREVIOUS INVESTIGATIONS

### Previous Exploration

Regional stream sediment geochemical surveys were conducted throughout Korea during 1971. Follow up of stream sediment geochemical anomalies led to the discovery of a cluster of hydrothermal breccias pipes outcropping on the southeastern slopes of Sajasan mountain.

Exploration was conducted over the Jangheung area during 1977-1982 by the *Korean Institute of Energy & Resources* ("KIER"). KIER (1982) completed the following surveys at Jangheung, including:

1. Field prospecting and mapping located mineralized breccia outcrops during 1977-1979.
2. Soil geochemical survey over a 1500m x 2500m area. This survey locating 16 anomalous geochemical zones (labelled Anomalies A-P).
3. A VLF-Electromagnetic geophysical survey was completed by KIER over a 500m x 600m gridded area, which outlined coincidental EM anomalies with the H, G, I, and K Anomalies.
4. KIER subsequently drilled 12 diamond core holes, designed to test 5 of the soil geochemical anomalies, including Anomalous Zones B, C, E, G, and I. Significant intersections of >0.50% Cu and 5.0% Zn were reported from 3 of the 5 tested Anomalous Zones.

*Indochina Goldfields Limited* subsequently explored the Korean peninsula during 1994-2000, mainly focused on epithermal gold exploration. A visit to the Jangheung prospect was made by Spadafora (1994), but only the Anomaly P breccia pipe was inspected. Rock chip sampling (5 samples) recorded maximum assays up to 4.85% Cu, 6.28% Pb, 9.27% Zn and 932g/t Ag. However, no anomalous gold was detected and so no further work was recommended.

### Historical Resource Estimates

Previous exploration by the *Korean Institute of Energy Resources* (KIER, 1982) has reported a combined historical inferred mineral resource<sup>2</sup> of 1.12Mt @ combined 5% Cu-Pb-Zn & 64g/t Ag, based on the results of the 12 drill holes. This combined resource was estimated from modelling of the drilled breccia pipes at Anomaly B, Anomaly E and Anomaly I, including:

#### Anomaly B (based on drillholes JD-10, JD-11 & JD-12).

Cylinder Resource Block model with dimensions as follows:

- ❖ Block 1 = 3.14 (Pi) x 20m (radius) x 20m (radius) x 160m (depth) x 2.8g/cc (SG) = 562,700 tonnes
- ❖ Block 2 = 3.14 (Pi) x 20m (radius) x 20m (radius) x 50m (depth) x 2.8g/cc (SG) = 175,800 tonnes
- ❖ Total = 738,500 tonnes

#### Anomaly E (based on drillholes JD-5, JD-6, JD-7 & JD-8).

Cylinder Resource Block model with dimensions as follows:

- ❖ Block 3 = 3.14 (Pi) x 5m (radius) x 5m (radius) x 90m (depth) x 2.8g/cc (SG) = 19,800 tonnes
- ❖ Block 4 = 3.14 (Pi) x 5m (radius) x 5m (radius) x 30m (depth) x 2.8g/cc (SG) = 6,600 tonnes
- ❖ Total = 26,400 tonnes

#### Anomaly I (based on drillholes JD-1, JD-2 & JD-3).

Cylinder + Cone Resource Block model with dimensions as follows:

- ❖ Block 5 = 3.14 (Pi) x 15m (radius) x 15m (radius) x 90m (depth) x 2.8g/cc (SG) = 155,400 tonnes
- ❖ Block 6 = 3.14 (Pi) x 20m (radius) x 20m (radius) x 30m (depth) x 2.8g/cc (SG) = 105,500 tonnes
- ❖ Block 7 = 3.14 (Pi) x 20m (radius) x 20m (radius) x 90m/3 (depth/3) x 2.8g/cc (SG) = 74,400 tonnes
- ❖ Block 8 = 3.14 (Pi) x 20m (radius) x 20m (radius) x 30m (depth) x 2.8g/cc (SG) = 32,700 tonnes
- ❖ Total = 368,000 tonnes

<sup>2</sup> Cautionary Statement: This resource was classified based upon the *Korean Institute of Energy Resources* resource estimation classification scheme and reporting nomenclature. The resource estimates are historical and do not comply with current NI-43-101 or 2012 JORC Code reporting requirements.

## 6.0 REGIONAL GEOLOGY OF KOREA

The Jangheung project is situated within the Jangheung-Boseong mining district, located in the southwestern coastal region of the Korean peninsula adjacent to Boseong Bay.

The geology and stratigraphy of Korea is well documented, being summarized below, using the main sources of Reedman and Um (1981), Lee (1988), KIGAM (1995) and subsequently revised by Chough et al (2000).

### Pre-Cambrian Cratonic Basement

Situated at the active margin of a stable craton known as the Sino-Korean craton or the North China-Korea Platform, the Korean Peninsula is divided into three Archean blocks (the *Nangrim-Pyeongnam Block*, *Gyeonggi* and *Ryeongnam Massifs*) separated by northeast-trending Phanerozoic mobile belts (the *Imjingang* and *Ogchon Belts*).

The crustal scale *Gyeonggi Shear Zone* forms the northern tectonic boundary of the *Gyeonggi Massif*, with the *Imjingang Belt* to the north and the north-northeast striking *Kongju Fault* forms the southern tectonic boundary of the *Gyeonggi Massif* with the *Ogchon Belt* to the south.

The *Imjingang Belt* and the southwestern sector of the *Gyeonggi Massif* is considered to be an extension of the Triassic *Dabie-Sulu collision belt* of the *Yangtse Craton* (Lee et al, 2003; Oh et al, 2005).

### Archean

The *Gyeonggi* and *Ryeongnam Massifs* consist of gneiss, porphyroblastic gneiss, augen gneiss, granite gneiss, migmatite, minor schist amphibolite and limestone/calc-silicate lenses, interpreted as a deep marine sedimentary sequence intruded by granite. The crystalline basement core of the *Gyeonggi Massif* is believed (Lee et al, 2003) to have formed during the Late Archean (2.9-2.5Ga), but may be as old as the Middle Archean (3.0Ga).

### Early Proterozoic

Leucogranites were emplaced into the northeastern sector of the *Yeongnam Massif* at about 1.93-1.86Ga and was accompanied by widespread regional low-pressure type metamorphism (Kim & Cho, 2003). A large rapakivi granite batholith intruded the *Gyeonggi Massif* at 1.84Ga (Zhai et al, 2005). This felsic magmatism is correlated with the *Luliangian Orogeny* of the North China craton.

### Late Proterozoic

The **M1** regional metamorphic event took place in the cratonic basement at about 888-820Ma, during the Late Proterozoic. The widespread upper amphibolite to granulite facies indicates high-temperature, medium-pressure type metamorphism. This event is attributed by Lee and Cho (1995) and Sagong et al (2003) to the collision and amalgamation of continents during the Late Proterozoic (the *Jinlingan Orogeny* in the Qinling Belt of China).

The **M1** regional metamorphism was accompanied by syn-tectonic deformation and emplacement of deep-seated, mantle-derived syn-kinematic intrusions (Sennitt & Kim, 2012). Layered ultramafic intrusive complexes were emplaced at about 822-812Ma (Cho, 2001), along northeast-striking structures in a rift setting (Seo et al, 2013).

Peralkaline A-type meta-granitoids were emplaced along the major bounding faults of the *Ogchon Belt*. This alkaline magmatism is considered to be rift-related, associated with the break-up of the *Rodinia* (Li & Powell, 2001) or *Columbia* (Zhang et al, 2010) supercontinents and may be correlated with the *Yangtse Craton* of southern China (Chough et al, 2000).

## Cambrian - Ordovician

During the mid-late Cambrian, a subsiding geosynclinal zone developed between the *Gyeonggi* and *Ryeongnam Massifs*, which evolved into the Ogchon and Taebaeksan Basins. This geosynclinal zone probably formed in an extensional rift tectonic setting, between the *Honam Shear Zone* and the *Kongju Faults*, possibly related to the break up of the *Rodinia* super-continent about 750Ma (Koh et al, 2005).

Deep-trough sedimentary sequences (*Ogchon Group*) were deposited into the Ogchon Basin and shallow marine platform facies (*Choson Group*) into the Taebaeksan Basin. Although stratigraphic relationships are poorly constrained (Chough et al, 2000), Cluzel and others (1990) consider the *Choson Group* is a lateral equivalent of the *Ogchon Group*, representing different palaeogeographic zones of essentially the same basin.

### Ogchon Basin

The Ogchon Basin is distinctly tiled, with the northeast part comprising a non-metamorphosed zone with partly uplifted Precambrian granite gneiss basement. The central and southwestern portions of the geosyncline have undergone subsidence, resulting in progressive lower greenschist facies metamorphism.

Multiple deformation events and metamorphism have resulted in a complex geological framework which is still poorly understood (Lee *et al*, 1986). Structural unravelling by Park and So (1980) of the overturned and folded Ogchon Basin sequence and the use of quartzite and limestone “marker horizons” has resulted in a better understanding of the stratigraphic sequence of the *Ogchon Belt* (Sennitt & Kim, 2012).

The lower sequence of the *Ogchon Group* consists of basal pebbly mudstones (Hwanggangri & Pugnori Formations), phyllite and schist (Changri & Munjuri Formations), U-V-Mo-enriched black shales of the Guryongsan Slate, and a thin dolomitic limestone bed (Geumgang, Hansu & Bibong Limestone). The upper section of the *Ogchon Group* consists of limestone and calcareous slate (Hwajeonri & Kounri Formations), quartzite beds (Midongsan & Taehyangsan Quartzites) and phyllite (Ungyori & Baegbongri Formations), broadly correlating with the *Great Limestone Series* of the Taebaeksan Basin (Sennitt & Kim, 2012).

The *Ogchon Belt* has been interpreted to be the eastward extension of the *Nanhua Basin* of southeastern China (Gi, 2006), but correlations are difficult (Fitches & Zhu, 2006).

### Taebaeksan Basin

The *Choson Group* unconformably overlies the *Yongnam Massif* (northern sector of the *Ryeongnam Massif*) and was deposited into the Taebaeksan Basin in a shallow marine and tidal environment and was likely open to the deeper ocean. The *Choson Group* consists of the lower *Yangdok Series* and upper *Great Limestone Series*, based on distinct lithostratigraphic successions and geographic distribution, with variations in the sequence reflecting numerous sea-level fluctuations (Kwon & Chough, 2006).

Alluvial fans entered into shallow marine tidal environments (Jangsan Quartzite & Myobong Slate). A shallow carbonate shelf setting developed within this marginal shallow lagoonal environment (*Pungchon Limestone*, *Hwajeol Limestone*, *Dumudong Formation* & *Maggol Limestone*). Carbonate sedimentation was periodically terminated by the influx of terrigenous clastic sediments (*Sesong Shale*, *Dongjeum Quartzite*).

The basin evolved from a slowly subsiding carbonate platform into a rapidly subsiding intracontinental rift basin during the Middle Ordovician (Ryu et al, 2005). Lithofacies distribution and rich faunal assemblages indicate a deeper seafloor was present in the western sector of the basin that correlates with sequences in North China and Australia (Chough et al, 2000). Marine sedimentation ceased during the Late Ordovician and the basin was emergent until marine transgression resumed in the Late Carboniferous.

## Silurian - Devonian

The **M2** regional thermal metamorphic event took place at 438±99 Ma (Suzuki et al, 2010), consisting of transitional greenschist-amphibolite facies conditions (Cho et al, 2010). This Late Silurian-Devonian *Ogchon Orogeny* resulted in the ductile piling up of syn-metamorphic, southeastward verging nappes (Cluzel, 1987) of the *Ogchon Belt*.

## Carboniferous – Permian - Triassic

### Pyongnam Supergroup

Compression and collision of the *Sino-Korea*, *Yangtse* and *Russian Far East (Primorye) Cratons* occurred during the Late Carboniferous and Early Triassic (Kim et al, 2000), producing increasing emergence of uplifted continental areas. This uplift resulted in the deposition of distal siliciclastic rocks of the *Pyongnam Supergroup* in numerous, scattered, rapidly subsiding, hinterland troughs, intermontane half grabens and limnic coal basins, under high burial-pressure metamorphic conditions, probably in response to the *Songrim Orogeny*. The *Pyongnam Supergroup* has been correlated with the *Yangtse Craton* of southern China (Jeon et al, 2007).

### Triassic - Jurassic

The *Songrim Orogeny* is the **M3** regional metamorphic event recorded throughout the Korean Peninsula during the Triassic between 252-220Ma (Kim et al, 2008; Ree et al, 2008), coinciding with compression and continental collision along the *Qinling-Dabie-Sulu Collisional Belt* between the *North China* and *Yangtse Blocks* (Kwon et al, 2009) and the Circum-Pacific (Egawa & Lee, 2009).

A post-collisional feature is the development of transcurrent tectonics, medium-low pressure metamorphism and emplacement of related syn-kinematic plutons of the Middle Jurassic *Daebo Granite Series*. A series of extensional shear zones related to these events were active during this period, including the *Gyeonggi Shear Zone* (Kim et al, 2000), *Kongju Fault* and the *Honam Shear Zone*. These extensional shear zones display dextral movements and are thought to have evolved from deep crustal ductile into a shallow crustal brittle regime, associated with the rapid uplift of the *Gyeonggi Massif* (Kim et al, 2000).

### Daebo Granite Series

The *Daebo Granite Series* plutons have been emplaced into the margins of the Ogchon Basin along northeast-southwest striking fault corridors, including the *Honam Shear Zone*, as a huge northeast trending batholith between the *Gyeonggi* and *Ryeongnam massifs*. The *Daebo Granite Series* is a per-aluminous S-type, ilmenite series granitoid, generated by partial melting of metasedimentary rocks. This intrusive suite consists of two-mica, biotite and muscovite granite, foliated porphyroblastic biotite granite, schistose and gneissic granite which were probably emplaced syn-tectonically and syn-kinematically. Slow cooling rates in these intrusions suggest they may have been initially emplaced in the Late Triassic (KIGAM, 2001).

## Cretaceous

During the Cretaceous, East Asia was characterized by Andean-type continental margin formed by the subduction of the Kula Plate and the Kula-Pacific Ridge. This marginal zone was subjected to extensional tectonism of the magmatic arc, resulting in the development of fault-bounded continental depressions, including the Gyeongsang Basin. This tectonism eventually led to the opening of the Sea of Japan.

The Gyeongsang Basin developed as an intra-arc basin followed by the development of a mature volcanic arc, with the coeval intrusion of stocks and batholiths of the late Cretaceous *Bulgugsa Series* and co-magmatic volcanic sequences.

During Cycle 1 (Sennitt, 2010), the Gyeongsang Basin developed initially as an intra-arc basin with deposition of a non-marine sequence comprising the basal Early Cretaceous continental "red bed" Sindong Group into the Nakdong Trough. During Cycle 2 in the Middle Cretaceous, scattered centers of andesitic and basaltic-andesitic volcanism formed, resulting in deposition of the volcano-sedimentary *Hayang Group*. The basin then evolved rapidly during Cycle 3 into a mature volcanic arc during the Late Cretaceous, with extrusion of alternating lava flows and pyroclastics of the volcanic-dominated *Yuchon Group*.

## Tertiary

During the Tertiary, trans-tensional rifting was responsible for the development of sub-basin grabens along with calc-alkaline effusive and explosive activity along the east coast of the peninsular. Deposition initially consisted of terrestrial fluvio-lacustrine sequences (*Yangbug Group*), followed by marine sedimentation (*Yeonil Group*) with minor andesitic-dacitic volcanism.

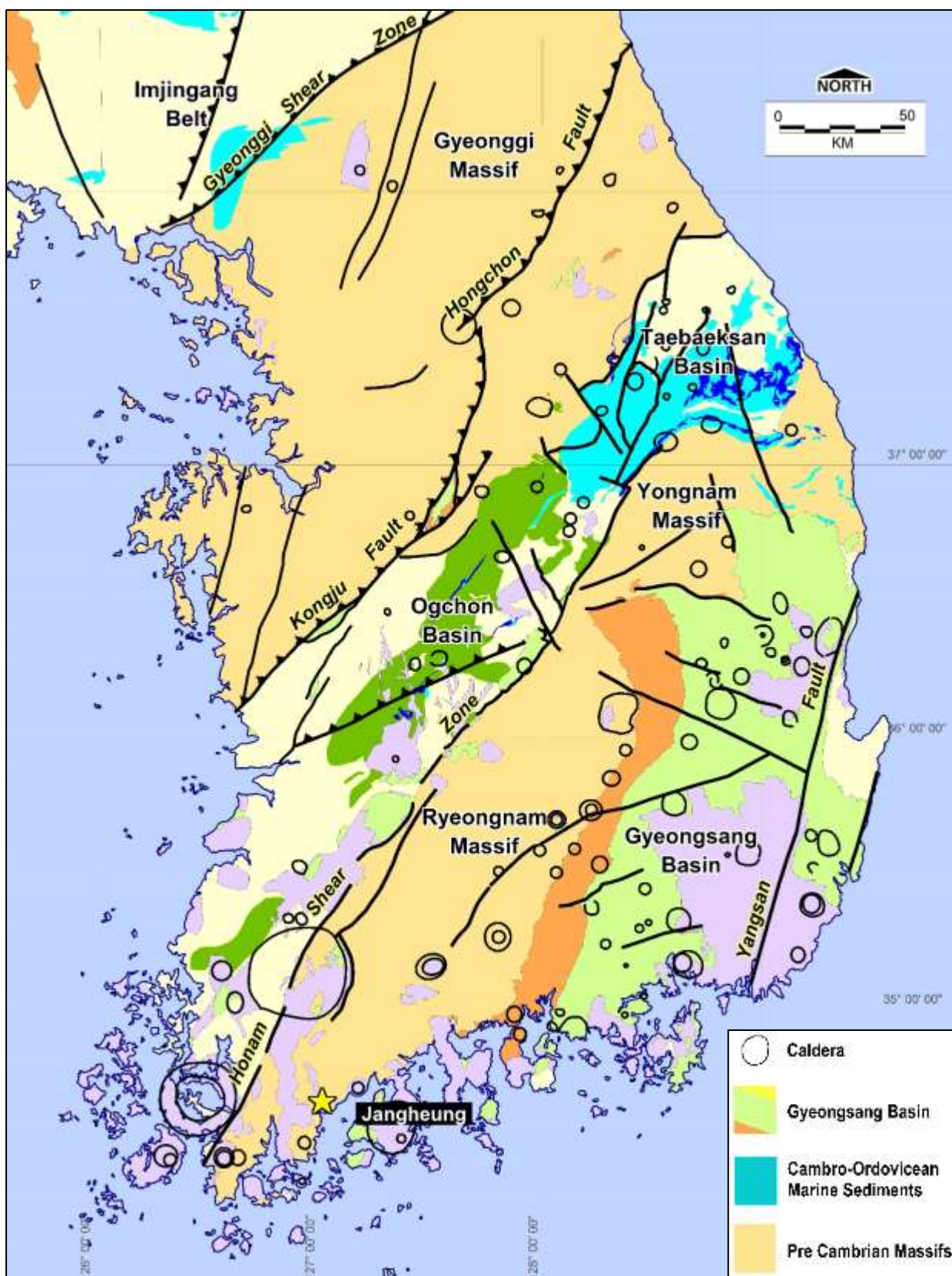


Figure 11. Tectonic Elements Map of South Korea. The Jangheung project is indicated together with major structural features.

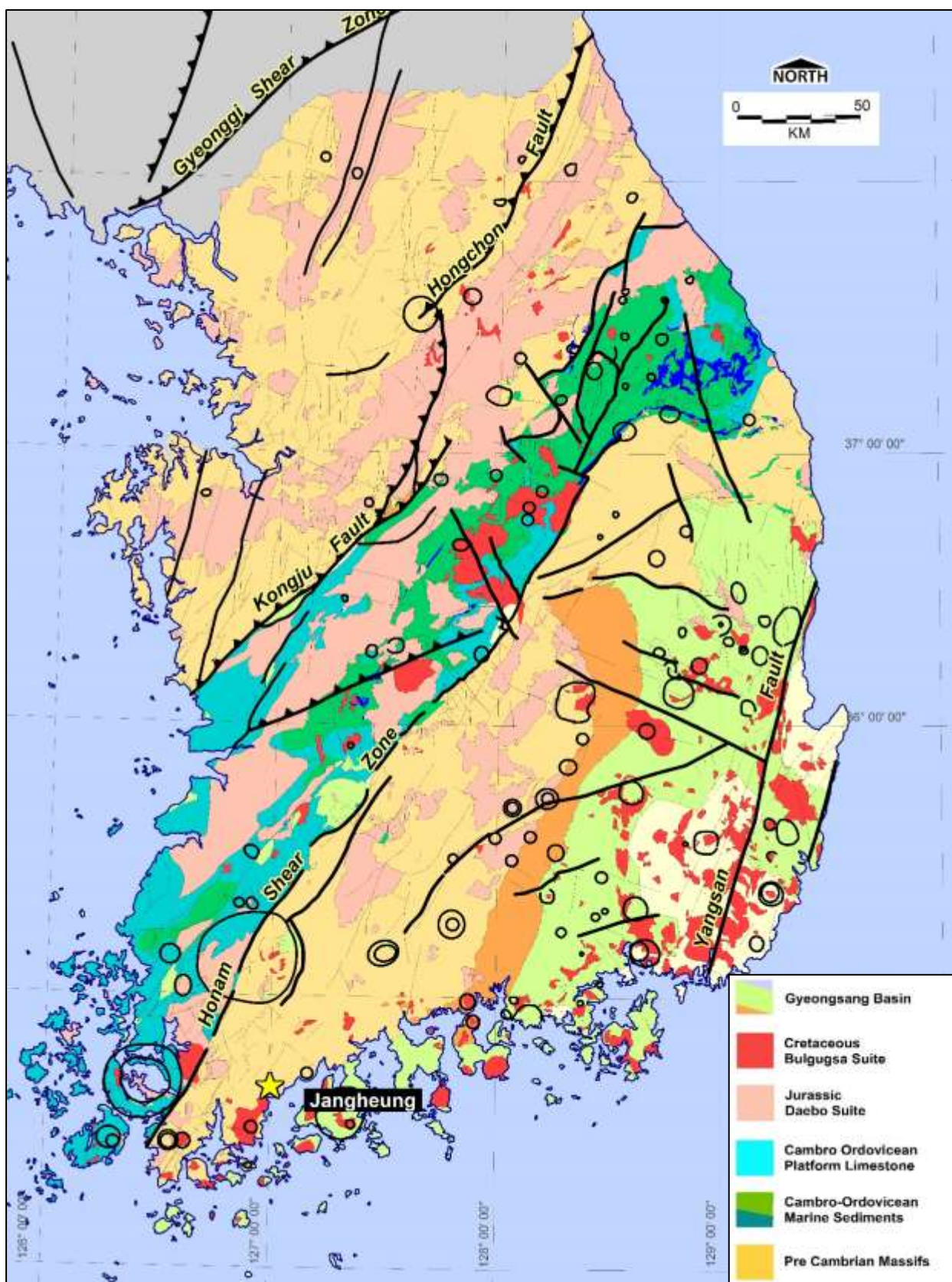


Figure 12. Regional Geological Map of South Korea. The location of the Jangheung Cu-Ag-Pb-Zn Project and the distribution of Jurassic and Cretaceous igneous intrusive complexes are indicated, along with the simplified geology.

## 7.0 STREAM SEDIMENT GEOCHEMISTRY SURVEY

The Korea Institute of Geoscience and Mineral Resources conducted a country-wide stream sediment geochemical survey in 1971 to provide an excellent geochemical background database for the entire country (KIGAMM, 2001). The data is primarily used for lithological characterization and environmental background purposes, but can also be used for mineral exploration purposes.

### Data Processing

The individual map sheets were scanned as JPEG files and registered for use in the *MAPINFO*™ GIS database using control points.

### Sampling Methodology

Stream sediment samples were collected at a density of about 1 sample per 3.5km<sup>2</sup> area on a provincial wide basis. Samples were collected from the active fine sand fractions and sieved in the field to -100# (-150µm) and approximately 70-100g of sample collected. A total of 3,140 stream sediment sites were sampled in Chollanam-Do Province, sufficient for meaningful statistical analysis. Elements analyzed included Ba, Be, CaO, Co, Cr, Cu, Fe<sub>2</sub>O<sub>3</sub>, K<sub>2</sub>O, Li, Mg, Na<sub>2</sub>O, Ni, Pb, Rb, Sr, Ti, V, Zn, Zr, and Ph.

### Statistical Geochemical Colour Plots

Results were statistically treated to determine maximum, minimum, mean, median, standard deviation and frequency on a provincial basis. Anomalous threshold values were determined by the 95% and 99% statistical values and colour-coded for each drainage catchment area (Table below). The colour anomaly plots for each element are presented in the following Figures.

**Table 3. Anomalous Threshold Levels for Selected Elements, Stream Sediment Geochemical Survey.**

Element	99% Percentile (dark brown)	95% Percentile (red-brown)	90% Percentile (orange)
Barium	>2327ppm Ba	1930-2327ppm Ba	1790-1930ppm Ba
Beryllium (eH)	>4.5ppm Be	3.2-4.5ppm Be	2.8-3.2ppm Be
Cobalt	>30.0ppm Co	21.7-30.0ppm Co	19.3-21.7ppm Co
Copper	>63ppm Cu	40-63ppm Cu	35-40ppm Cu
Iron	>10.5% Fe <sub>2</sub> O <sub>3</sub>	9.2-10.5% Fe <sub>2</sub> O <sub>3</sub>	8.4-9.2% Fe <sub>2</sub> O <sub>3</sub>
Lead	>44ppm Pb	29-44ppm Pb	26-29ppm Pb
Magnesium	>2.77% MgO	2.16-2.77% MgO	1.91-2.16% MgO
Manganese	>0.27% MnO	0.18-0.27% MnO	0.16-0.18% MnO
Nickel	>66ppm Ni	44-66ppm Ni	38-44ppm Ni
Potassium	>4.8% K <sub>2</sub> O	4.2-4.8% K <sub>2</sub> O	3.8-4.2% K <sub>2</sub> O
Strontium	>303ppm Sr	222-303ppm Sr	189-222ppm Sr
Titania	>1.65% TiO <sub>2</sub>	1.31-1.65% TiO <sub>2</sub>	1.18-1.31% TiO <sub>2</sub>
Vanadium	>138ppm V	110-138ppm V	97-110ppm V
Zinc	>484ppm Zn	256-484ppm Zn	194-256ppm Zn
Zirconia	>185ppm Zr	145-185ppm Zr	129-145ppm Zr
Acidity (pH)	<5.9 pH	6.3-5.9 pH	6.5-6.3 pH

### Results

The stream sediment geochemical survey identified the following anomalous catchments:

- ❖ Cu, Pb, Zn, Ba, Cr and Ni display anomalies coincidental with streams draining southeast off the Jangheung mineralized breccia pipes. These streams are also weakly anomalous in V and Mn.
- ❖ Streams draining to the west of the diorite porphyry of Sajasan are anomalous in Co, Fe, Ti, Mg, Be, and Sr, and weakly anomalous in Mn.

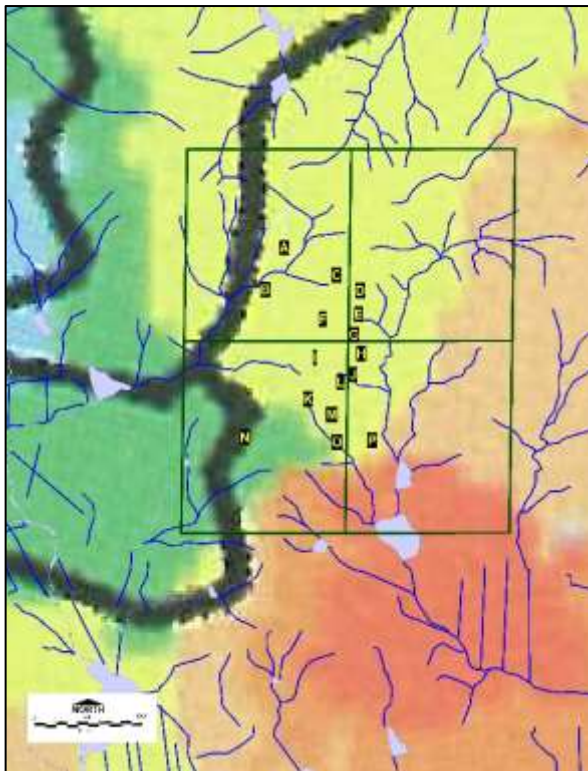


Figure 13a. Cu Stream Sediment Geochemistry.

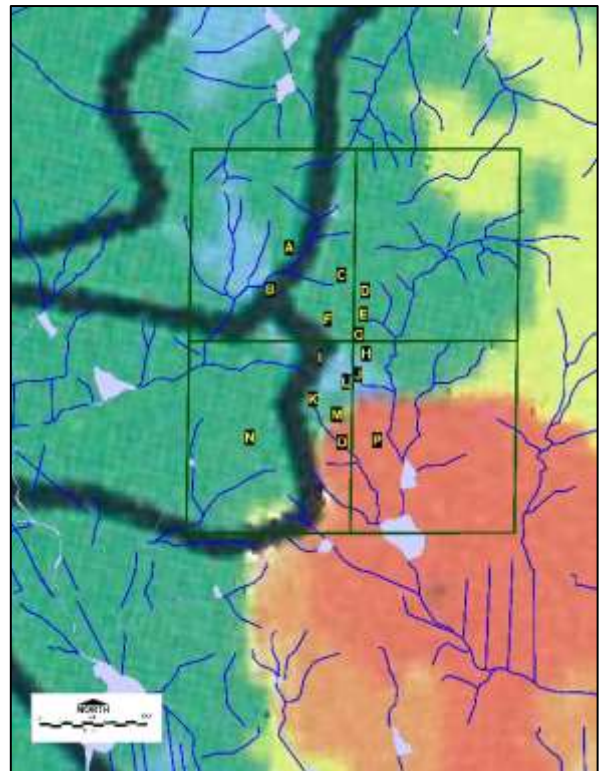


Figure 13b. Pb Stream Sediment Geochemistry.

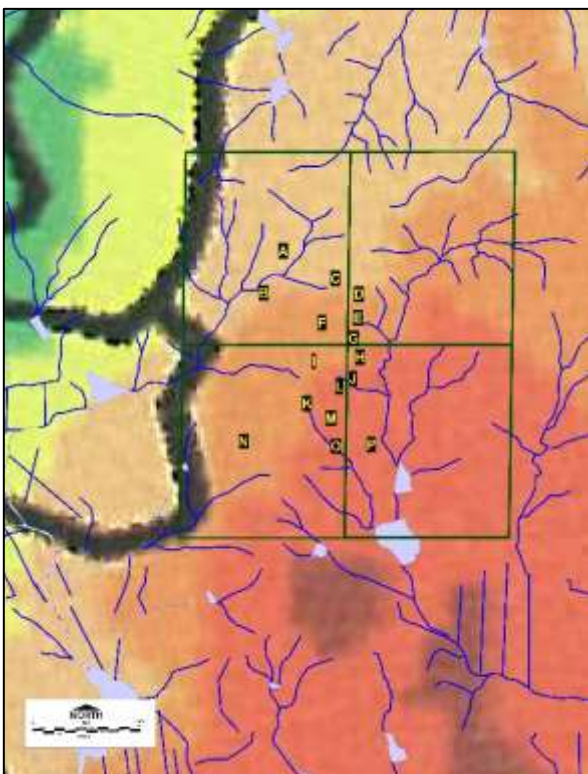


Figure 13c. Zn Stream Sediment Geochemistry.

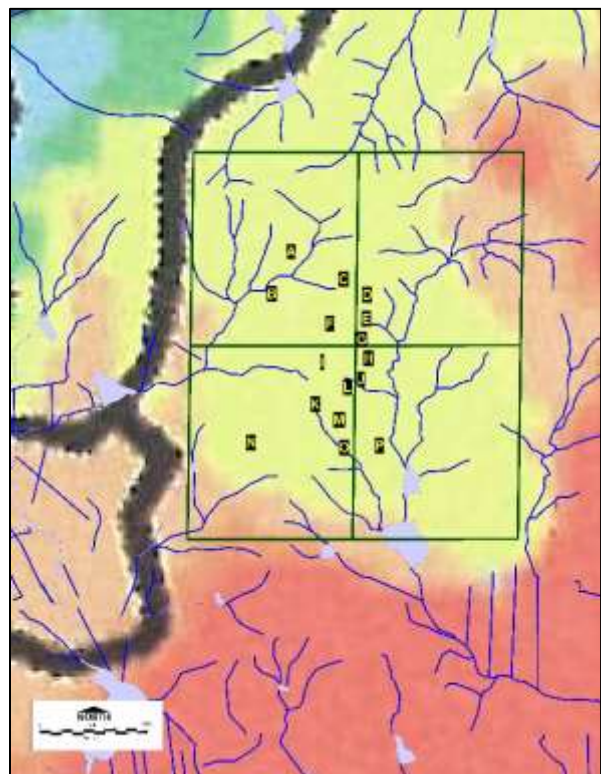


Figure 13d. Ni Stream Sediment Geochemistry.

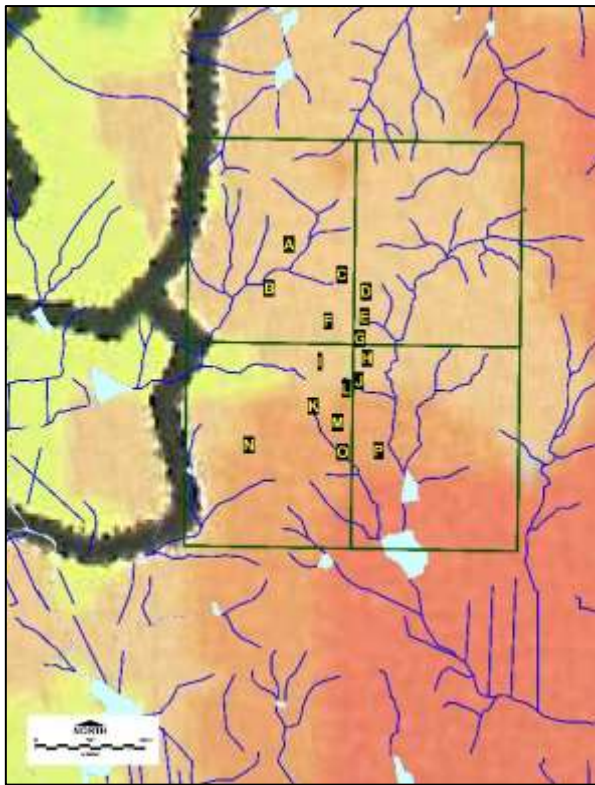


Figure 13e. Ba Stream Sediment Geochemistry.

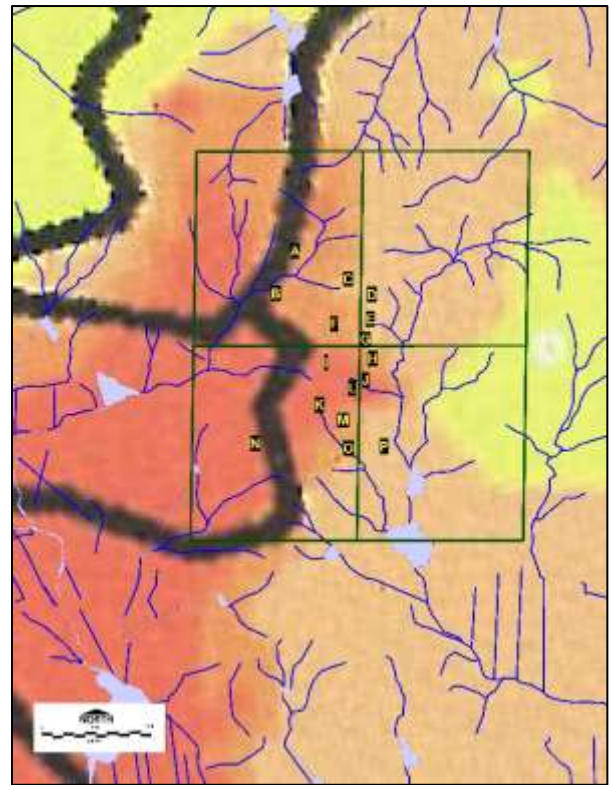


Figure 13f. Fe Stream Sediment Geochemistry.

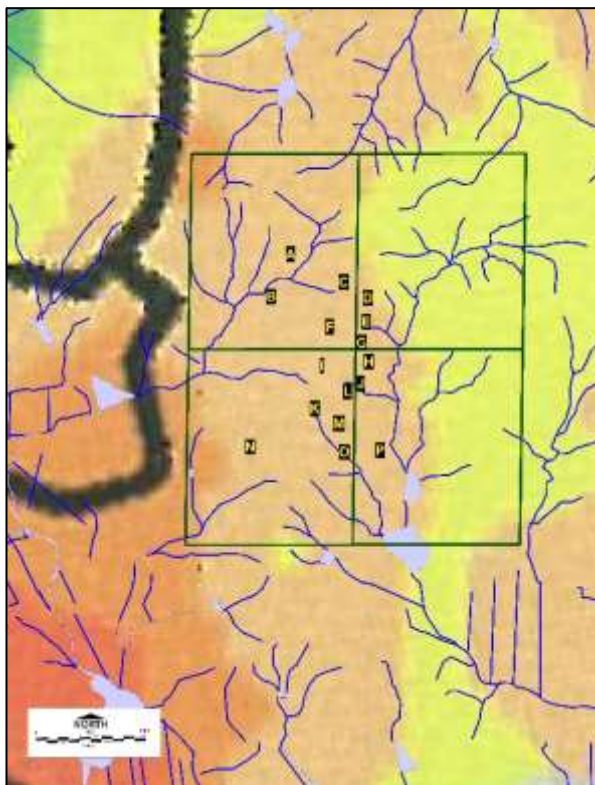


Figure 13g. Co Stream Sediment Geochemistry.

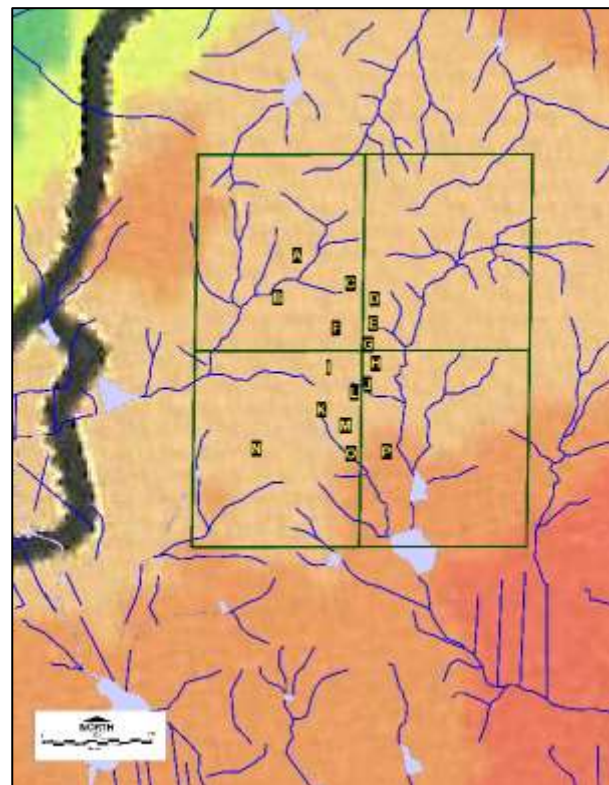


Figure 13h. Cr Stream Sediment Geochemistry.

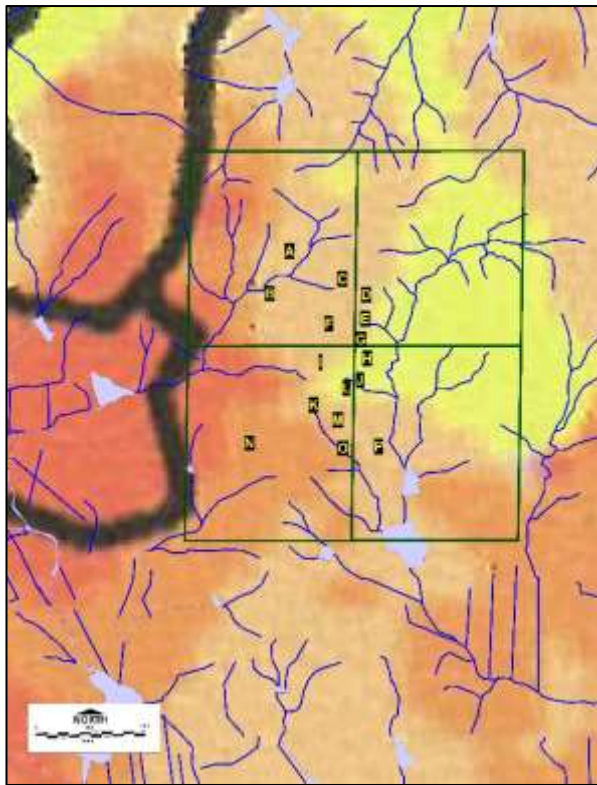


Figure 13i. Mg Stream Sediment Geochemistry.

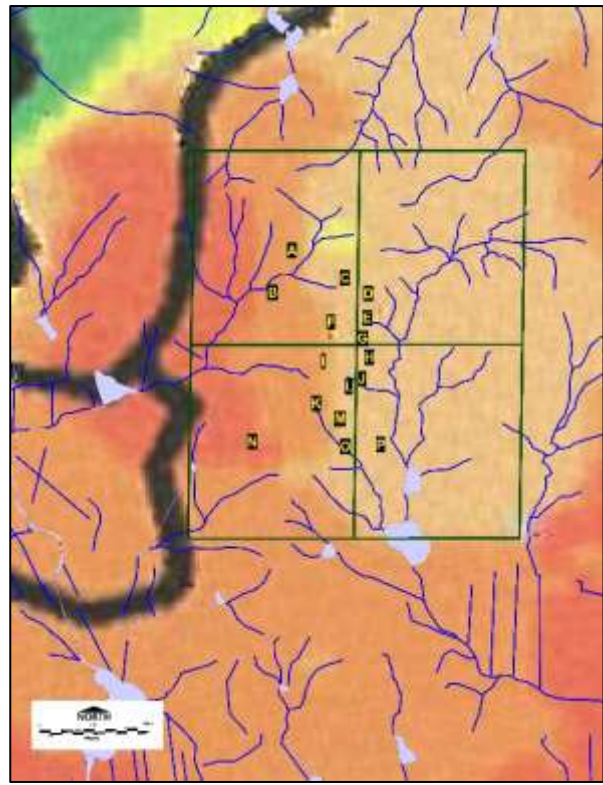


Figure 13j. Ti Stream Sediment Geochemistry.

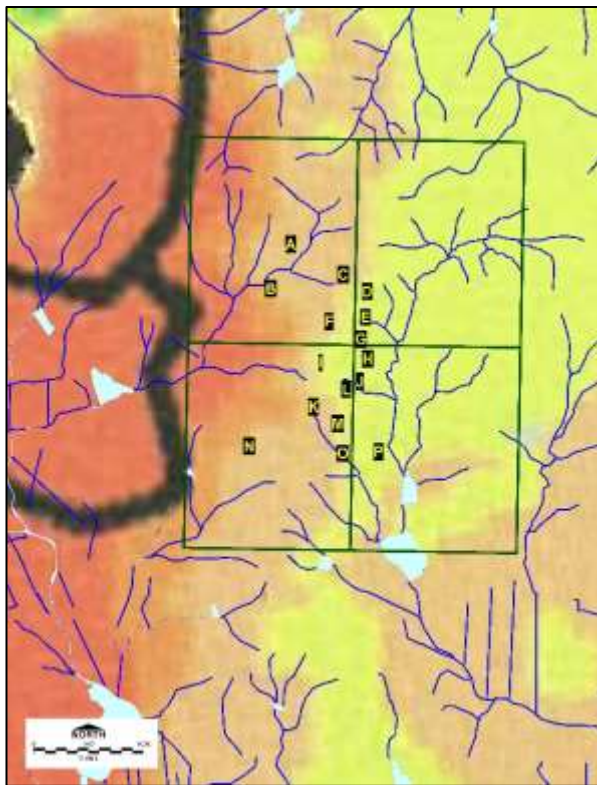


Figure 13k. Be Stream Sediment Geochemistry.

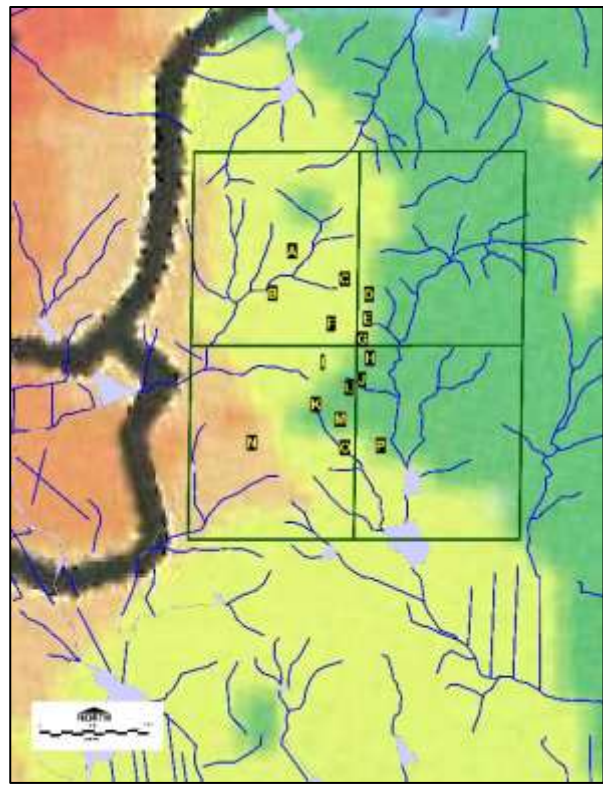


Figure 13l. Sr Stream Sediment Geochemistry.



Figure 13m. V Stream Sediment Geochemistry.

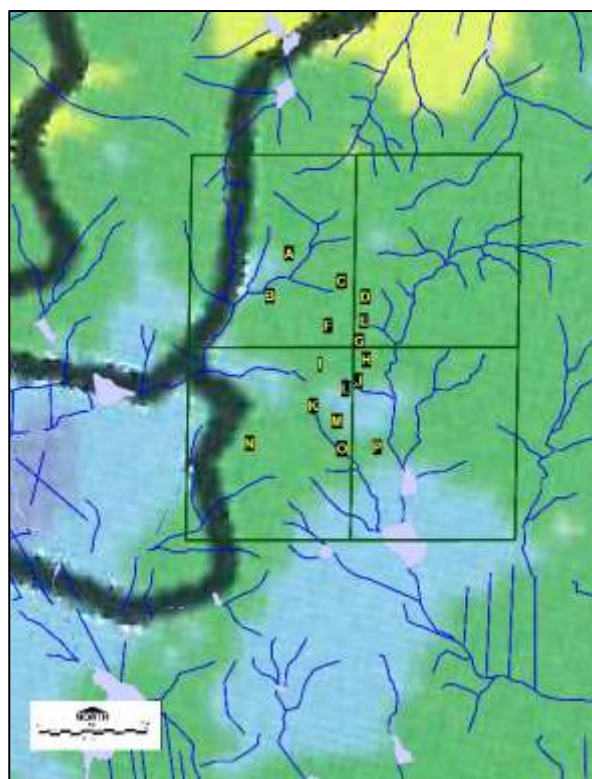


Figure 13n. Zr Stream Sediment Geochemistry.

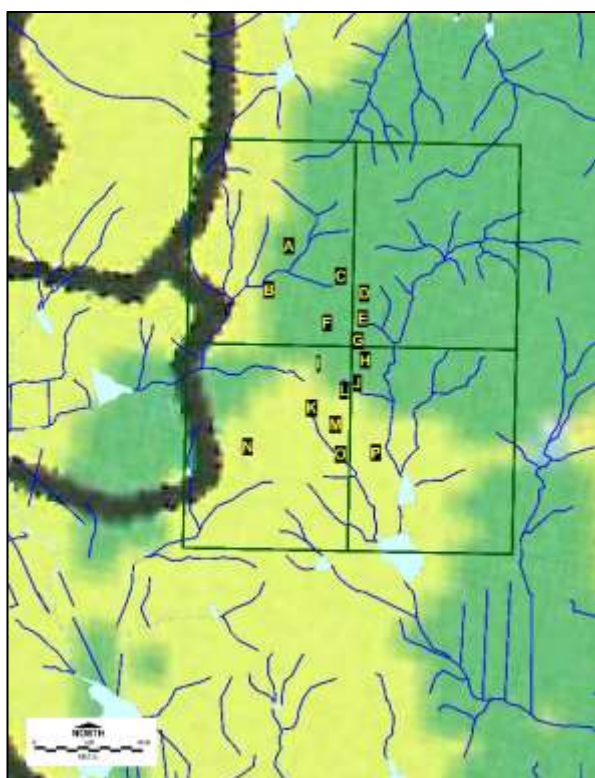


Figure 13o. pH Stream Sediment Geochemistry.



Figure 13p. Mn Stream Sediment Geochemistry.

## 8.0 AIRBORNE GEOPHYSICAL SURVEYS

The *Korean Institute of Geology Mining & Materials* (“KIGAMM”) conducted a combined magnetic-radiometric airborne geophysical survey during 1989-1991 over the Korean peninsula.

### Survey Parameters

The airborne geophysical survey used a BK-117 helicopter flown at a terrain clearance altitude of 120m.

The survey used East-west flight lines flown at a very wide spacing of 1.5km. North-south tie lines were flown at a very wide 8km spacing.

The helicopter was equipped with a *Geometrics G-813* proton precision magnetometer, a *Geometrics G822A* Cesium magnetometer and a GR-800B multi-channel spectrometer (1024 CI). The spectrometer collected data on the Uranium (U), Thorium (Th) and Potassium (K) channels.

### Data Processing

The source airborne geophysical data is not available for purchase from KIGAM and so the published geophysical maps for the 1:50,000 scale Jangheung and Hoecheon map sheets were purchased, including Total Magnetic Intensity (“TMI”), Residual Magnetic Intensity (“RMI”), Total Count, K-channel, U-channel and Th-channel contoured data.

The *Korean Institute of Geoscience and Mineral Resources* subsequently reprocessed the data and produced colour contoured magnetic anomaly maps for the entire country (KIGAM, 2008).

The individual map sheets were scanned as high-resolution JPEG files and then registered for use in the *MAPINFO™* GIS database using control points. *Senlac Geological Services Pty Ltd* then digitized the contours. The digitized contours were then converted to data coordinate points and then processed and manipulated using *SURFER™* software.

The Magnetic Anomaly and Radiometric Channel colour plot maps are presented in the Figures below.

### Airborne Magnetic Survey Interpretation

Interpretation of the Magnetic Anomaly map indicates the following features:

- ❖ A strong magnetic high anomaly of >0nT (peaking at 200nT) closely corresponds to Sajasan and Jeamsan mountains and the distribution of the mapped Cretaceous andesite tuff unit (Yuchon Group equivalent). The andesite tuff forms a cap that sits on top of a diorite porphyry intrusion. It is possible the elevated magnetic response is due to the andesite tuff or the underlying diorite porphyry.
- ❖ A magnetic low anomaly of -200nT coincides with the granite gneiss unit mapped within the Precambrian basement rocks, as well as breccia-pipe outcrops and geochemical anomalies. This magnetic low feature could potentially represent a magnetite-destructive hydrothermal alteration zone.
- ❖ The survey flight line spacing is too wide to define small, subtle magnetic features. A closer-spaced survey of 50m line spacing with continuous readings is recommended for use in mineral exploration to locate the discrete mineralized breccia pipes. A DGPS-controlled Drone UAV is a good platform for this role in the steep terrain and dense thorny scrub vegetation.

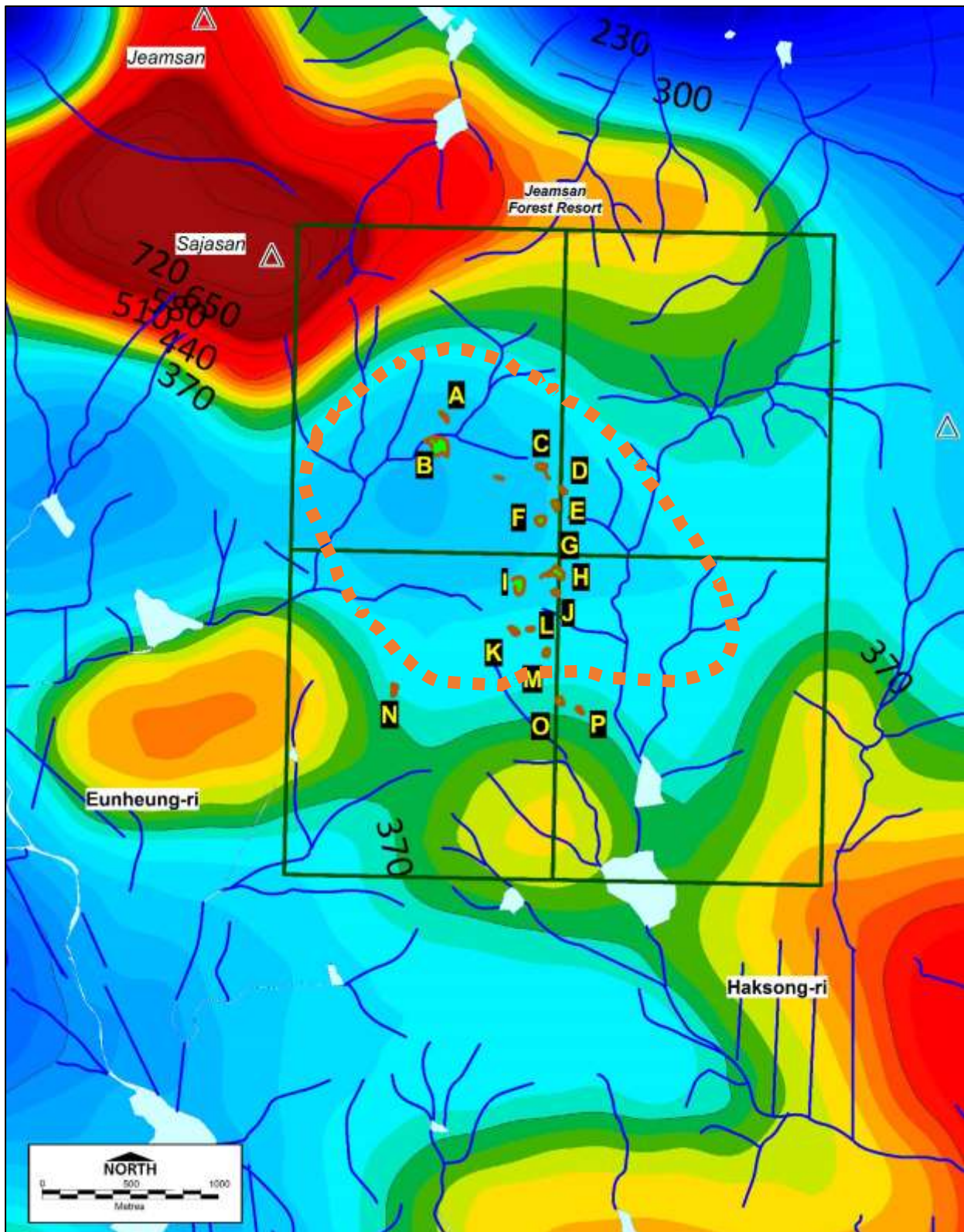


Figure 14. Regional Magnetic Anomaly Map of the Jangheung Cu-Ag-Zn-Pb Project (1:50,000 scale). The prominent magnetic high anomaly developed over Sajasan and Jeamsan corresponds closely to the mapped andesite tuff cap sitting over diorite porphyry. The mapped outcrops of breccias and Soil Geochemical Anomalies (labelled A-P) correspond to a broad magnetic low feature (outlined in brown dashed line) and could possibly indicate a magnetite-destructive alteration zone within the Pre-Cambrian basement gneiss, granite gneiss and schist.

### **Airborne Radiometric Survey**

Interpretation of the K-Channel, U-Channel, Th-Channel and Total Count radiometric geophysical survey maps indicate the following features:

- ❖ The K-Channel image shows a series of anomalous highs that form a broad ring surrounding the magnetic low feature. Potassium-channel anomalies can often reflect potassic or sericite alteration developed in the underlying rocks.
- ❖ The U-Channel image shows 2 anomalies, one anomaly orientated NNE in the south and another to the southwest, orientated E-W. The southwestern anomaly corresponds to mapped granite gneiss.
- ❖ The Th-Channel image shows a coherent large anomaly, roughly orientated NNE, that coincides with the topographic high ridge. This anomaly corresponds well to the mapped granite gneiss. The breccia pipes appear to be distributed/surround the highest peak response/core of this anomaly.
- ❖ The Total Count image shows a large anomaly that coincides with mapped granite gneiss.
- ❖ A deep radiometric anomalous low response from all Channels is present over Sajasan and Jeamsan, clearly corresponding to the mapped andesite tuff unit.

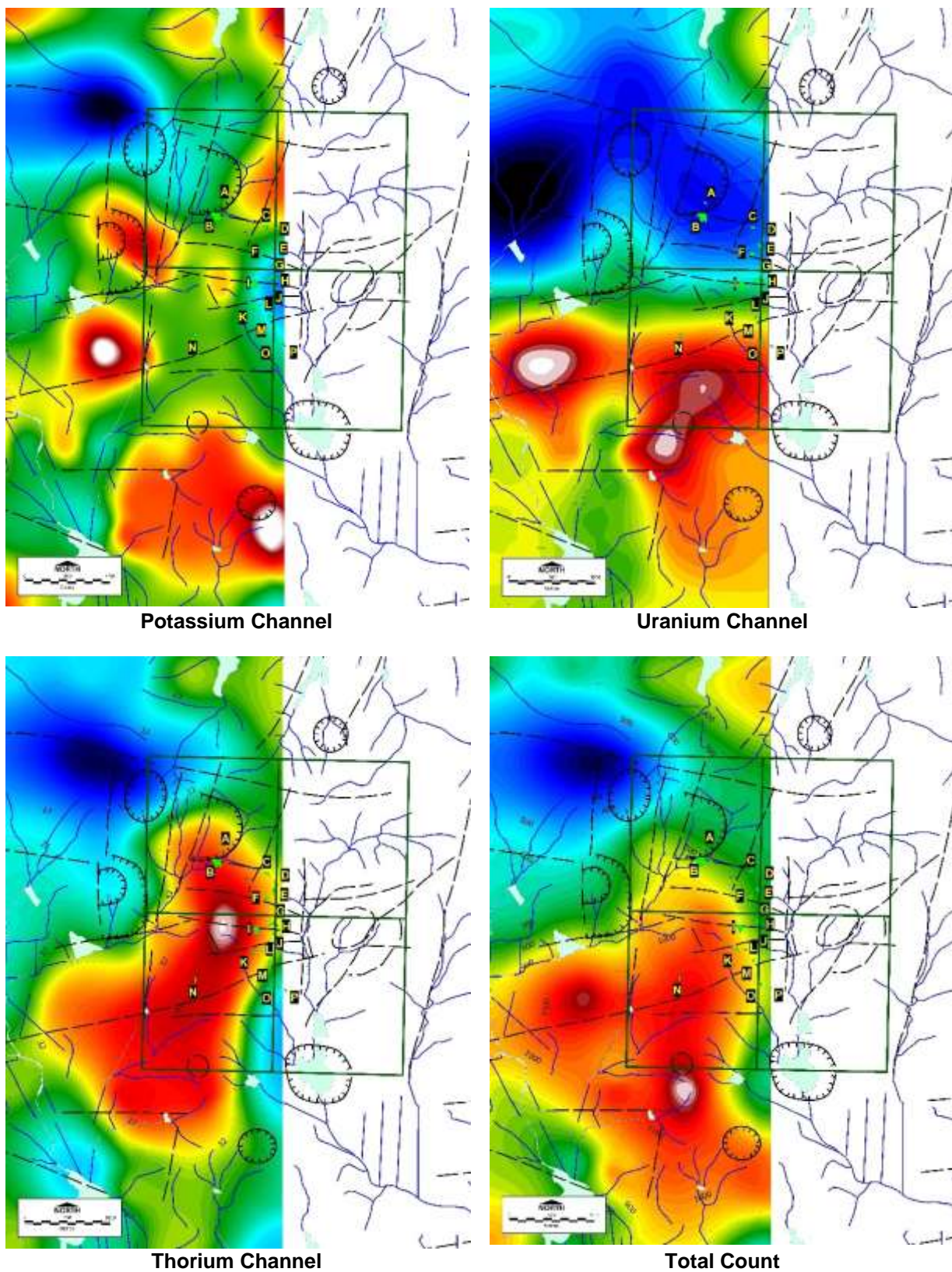


Figure 15. Radiometric Channel Response Maps of the Regional Geophysical Survey over the Jangheung Cu-Ag-Zn-Pb Project (1:50,000 scale Jangheung Sheet). Note the radiometric data for the Hoechong Sheet was unavailable.

## 9.0 PROSPECT GEOLOGY

### 9.1 PROSPECT GEOLOGY

The Jangheung Cu-Pb-Zn-Ag project is situated within the Suncheon Metallogenic Province of Choi et al (2006). The *Atlas of Mineral Resources – Republic of Korea*, compiled by the United Nations (ESCAP, 1987) lists the Jangheung deposit as Cu mineral occurrence No 1 and Pb-Zn mineral occurrence No 40.

Geological prospecting and mapping surveys (KIER, 1982) conducted during 1977-1979 located 5 outcrops of mineralized breccia, which KIER identified as Areas A, B, C, D and F. Subsequent soil geochemical and geophysical exploration and drill testing located another 10 anomalies which were confusingly labelled A-P, with differing identification labels. In order to avoid ongoing confusion, the soil anomaly labels are identified in this report as Areas A, B, C, D, E, F, G, H, I, J, K, L, M, N and P and the original breccias were re-labeled to correspond to the soil anomaly nomenclature.

#### Precambrian Basement

The basement rocks of the Jangheung area are composed of gneiss, granite gneiss and schist of the Precambrian Sobaegsan Massif (Lee, 1987). The regional foliation trend displays a reasonably consistent NE strike, with moderate dips to the NW.

Granitic gneiss is mapped as a NNE orientated block in the Jangheung prospect area. The granite gneiss displays strong porphyroblastic textures, formed by rounded quartz, plagioclase and k-feldspar grains. A weak-moderately developed foliation is developed, formed by aligned biotite mica flakes and crude elongation of the porphyroblasts.

Petrological study of the granite gneiss by KIER (1982) indicate myrmekitic quartz vermicule texture is commonly developed within the plagioclase (albite) grains, suggesting replacement of primary K-feldspar by plagioclase and quartz vermicules has occurred. This feature is interpreted as indicating a constant Na/Ca composition was present within the calcic plagioclase, which released enough silica for the myrmekite quartz vermicule structures to form. The metamorphic textures and mineralogy are consistent with recrystallization of an original granitic precursor.

Plagioclase feldspar has been altered to a “saussurite assemblage”, comprising zoisite, chlorite, amphibole, and carbonates. This suggests residual fluids present during the late stages of magmatic crystallization have reacted with previously formed plagioclase feldspar to form saussurite near its outer margin. The plagioclase may be reconstituted into a more sodium-rich variety (albite). Later hydrothermal alteration can produce the same result. The process commonly takes place during the low-grade regional metamorphism of mafic rocks which contain Ca-plagioclase as an essential component.

Recent studies by Song et al (2015) have obtained a much younger age of 250Ma (Early Triassic) for the granite gneiss basement rocks, located northeast of Jangheung (*Sobaegsan Gneiss*). The younger age date obtained by Song et al (2015) could be attributable to recrystallization of much older basement rocks during the widespread *Songrim Orogeny M3* regional metamorphic event, recorded throughout the Korean Peninsula during the Triassic between 252-220Ma (Kim et al, 2008; Ree et al, 2008). The *Songrim Orogeny M3* coincides with compression and continental collision along the *Qinling-Dabie-Sulu Collisional Belt* between the *North China* and *Yangtse Blocks* (Kwon et al, 2009) and the Circum-Pacific Plate (Egawa & Lee, 2009).



**Photograph 9. Outcrop of sericite-argillic clay altered, decomposed granite gneiss located along a track near Anomaly K. Gently-dipping foliation ( $060^{\circ}/10^{\circ}$ ) and weak quartz veinlet-fracturing is evident in the outcrop, along with some jarosite-limonite staining. Sample 243429.**



**Photograph 10. Cut slab of coarse-grained porphyroblastic granite gneiss, with dark biotite micas, quartz, white plagioclase and pink k-feldspar grains. Plagioclase feldspar has been altered to zoisite, chlorite, amphibole and carbonate (saussurite assemblage). Limonite staining. Sample no 243428.**



Photograph 11. Cut slab of coarse-grained porphyroblastic textured granite gneiss. Myrmekitic quartz vermicule texture is commonly developed within the plagioclase (albite) grains. Sample no 243284.

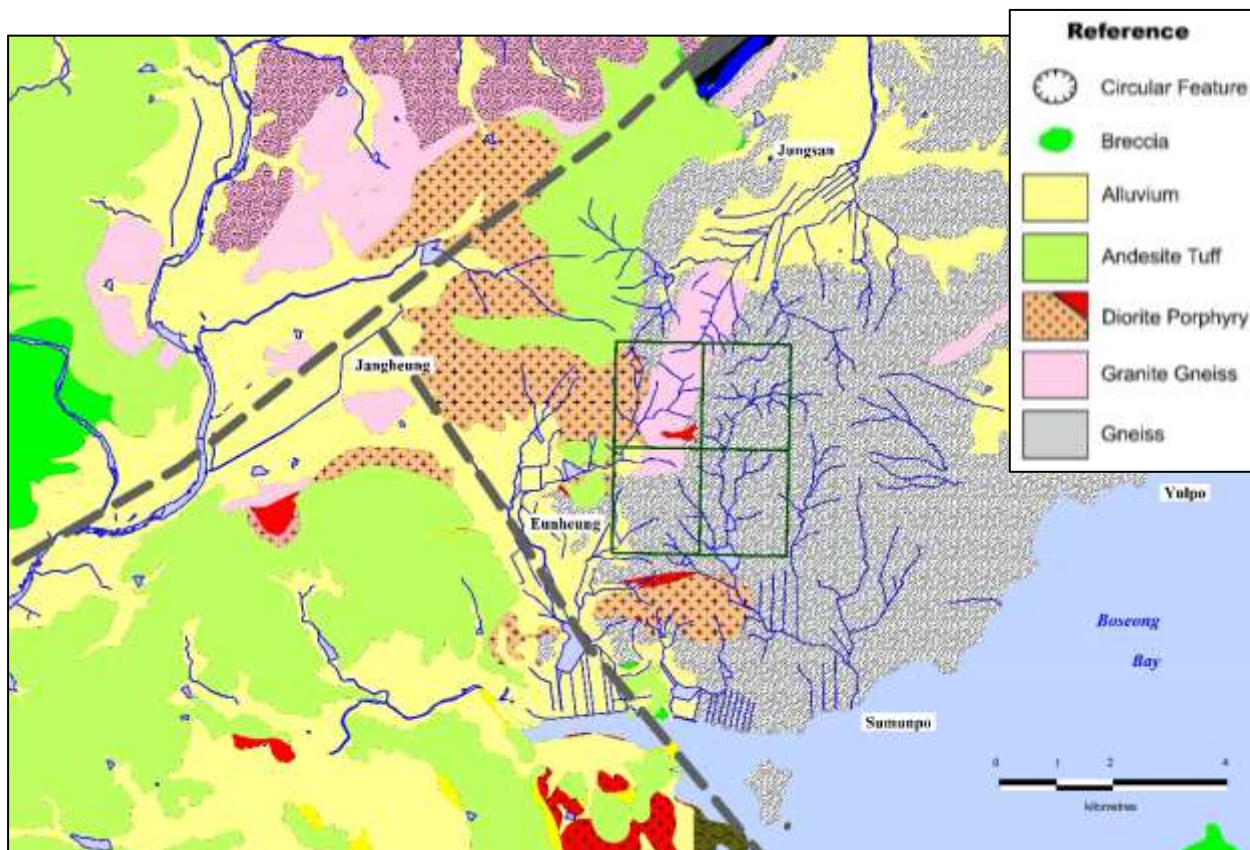


Figure 16. Regional Geology Map, Jangheung project. The Cretaceous diorite porphyry intrusion and andesite volcanics appear to be localized and emplaced along an older NW structure at its intersection with a major NE transfer fault structure.

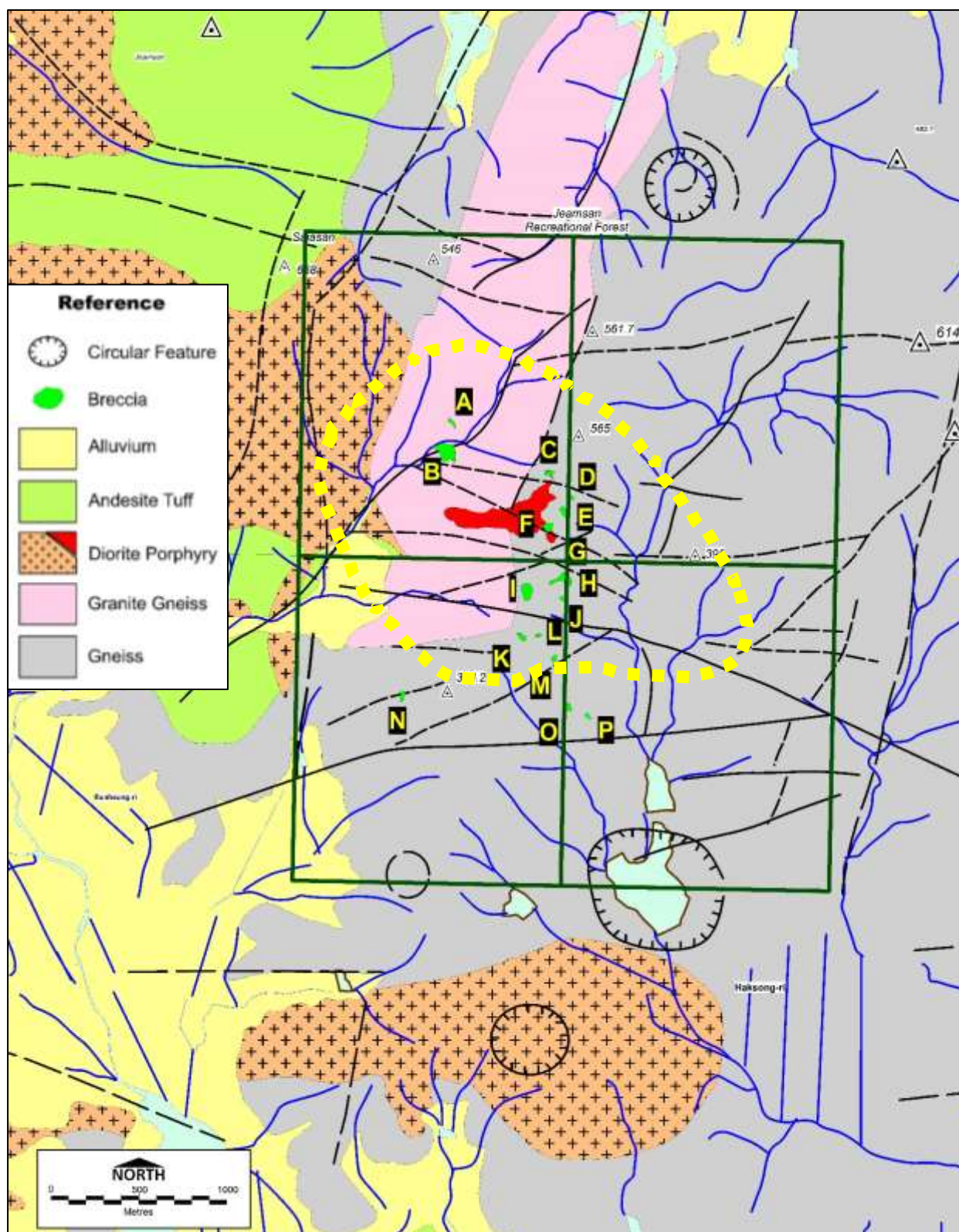


Figure 17. Geological Map of the Jangheung Cu-Ag-Zn-Pb Project (1:50,000 scale). The mapped breccia pipes are highlighted in green and Anomalies A-P are labelled. Linear and circular structures interpreted from satellite imagery are shown. The broad magnetic low feature (yellow dashed line) could possibly indicate a magnetite-destructive alteration zone within the Pre-Cambrian basement gneiss, granite gneiss and schist. A diorite porphyry intrusion is mapped in the core of this magnetic low feature.

### **Cretaceous Bulgugsa Series Diorite Porphyry**

At Sajasan, diorite porphyry is mapped as intruding the Precambrian granite gneiss basement and small dykes of diorite and andesite porphyry are present near some of the breccia outcrops. In a regional sense, the diorite porphyry intrusion has been emplaced along an older NW structure, localised at its intersection with a major NE transfer fault structure.

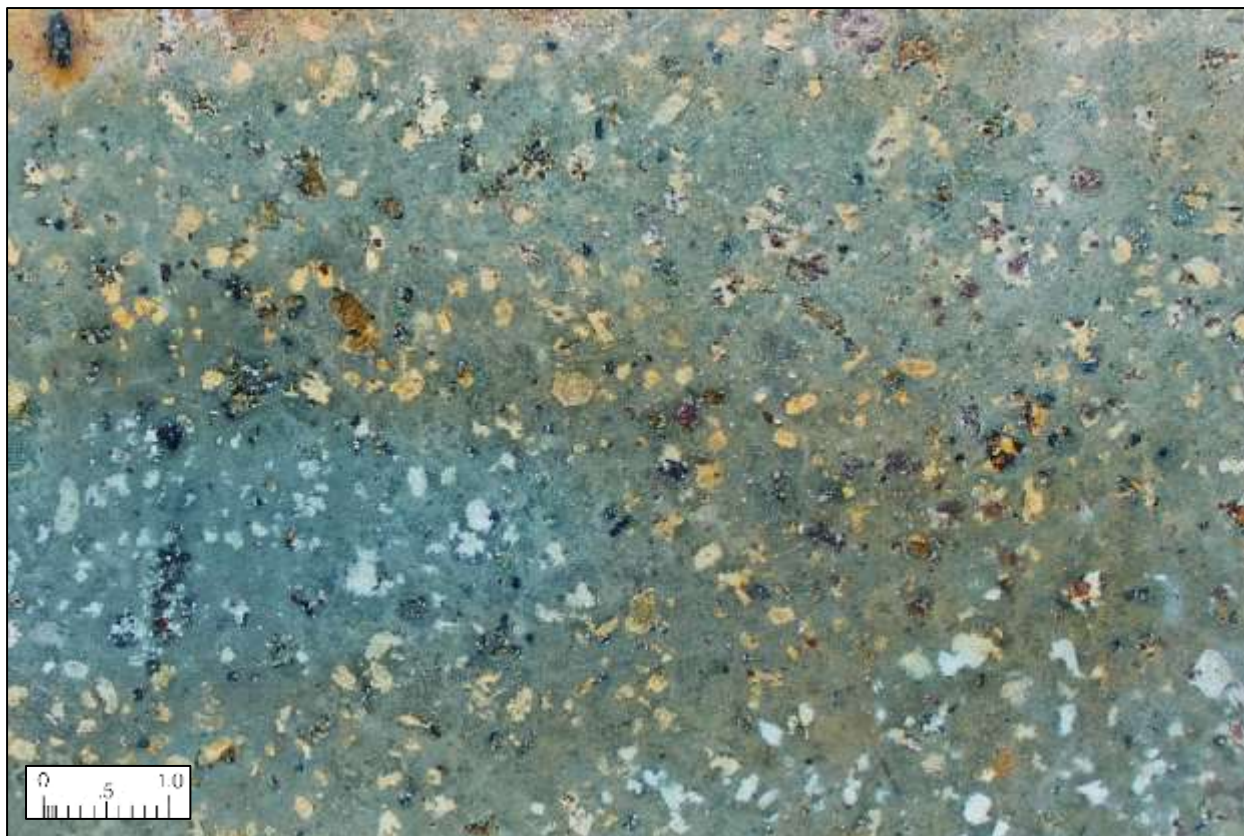
The diorite is composed mainly of oligoclase, hornblende, biotite and quartz, accompanied by minor calcite and magnetite.

Interpretation of the petrochemical characteristics suggest the diorite porphyry was emplaced in a compressional regime at a continental margin, during subduction of the proto-Pacific plate beneath the Eurasian plate and probably represents a more evolved, fractionated I-type intrusive phase (Soo et al, 2005).

During the late Jurassic to early Cretaceous, southern Korea was a continental margin of Andean type before the opening of the Sea of Japan. During the Cretaceous, extensional tectonism of this magmatic arc resulted in the emplacement of the *Bulgugsa Granite Series* intrusive rocks as stocks, plugs and dykes throughout the Korean Peninsula along orthogonal transfer fault structures.



**Photograph 12. View of Sajasan peak (668masl), The bare rocky bluffs are composed of diorite-andesite porphyry. The vertical flow banding evident in the outcrop is suggestive of a flow dome intrusion.**



**Photograph 13. Cut slab of diorite porphyry. Angular grains of plagioclase, argillic altered and leached mafics & sulphides are set in a fine dark grey matrix. Sample no 243417.**

### **Cretaceous Andesitic Volcanics**

Late Cretaceous age andesite tuff, pyroclastics and volcanic breccia outcrop on the higher elevations, resting as a cap over basement gneiss and diorite porphyry. The unit is best developed at Jeamsan and the surrounding ridges.

Abundant xenoliths of fine-grained sediments are incorporated within the tuff within a densely packed, poorly sorted mass of inequigranular grains of feldspar, quartz and mafics.

The andesite tuff probably represents the “surge” eruptive product phase associated with the *Bulgugsa Series* igneous activity (equivalent to *Yuchon Group*).



Photograph 14. Outcrop of gently dipping andesite tuff and pyroclastic breccia cap forming the peak at Jeamsan. The outcrop displays prominent subvertical jointing. The vegetation is noticeably sparser and soil cover thinner on the peaks and ridges.



Photograph 15. Cut slab of blue-tinged uralite (deuteric alteration) and chlorite altered porphyritic andesite tuff. Sample no 243425. Abundant xenoliths of fine sediments are evident (dark grey clasts) within a densely packed, poorly sorted mass of inequigranular grains of feldspar, quartz and mafics.

### Breccia Pipes

A “cluster” of sixteen (16) base metal breccia pipes have been identified at Jangheung by mapping and soil sampling (KIER, 1982) and are referred to sequentially as Anomalies A to P. The pipes were discovered in the late 1970s by follow up prospecting of regional stream sediment geochemical anomalies, mainly by tracing mineralized breccia talus scree in creeks back uphill to their source outcrops.

The 16 breccia pipes occur as small outcrops, subcrop scree and talus, distributed sporadically over an area of 2000m x 740m that is roughly orientated NNW in a crude sense. Because of the nature of the terrain, scree cover, and dense secondary thorny “gashin” vegetation making ground traversing difficult, there is an expectation that there could be other pipes remaining undetected in the area.

### Clasts

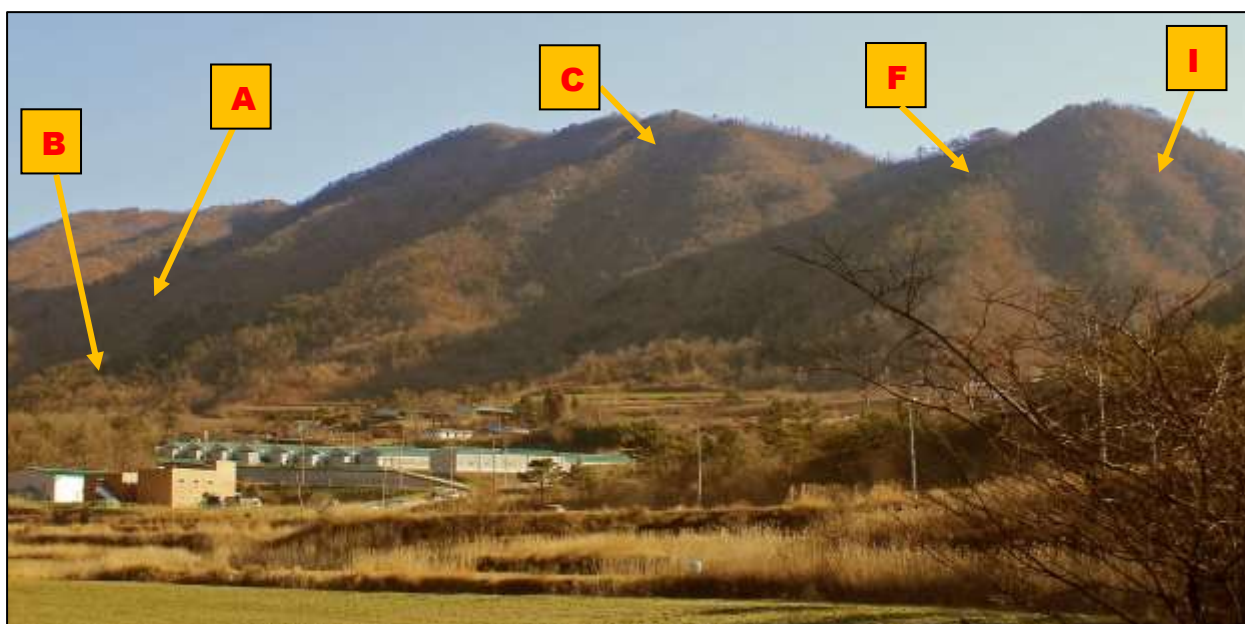
The breccia pipes are composed of variably-sized, sub-rounded, sub angular to angular clasts and fragments of diorite porphyry and basement gneiss and schist (Spadafora, 1994). Most of the breccia clasts are porous, angular and apparently corroded. The angularity of most clasts and fragments, suggests fluidized “streaming” movement, fragment attrition or abrasion did not occur.

Sillitoe and Sawkins (1971) suggest that clast-fragment corrosion occurs mainly in the upper portions of these pipes. The more abundant open-space voids and corrosion observed in the upper levels of the pipes are interpreted to be the result of gaseous volatiles preferentially concentrating towards the top of the breccia pipe column.

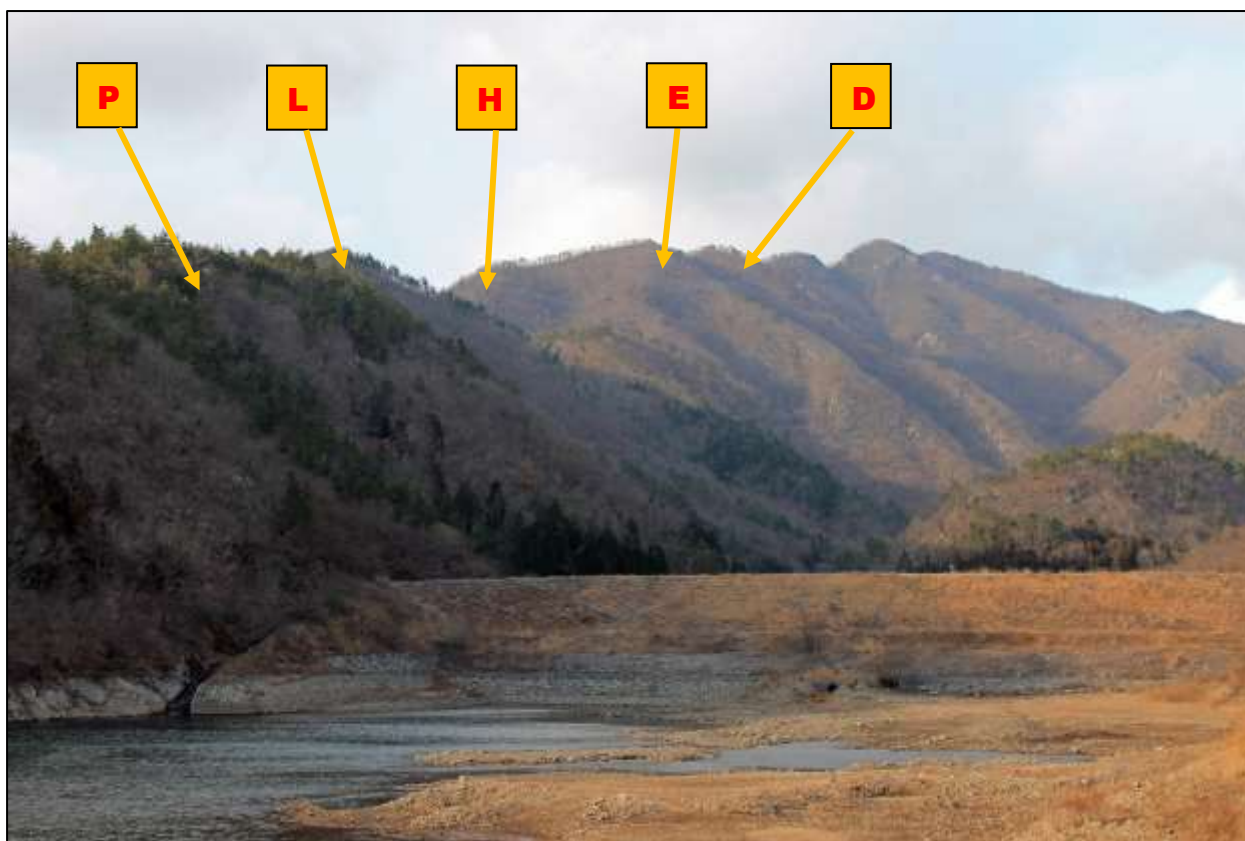
Some of the larger porphyry clasts tend to be more rounded and display a zoned alteration pattern. The inner core of these clasts is relatively unaltered and a primary igneous texture is still discernable. This core is surrounded by an inner halo of epidote-chlorite-quartz alteration (inner propylitic assemblage). This zone then grades into a halo of chlorite-epidote-sericite alteration (propylitic) and then into an outer rim or rind of sericite-quartz-sulphide (phyllic assemblage). The presence of these rounded clasts is attributed by Sillitoe and Sawkins (1971) to be due to spalling off of the softer, hydrothermally altered rims during collapse of the breccia pipe column, rather than resulting from abrasive milling effects produced by “streaming” or rapid/prolonged movement.

### Matrix

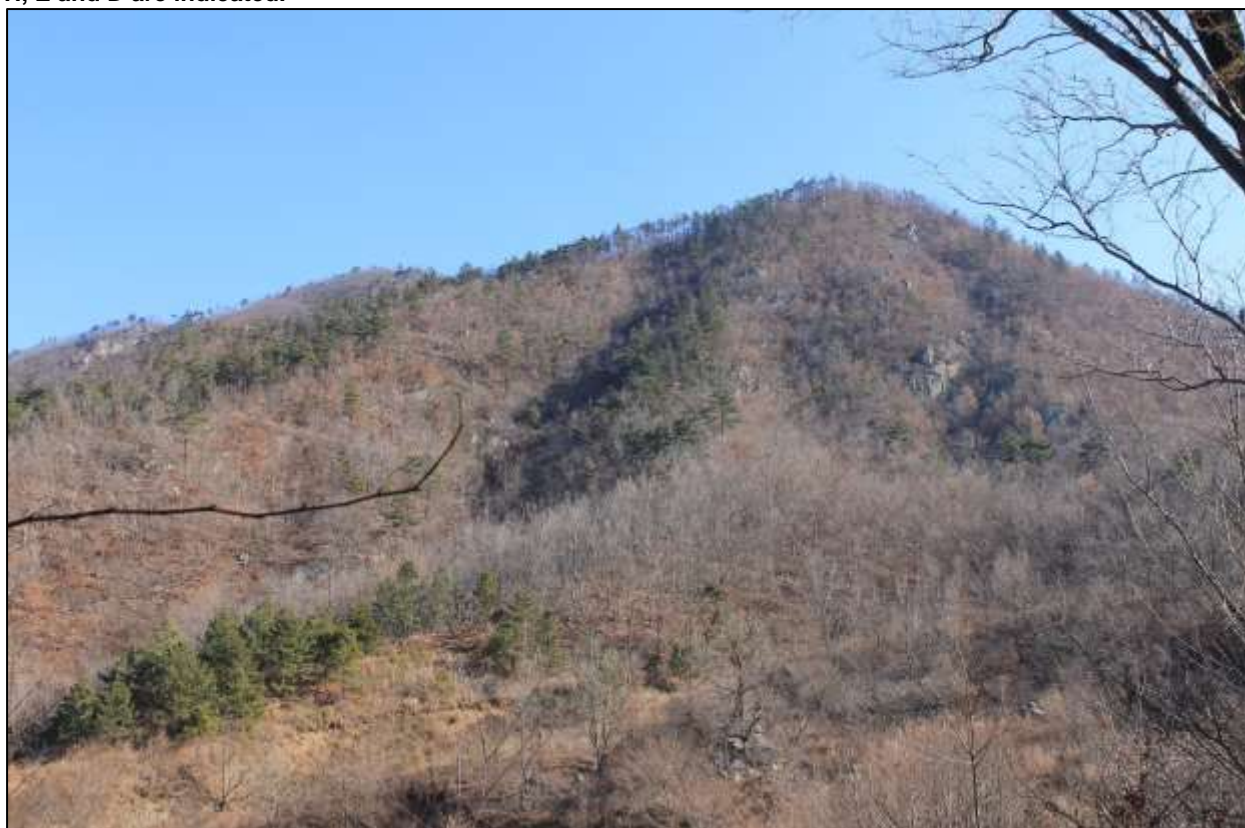
The matrix of the breccia is composed of a vughy, porous cement made up of quartz, chlorite, clay, specular hematite and secondary minerals that have replaced primary sulphides (Spadafora, 1994). There is a noticeable lack of rock flour in the matrix. The scarcity of rock flour and the angularity of most clasts-fragments, suggests fluidized “streaming” movement, fragment attrition or abrasion has played a relatively minor role.



Photograph 16. View looking northeast from the Eunheung-ri road over the feedlot-agricultural factory complex towards the hills beyond. The locations of the breccia zones at Soil Geochemistry Anomalies B, A, C, F and I are indicated.



Photograph 17. View of the reverse side of the above photograph, looking northwest from the dam upstream from Haksong-ri village, towards the breccia zones on ridges. Breccia pipe-Soil Geochemistry Anomalies P, L, H, E and D are indicated.



Photograph 18. View looking east towards the breccia outcrops of Anomaly I.



Photograph 19. Outcrop of leached, gossanous, vughy hydrothermal breccia at Anomaly I.



Photograph 20. Outcrop of mineralized gossanous hydrothermal breccia at Anomaly I, showing cockscomb quartz lined breccia clasts, with secondary replacement minerals (after sulphide) infill of matrix and some open cavities. Sample no 243423 (8g/t Ag, 0.13% Cu, 0.30% Pb & 0.14% Zn).

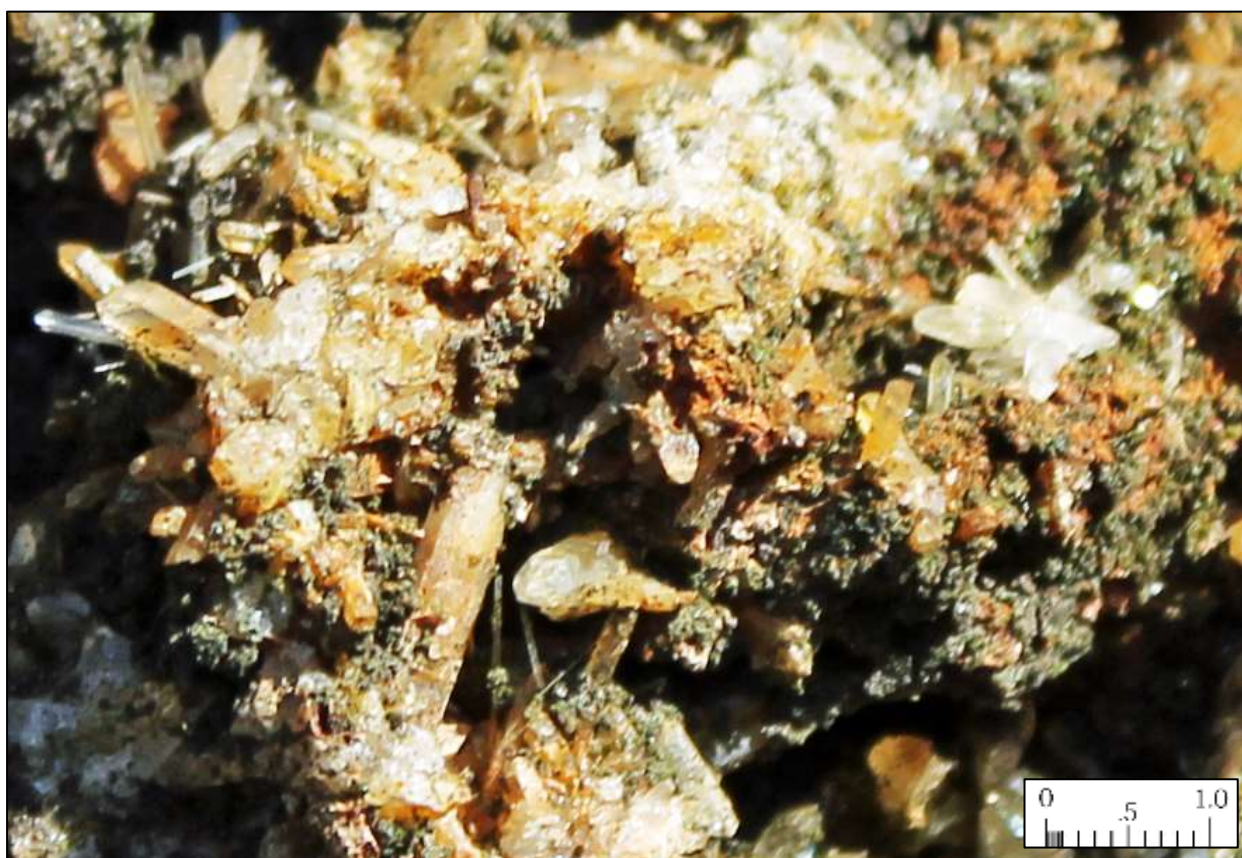
## 9.2 MINERALIZATION

Primary sulphides are only rarely observed in surface outcrops or talus scree, being typically evident only in drill core (KIER, 1982). The primary sulphides have been replaced by secondary minerals in the supergene, oxidized weathering zone. The primary sulphide minerals identified by KIER (1982) in drill core consist of pyrite, sphalerite, galena, chalcopyrite and arsenopyrite.

The cavities/vughs between the breccia clasts are often lined with cockscomb and comb quartz crystals, exhibiting well-formed prismatic grains, suggesting a relatively gaseous-rich, fluidized hydrothermal breccia mineralizing event took place.

Goethite-limonite-hematite-jarosite gossan is common in the breccias and fracture stockworks, and is accompanied by a diverse mix of supergene secondary minerals, including adamite (zinc-arsenic hydroxide), cerussite (lead carbonate), anglesite (lead sulphate), smithsonite (zinc carbonate), black “sooty chalcocite” (copper sulphide), covellite (copper sulphide), chrysocolla (hydrated copper silicate), azurite (copper carbonate), malachite (hydrated copper carbonate), cuprite (copper oxide) and native copper (KIER, 1982).

The abundance of secondary minerals suggests supergene weathering, thermal oxidation, hypogene leaching, or other telescoping “overprinting” effects occurred during the late stages of the brecciation and hydrothermal mineralization process.



Photograph 21. Prismatic quartz and uralite crystals partially infilling vugh in breccia at Anomaly I. Uralite is common low-temperature alteration mineral replacement of pyroxene (actinolite) that forms during crystallization of a magma.

### 9.3 ROCK CHIP GEOCHEMISTRY

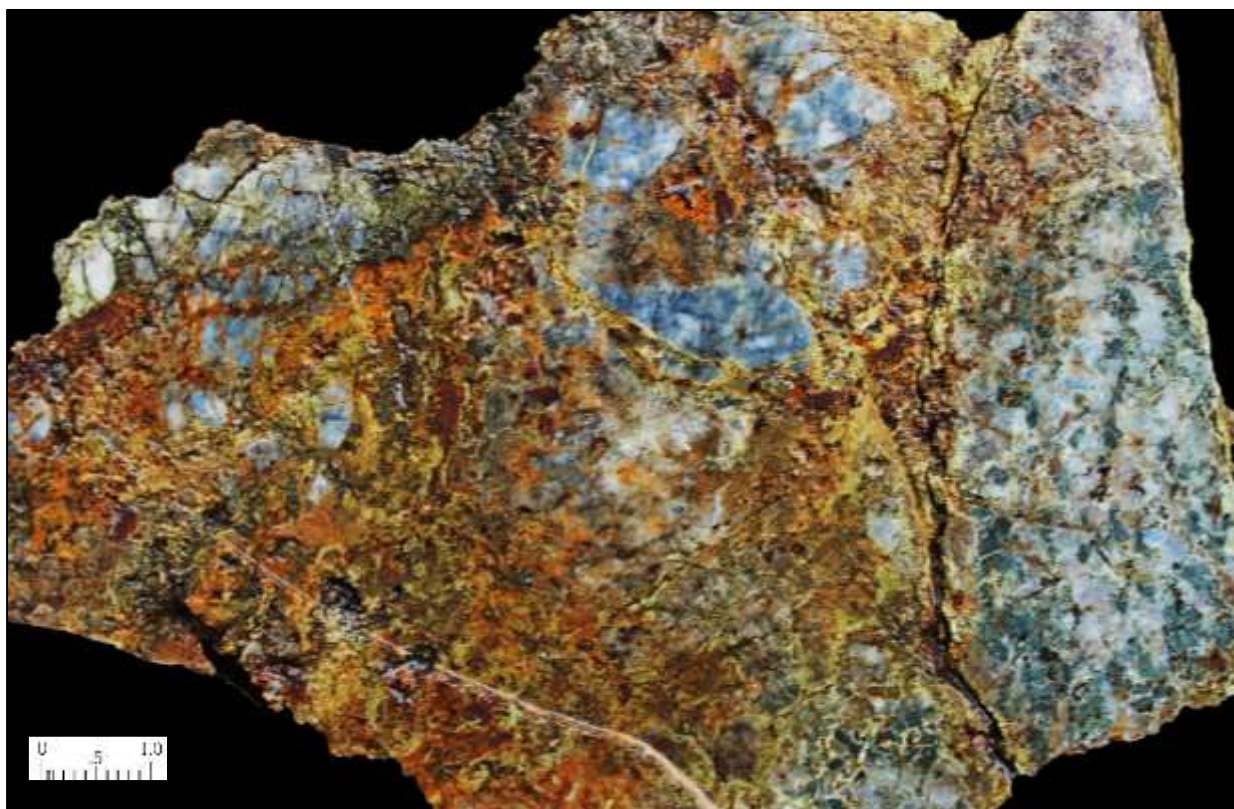
Historical rock chip sampling by Spadafora (1994) was undertaken on behalf of *Indochina Goldfields Ltd.* Five (5) samples were collected from Anomaly E recorded maximum assays of 4.85% Cu, 6.28% Pb, 9.27% Zn, 932g/t Ag and 0.06g/t Au. This silver assay result is exceptional and significant, as historical sampling by KIER (1982) makes little mention of silver assays apart from a metallurgical sample which assayed 143g/t Ag.

During the site visit to Jangheung by *Senlac Geological Services Pty Ltd* in January 2016, a total of 26 rock chip samples were collected from surface outcrops. Rock chip sample descriptions and assay results are presented in Appendix II. The samples were dispatched via *DHL Air Courier* to *Australian Laboratory Services* laboratory in Brisbane for analysis (BR16033324).

The highest assay results recorded were 172g/t Ag, 0.13% Cu, 0.31% Pb, 0.23% Zn and 0.26% As for the principal elements, with other anomalous elements including 0.25% Ba, 61ppm Bi, and 48ppm Mo. Analysis of the rock chip samples show the anomalous thresholds for the main elements are 8g/t Ag, 150ppm As, 10ppm Bi, 300ppm Cu, 5.0% Fe, 5ppm In, 0.1% Mn, 30ppm Mo, 400ppm Pb and 500ppm Zn.

The tenor of the surface rock chip base metal assay results do not compare well with the drill intersection results reported by KIER (1982), suggesting some depletion (particularly in zinc) may have occurred in the surficial oxidized weathering regime and the underlying supergene zone.

All the rock chip analyses confirm the presence of significant silver grades associated with the base metal mineralization. Further confirmation of significant silver values is also provided in the historical bulk metallurgical sample collected from Anomaly E by Hwang and Yang (1977) which assayed 143g/t Ag. Unfortunately, the drill core from the historical drilling program was not analyzed for silver.



Photograph 22. Sample of breccia collected from exposure on old track, located mid-way between Anomaly B and Anomaly E. The breccia consists of subrounded-subangular corroded clasts of granitic gneiss, set in a yellow-orange-brown coloured, jarosite-goethite-limonite matrix cement, which has likely replaced original epidote and sulphides. It is uncertain if this breccia is a manifestation of another pipe, or is a fault-breccia structure as suggested by coincidental anomalous Cu-Pb soil geochemistry. Sample 243276; 172g/t Ag, 273ppm As, 0.13% Cu, 9.44% Fe, 0.22% Pb, 55ppm Sn, 1.45ppm Te, 54 ppm U and 107ppm V.

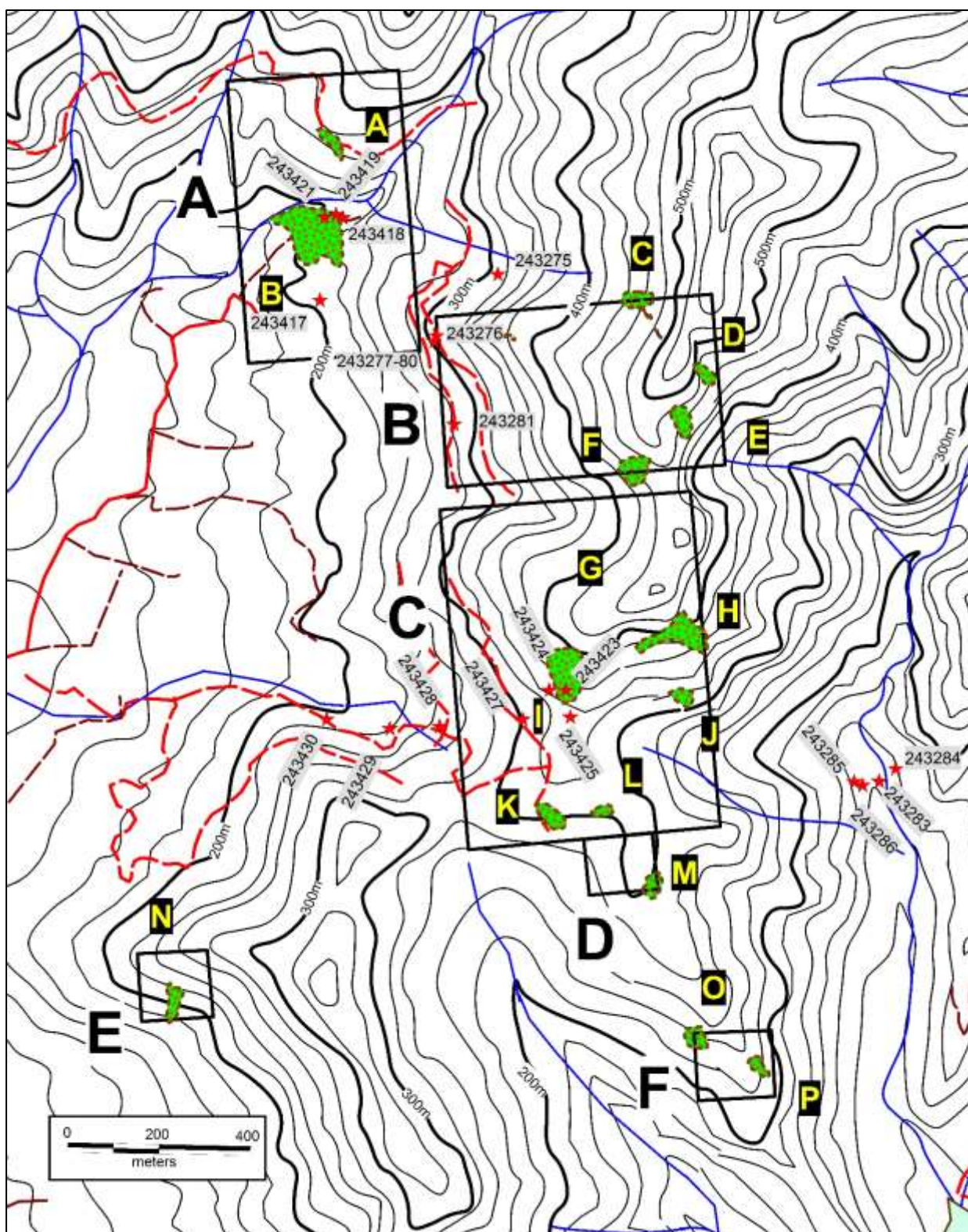
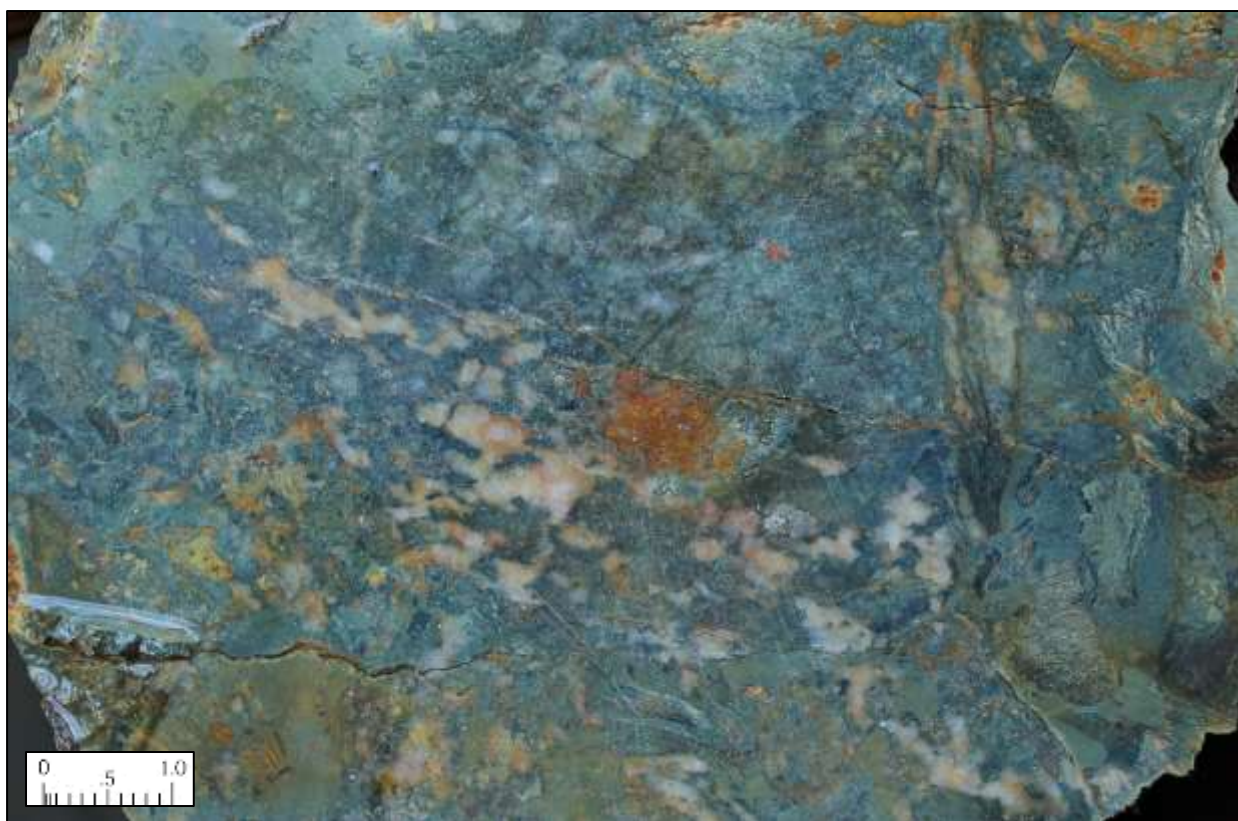


Figure 18. Rock Chip Sample Location Map of the Jangheung Cu-Ag-Zn-Pb Project. The mapped breccia outcrops are indicated in green and labelled A-P, superimposed on topographic contours.



Photograph 23. Cut slab of mineralized breccia dominated by entrained angular schist fragments, with somewhat diffuse granite gneiss and quartz vein clasts, cemented in a silica-sericite rock flour matrix. Anomaly B, Sample No 243421 (8g/t Ag, 0.31% Pb).



Photograph 24. Cut slab of limonite stained, brecciated, sericite altered, coarse-grained granite gneiss. Anomaly B, Sample No 243420 (0.15% Pb).



Photograph 25. Cut slab of gossanous quartz vein-fracture stockwork in leached, porous, brecciated diorite porphyry. Anomaly I, Sample no 243423 (8g/t Ag, 0.13% Cu, 0.30% Pb & 0.14% Zn).



Photograph 26. Cut slab of leached, porous breccia composed of diorite porphyry and granite gneiss clasts cemented by a vuggy matrix infill of quartz and gossan after sulphides. The clasts display diffuse embayed and corroded margins. Anomaly I, Sample no 243426 (9g/t Ag, 840ppm Cu, 0.20% Pb & 0.14% Zn).



Photograph 27. Cut slab of breccia dominated by gossanous granite gneiss clasts within a matrix of fine silica-chlorite cement. Anomaly B. Sample No 243418 (10g/t Ag, 518ppm Cu, 0.28% Pb & 0.23% Zn).



Photograph 28. Cut slab of leached, porous, brecciated mineralized diorite porphyry, with gossanous matrix. Anomaly I, Sample No 243427 (8g/t Ag, 0.12% Cu, 0.20% Pb & 0.15% Zn).



Photograph 29. Cut slab of leached, brecciated, sericite altered, coarse-grained granite gneiss. Anomaly B, Sample No 243419 (41g/t Ag, 0.13% Cu, 0.22% Pb & 0.12% Zn).



Photograph 30. Cut slab of leached, gossanous, porous, brecciated mineralized diorite porphyry. Anomaly F, Sample No 243281 (46g/t Ag, 0.11% Cu).

## 9.4 ALTERATION

The best chalcopyrite-galena-sphalerite mineralized diorite porphyry observed in drill core is recognised at **Anomaly I** (KIER, 1982). The diorite porphyry is described as intensely argillic clay and carbonate (mainly calcite) altered, associated with stockwork veinlet and disseminated galena, sphalerite and finer-grained chalcopyrite.

Argillic alteration is observed in surface outcrops of breccia, consisting of illitic clays and minor kaolinite.

Most biotite observed within granite gneiss is altered to chlorite and surface outcrops are weathered and decomposed, reflecting perhaps weak sericite and illite clay alteration overprint (argillic assemblage).

KIER (1982) observed that some of the larger porphyry clasts within the breccia at **Anomaly E** tend to be more rounded and exhibit a zoned alteration pattern and paragenesis, comprising:

- i. An inner core of relatively unaltered and a primary igneous texture still remains.
- ii. An inner halo of epidote-chlorite-quartz alteration (inner propylitic assemblage).
- iii. A halo of chlorite-epidote-sericite alteration (propylitic)
- iv. An outer halo or rind of sericite-quartz-sulphide (phyllic assemblage).

The presence of rounded clasts is attributed by Sillitoe and Sawkins (1971) to be the result of “spalling off” of the softer, hydrothermally clay altered rims during collapse rather than any “milling effects” induced by rapid/prolonged abrasive movements of material within the breccia pipe column.

From these observations by KIER (1982) and the 2016 field inspection by the author, it is possible to infer the following alteration sequence:

Alteration observed around the breccia-hosted base metal ore mineralization consists of:

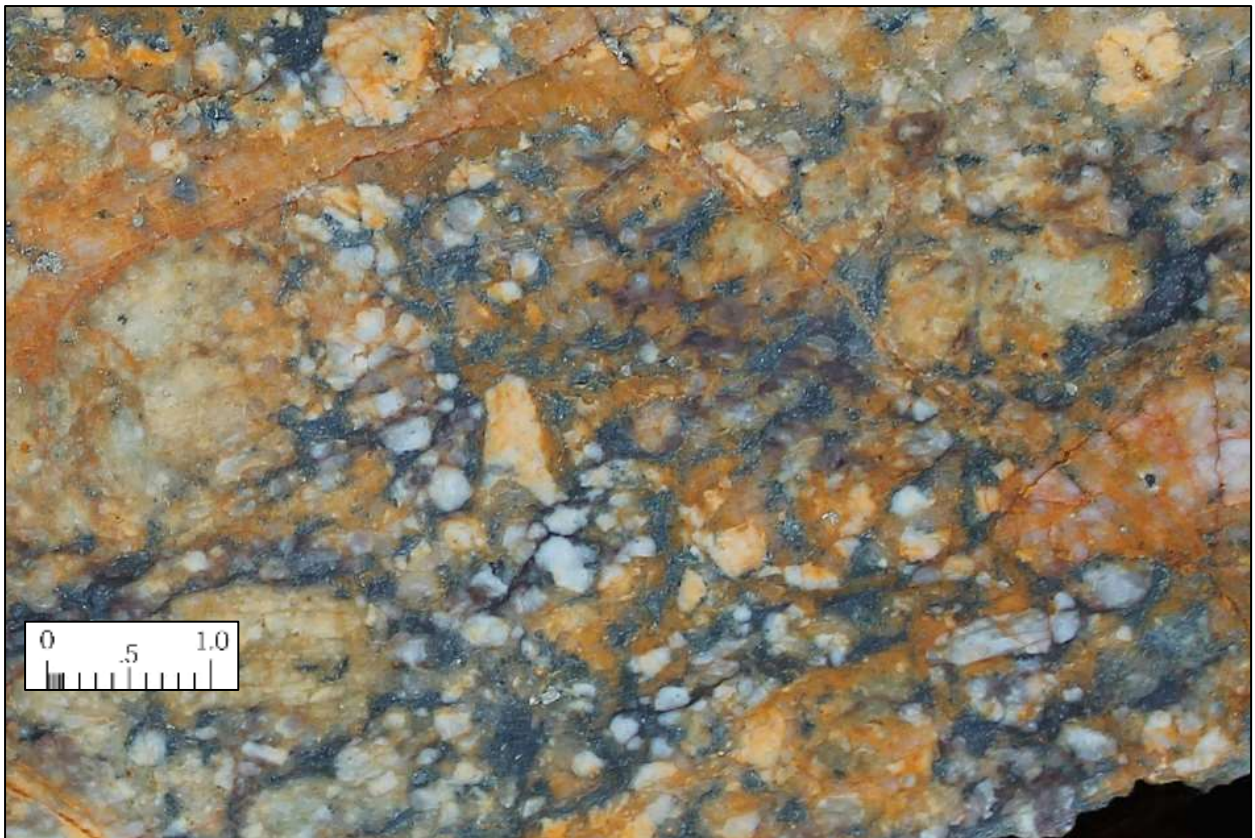
- ❖ Early epidote, chlorite and quartz alteration (inner propylitic assemblage).
- ❖ Halo of chlorite, epidote and sericite alteration (propylitic assemblage).
- ❖ Above the pipe, illite clay with lesser sericite and kaolinite clay (argillic assemblage).
- ❖ Main ore stage with base metal mineralization accompanied by sericite-quartz-carbonate alteration (intermediate argillic-phyllic assemblage).
- ❖ Late stage supergene alteration overprint, composed of secondary minerals after sulphides, limonitic gossan, hematite and jarosite replacement of sulphides.



Photograph 31. Intense leached and argillic clay altered diorite exposed by excavator digging. Sample 243417.



Photograph 32. Outcrop of argillic altered, decomposed granite gneiss near Anomaly K. Gently-dipping foliation and weak quartz veinlet-fracturing is evident in the outcrop, along with jarosite-limonite staining. Sample 243429.



Photograph 33. Cut slab of coarse-grained granite gneiss. Anomaly F, Sample No 243286.



Photograph 34. Cut slab of limonite stained, oxidized sericite-jarosite altered coarse-grained granite gneiss. Anomaly F, Sample no 243275.

## 9.5 SOIL GEOCHEMICAL SURVEYS

As part of an exploration program designed to follow-up stream sediment geochemical anomalies, the *Korean Institute of Energy & Resources* (KIER, 1982) established 6 separate grids (labelled A, B, C, D, E & F) to cover the areas of breccia outcrops.

A sample grid spacing of 20m x 20m was adopted. Samples were collected from the 'C' soil horizon, at depths of 10-60cm. Each sample was sieved to -80# and approximately 300g of sample collected from each site. A total of 1,491 samples were collected and the samples analyzed using AAS for Cu, Pb and Zn at the KIGAM laboratory in Daejeon.

The results were statistically treated. Mean background values for each element were determined to be 24ppm Cu, 105ppm Pb and 110ppm Zn respectively. Anomalous threshold values for the elements were determined as >54ppm Cu, >500ppm Pb and 350ppm Zn.

A total of 16 geochemical anomalies were identified, including **A, B, C, D, E, F, G, H, I, J, K, L, M, N, O** and **P**. These anomalous zones were plotted on the following geochemical maps for each soil grid and results summarized in the Table below. Significant results are highlighted in red, with maximum results of 3500ppm Cu, 6720ppm Pb and 2200ppm Zn recorded.

Lead is regarded as one of the least mobile elements in the weathering environment, and is least susceptible to enrichment or depletion in the supergene zone. As a consequence, lead is interpreted as indicating proximity to the mineralized source.

Soil anomalies **B, E, F, H** and **I** display large soil anomalies with significant Cu, Pb and Zn geochemical values that correspond to mapped outcrops of breccia. These anomalies represent the priority drill targets.

**Table 4. Summary of Soil Geochemical Anomalies.**

Anomaly	Soil Grid	Anomaly Size	Breccia Outcrop Dimensions	Cu Max (ppm)	Pb Max (ppm)	Zn Max (ppm)
<b>A</b>	<b>A</b>	80m x 50m	60m x 10m			
<b>B</b>	<b>A</b>	150m x 150m	150m x 150m	810	6720	680
<b>C</b>	<b>B</b>	50m x 50m	60m x 30m	260	1000	600
<b>D</b>	<b>B</b>	25m x 25m	50m x 10m	80	500	
<b>E</b>	<b>B</b>	200m x 150m	60m x 30m	2000	1000	1000
<b>F</b>	<b>B</b>	150m x 100m	60m x 50m	120	1000	750
<b>G</b>	<b>C</b>	50m x 25m	-		500	
<b>H</b>	<b>C</b>	150m x 100m	100m x 75m	70	600	370
<b>I</b>	<b>C</b>	100m x 100m	100m x 60m	3500	1000	2200
<b>J</b>	<b>C</b>	50m x 25m	30m x 20m		450	450
<b>K</b>	<b>C</b>	50m x 25m	60m x 25m		600	600
<b>L</b>	<b>C</b>	50m x 25m	30m x 15m		600	600
<b>M</b>	<b>D</b>	150m x 75m	15m x 15m	150	500	250
<b>N</b>	<b>E</b>	100m x 50m	60m x 20m	360	2400	330
<b>O</b>	<b>F</b>	75m x 50m	20m x 15m		460	530
<b>P</b>	<b>F</b>	75m x 50m	40m x 15m		460	540

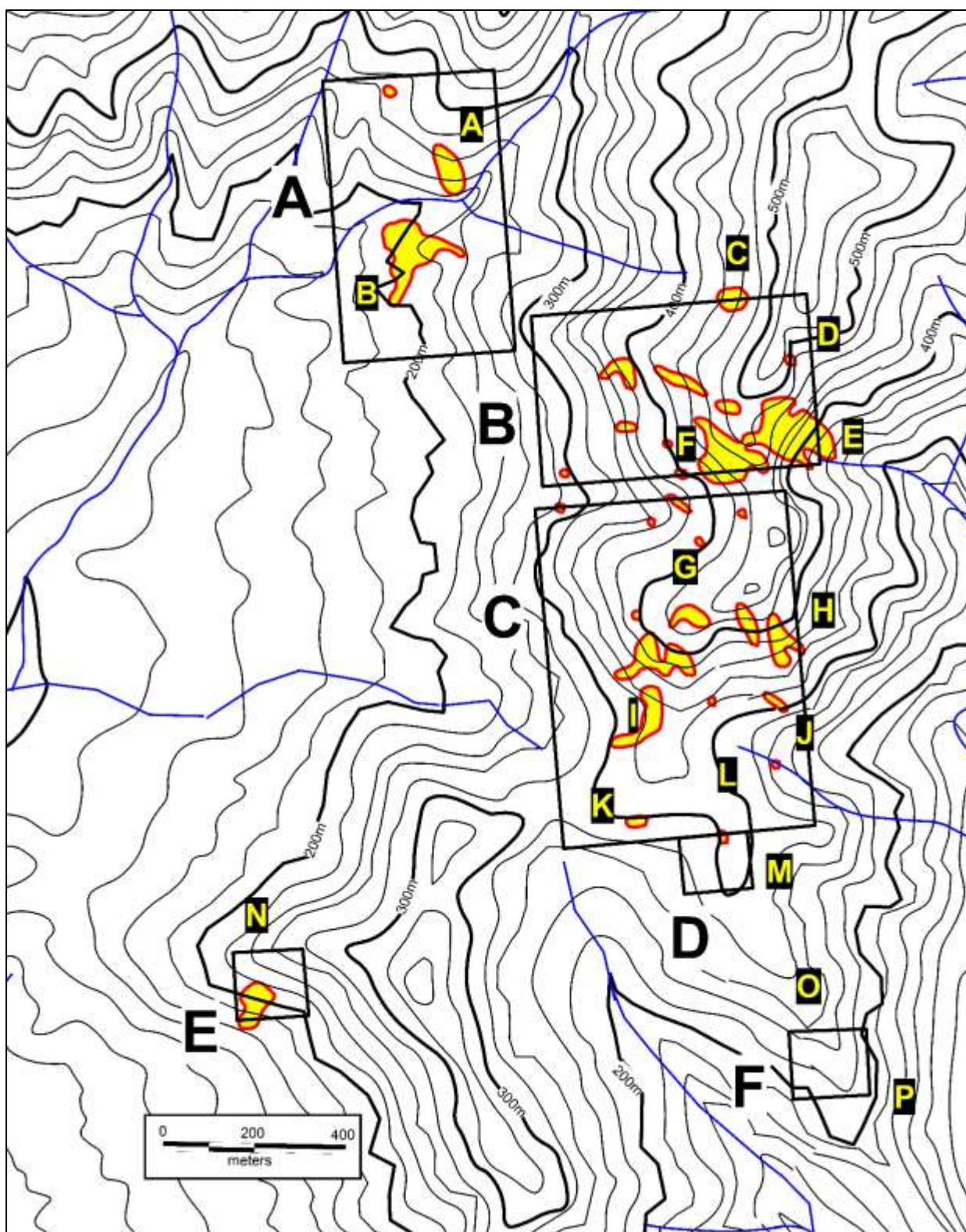


Figure 19. Copper Soil Geochemistry Map. The soil grids are indicated by boxes and labelled A-F. Anomalous copper zones (Cu > 54ppm) are highlighted in yellow.

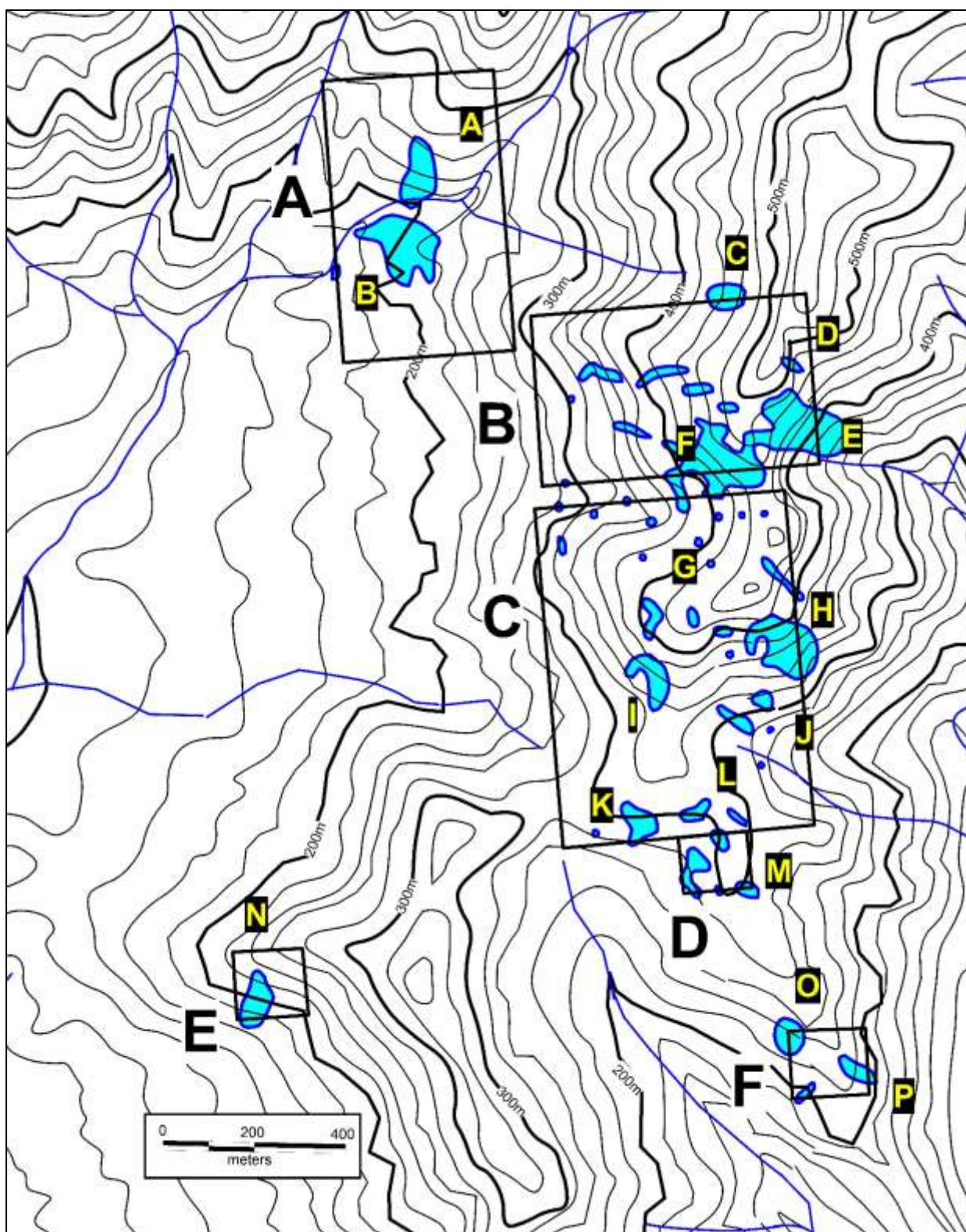


Figure 20. Lead Soil Geochemistry Map. The soil grids are indicated by boxes and labelled A-F. Anomalous lead zones (Pb >500ppm) are highlighted in blue. Lead is relatively immobile, not susceptible to supergene enrichment or depletion, and so is generally interpreted as indicating proximity to the mineralized source.

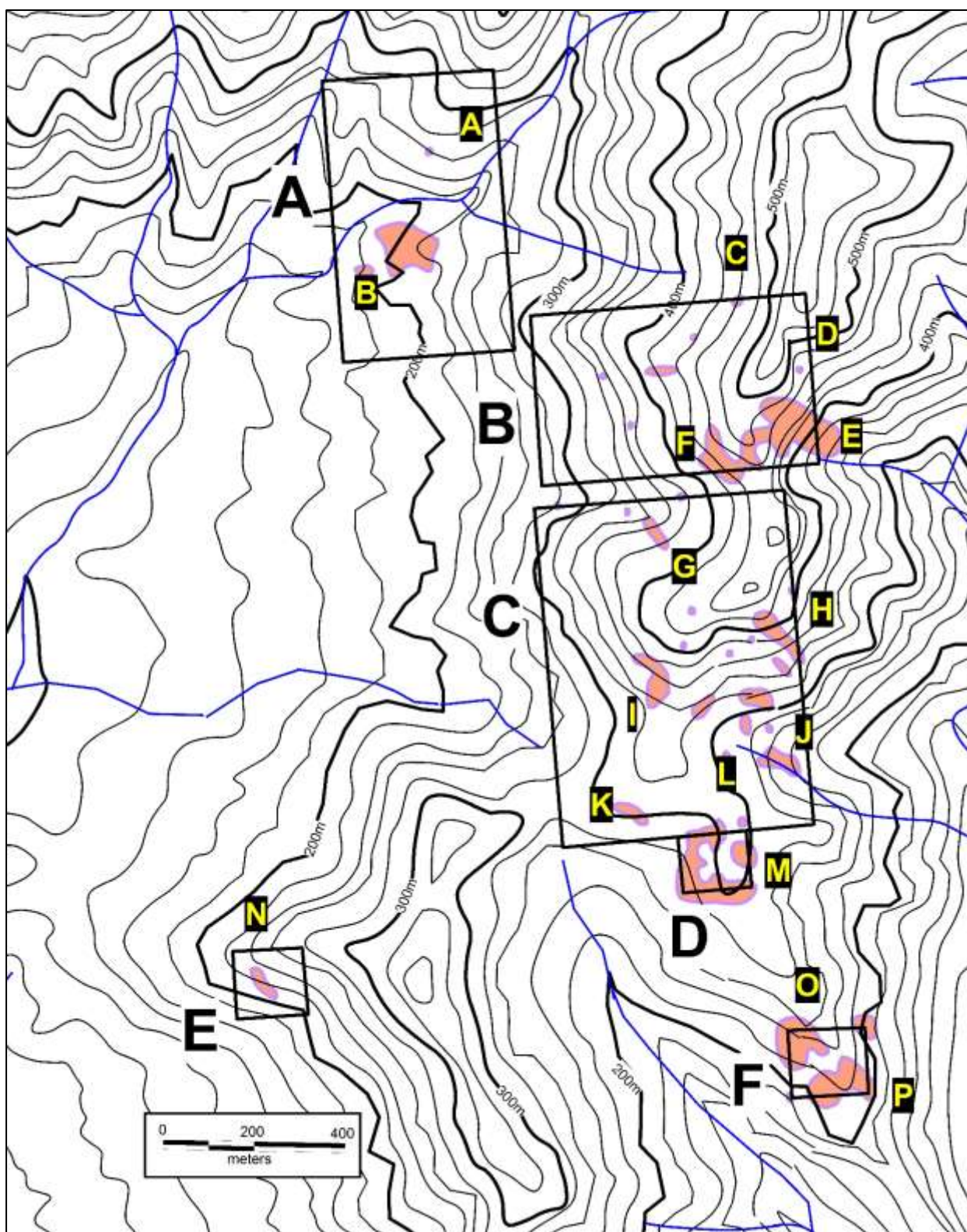


Figure 21. Zinc Soil Geochemistry Map. The soil grids are indicated by boxes and labelled A-F. Anomalous zinc zones ( $Zn > 350\text{ppm}$ ) are highlighted in pink.

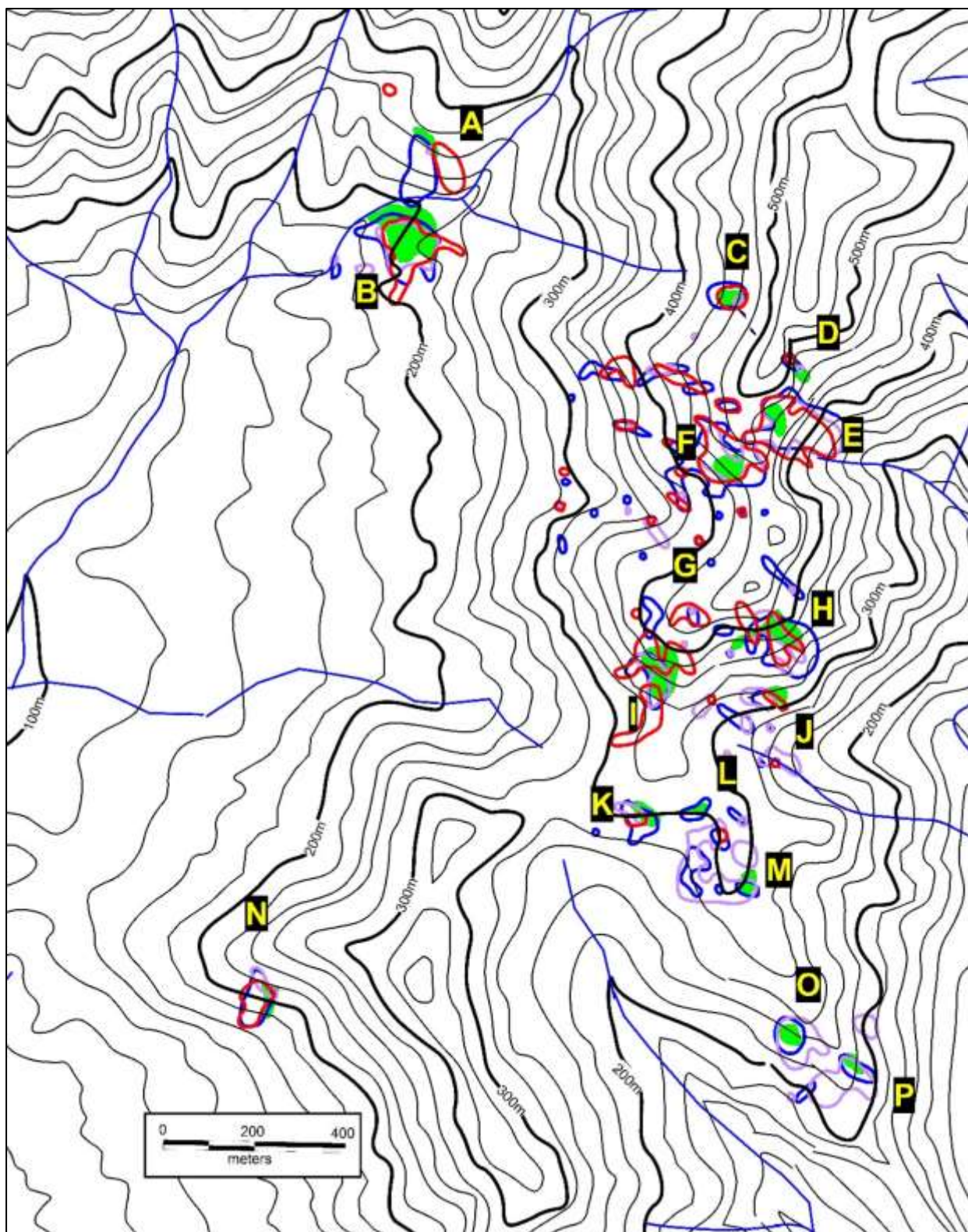


Figure 22. Soil Geochemistry Compilation Map. The anomalous soil zones are outlined (red = Cu, blue = Pb and purple = Zn) with the outcropping breccias highlighted in green. Coincidental multi-element soil anomalies with mapped breccia outcrops are evident at Anomalies A, B, C, E, F, H, I, J and K.

## 9.6 GROUND GEOPHYSICAL SURVEYS

The hilly terrain, soil and talus scree cover, thick secondary regrowth vegetation and poor outcrop make access and geological mapping difficult. The *Korea Institute of Energy and Resources* (KIER, 1982) completed some ground geophysical surveys to assist in locating base metal targets, as discussed in the following sections.

### VLF-EM Geophysical Survey

VLF is an electro-magnetic method using transmitted currents to induce secondary responses in conductive geological bodies and can be used to help map steeply dipping structures such as faults, fractures and shallow areas of potential conductive sulphide mineralization. The change in total magnetic field, vertical in-phase and out-of-phase quadrature component, and quadrature polarity data is recorded simultaneously. VLF is normally used to communicate with submarines using plane-wave radio signal frequencies of 15-30kHz, with several military radio transmitter stations providing world-wide signal coverage. In Korea, the VLF signals from transmitter stations located at Northwest Cape Australia (22.3KHz) and Ebina Japan (17.4KHz) can potentially be used, providing 2 possible signal directions and strengths for evaluation purposes. A Magnetometer is normally incorporated into the instrument configuration, providing significant additional geophysical information.

The optimal survey orientation is parallel to the strike of the target geological structure. The depth of penetration varies from 4-5 meters in conductive soils to 40-60 meters in highly-resistive soils, but >100m is possible with the VLF-EM system. VLF works best where the rocks are resistive and overburden is minimal, which is the situation for the Jangheung project area.

A filter is normally applied to average the data between the two stations. As the VLF-EM technique is usually associated with some surficial cultural and geological noise components, the data is also filtered again to reduce the noise and enhance conductivity anomalies (using a *Fraser Filter*).

The Jangheung VLF EM survey used readings taken at 30m spacing along east-west grid lines spaced 100m apart. VLF signals from (22.3KHz; NWC, Australia and 17.4KHz; NDT, Japan) were used to help map steeply dipping structures such as faults, fractures and shallow areas of potential conductive sulphide mineralization. The depth of penetration varies from 4-5 meters in conductive soils to 40-60 meters in highly-resistive soils. A Fraser filter was applied to average the data between stations.

Results from the VLF EM in-phase colour contour plot using the East Direction NWC Station show a 100-150m wide, NNE trending, EM conductor zone that runs from Anomaly K through Anomaly I and between Anomalies G and H.

Results from the VLF EM in-phase colour contour plot using the North Direction NDT Japan Station show an EW orientated, 200m x 90m elongate EM anomaly between Anomalies I, G and H and an EW orientated, 300m x 75m elongate EM anomaly just north of Anomalies K and L.

Anomalous conductive anomalies were identified using "Pseudo-sections". The main "Pants Leg" IP anomaly lies between 0E and 200E on Line 0 North, between Anomalies I and H.

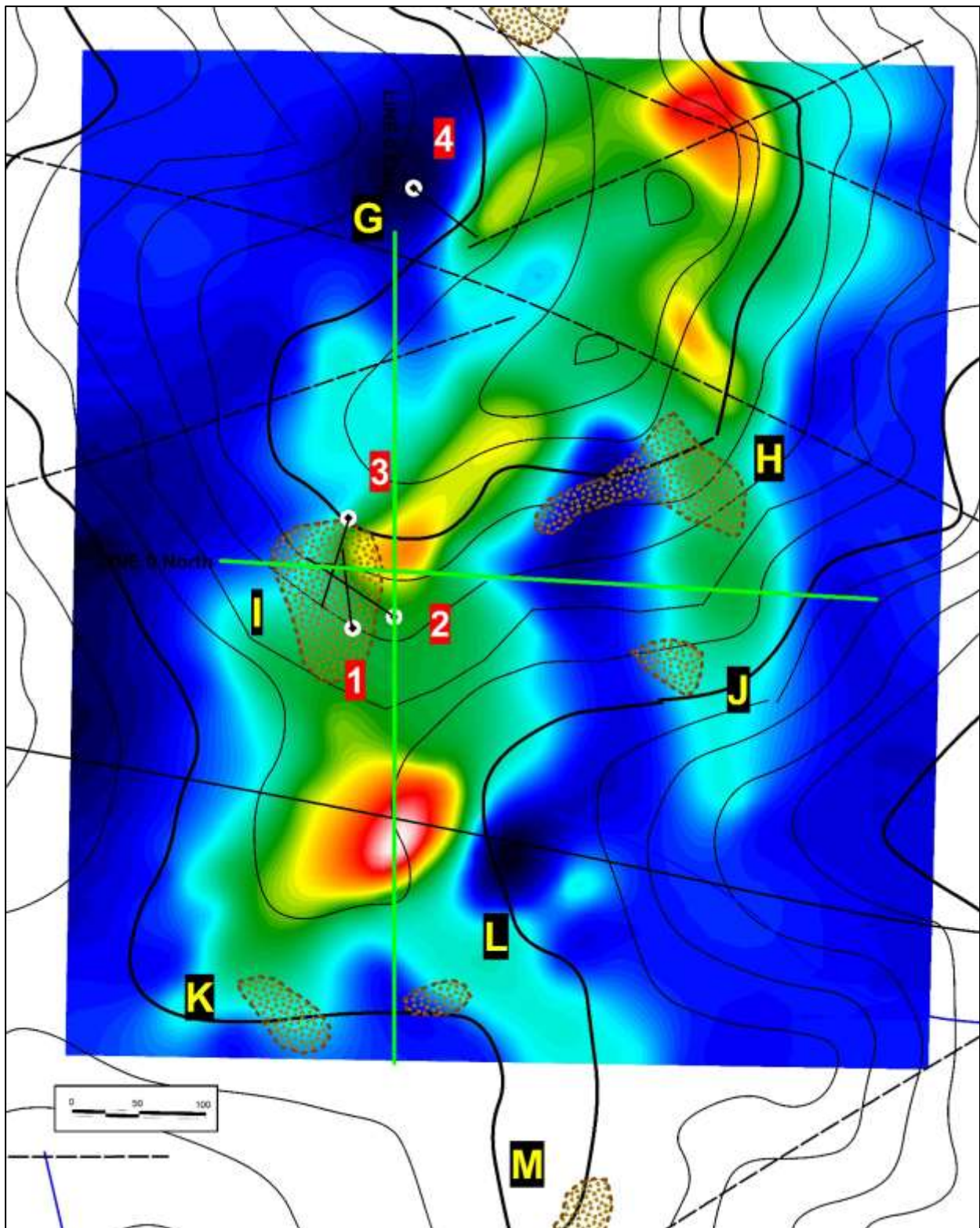


Figure 23. VLF EM Fraser Filter Contour Plot (East Direction-NWC Australia) conducted over Soil Geochemical Anomalies G, H, I, J, K and L. The VLF EM IP Pseudo-section Lines 0 East and 0 North are shown. The drill hole locations (JD-1, JD-2, JD-3 & JD-4) are indicated and the mapped outcrops of breccias outlined in brown.

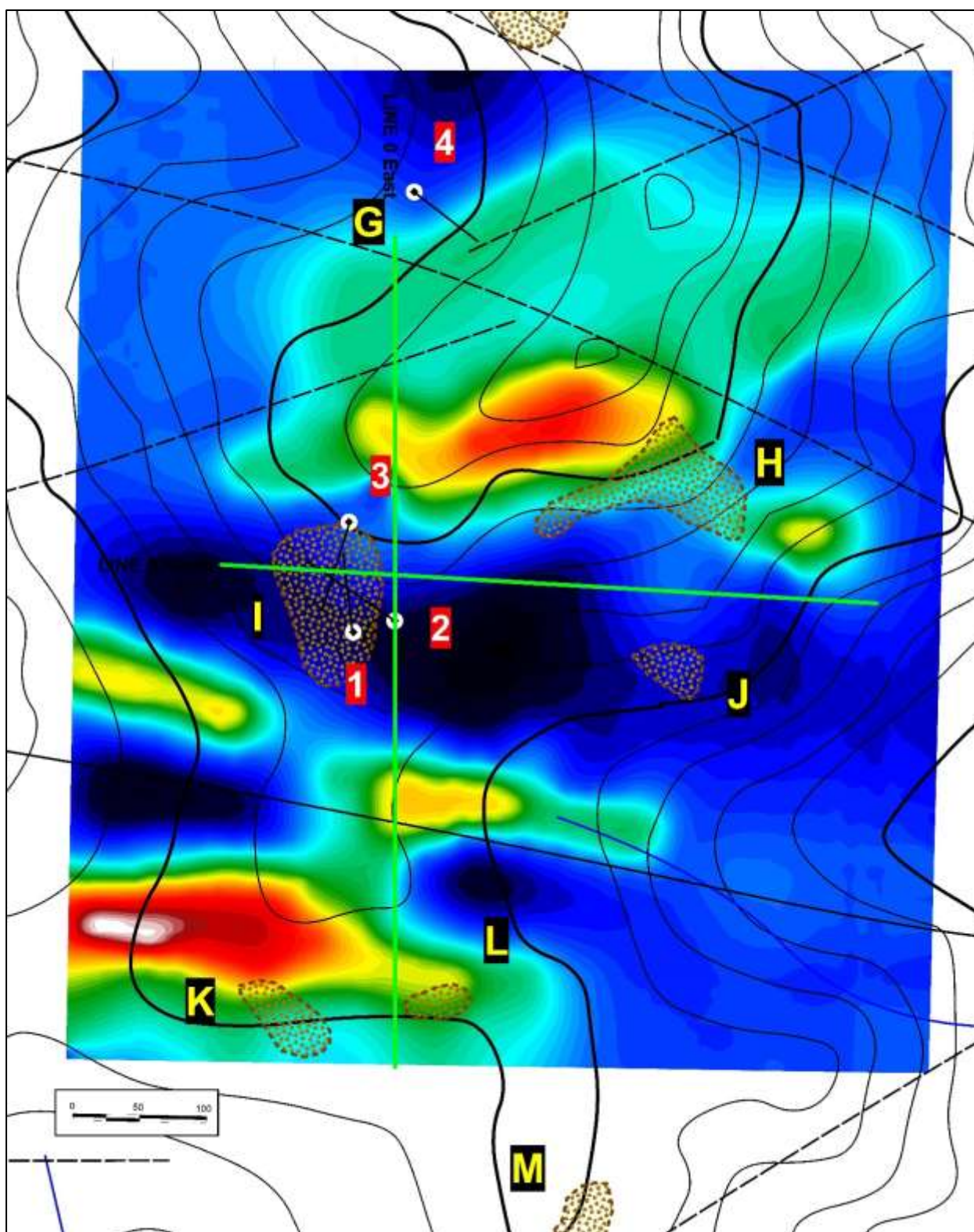


Figure 24. VLF EM Fraser Filter Contour Plot (North-NOT Japan) conducted over Soil Geochemical Anomalies G, H, I, J, K and L. The VLF EM IP Pseudo-section Lines 0 East and 0 North are shown. Drill hole locations (JD-1, JD-2, JD-3 & JD-4) are indicated and the mapped outcrops of breccias outlined in brown.

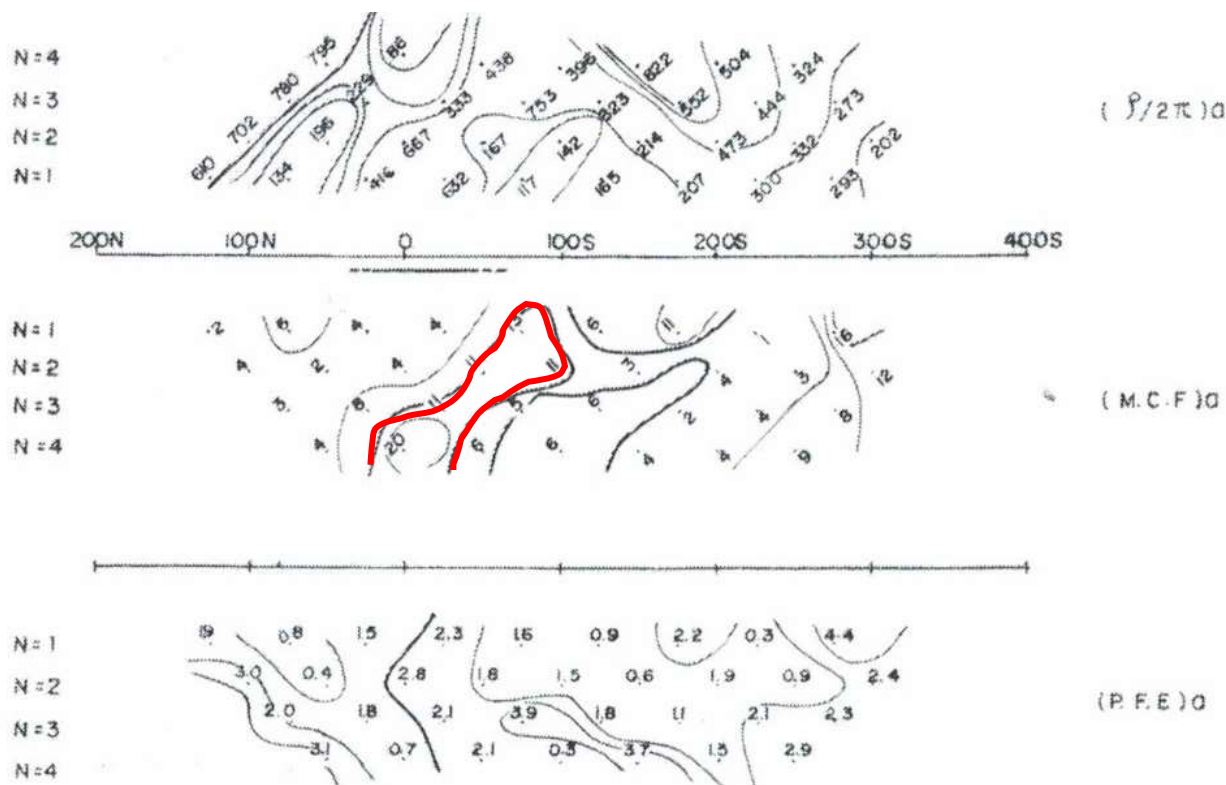


Figure 25. Line 0 East VLF-EM IP Pseudo-section. Nominal “pseudo-depths” are  $n = 4 = 100\text{m}$ , such that depth intervals are 25m. The conductive anomaly is outlined in red.

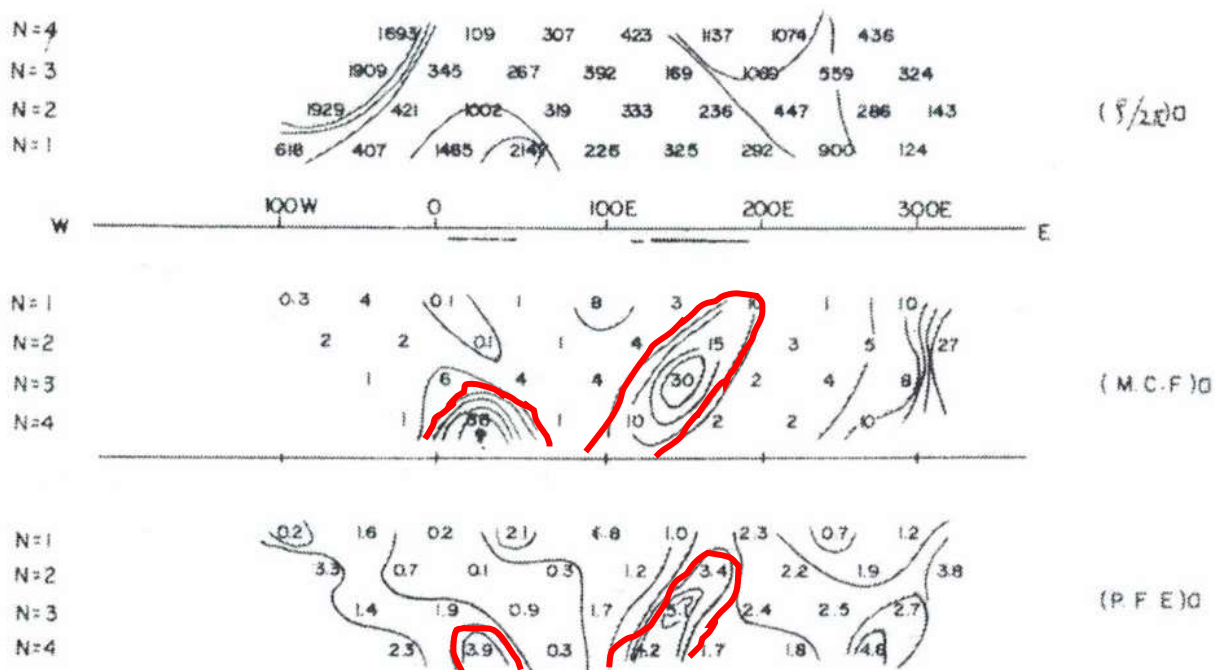


Figure 26. Line 0 North VLF-EM IP Pseudo-section. Nominal “pseudo-depths” are  $n = 4 = 100\text{m}$ , such that depth intervals are 25m. The conductive “Pant Leg” anomaly is outlined in red.

### TMI Geophysical Survey

In conjunction with the VLF EM geophysical survey, a ground magnetometer survey was conducted over a smaller area, covering only soil geochemical anomalies G and I.

The total magnetic intensity (TMI) colour plot indicates the presence of a series of NNE trending <500nT magnetic low anomalies (blue), located west of the breccia at Anomaly I. Magnetic high anomalies of >800nT (orange) are located to the east of Anomaly I and north of Anomaly G. The magnetic low features could represent magnetite-destructive alteration zones. The magnetic high anomalies are likely to be intrusive diorite porphyry bodies or possible magnetite alteration zones at depth.

The level of detail evident on the TMI image is considerable (particularly in comparison with the wide-spaced aeromagnetic survey; see earlier section in this report) and highlights the usefulness of a close-spaced magnetic survey for an exploration program.

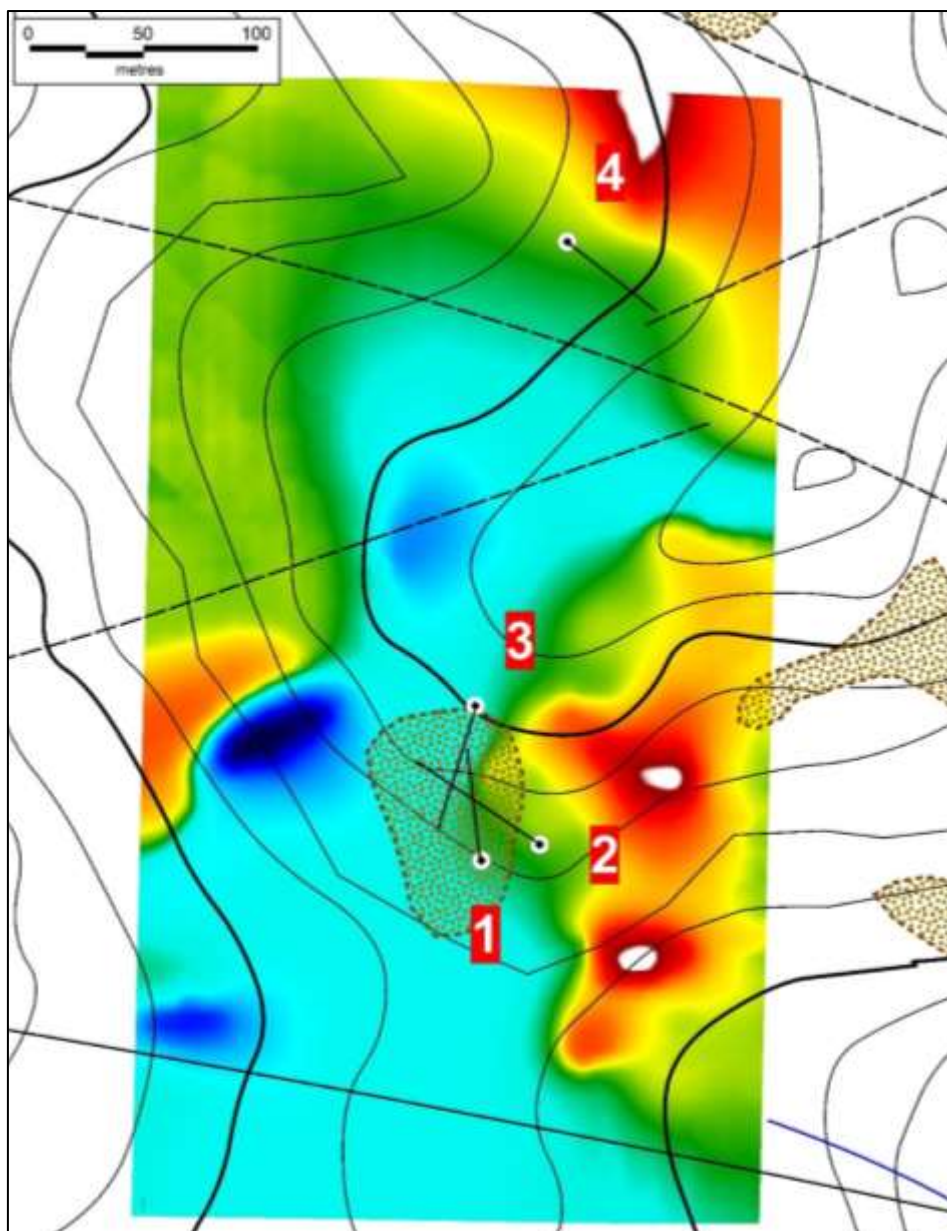


Figure 27. Total Magnetic Intensity Colour Image of ground magnetometer survey conducted over Soil Geochemical Anomalies G, H, I, J, K and L. The drill hole locations (JD-1, JD-2, JD-3 & JD-4) are indicated and the mapped outcrops of breccias outlined in brown. The map indicates the more intense NNE trending magnetic low response (blue) has not been tested by the drilling. The magnetic highs (red) were also not tested and may be related to an underlying 'blind' diorite porphyry intrusion or possibly magnetite alteration.

### IP Geophysical Survey

In conjunction with the VLF EM geophysical survey, an IP dipole-dipole ground geophysical survey was conducted over the area covered by soil geochemical anomalies I, K and L (Figure 22).

Results indicate there is a linear, 300m x 50m wide, strong -60mev conductive zone, trending ENE just north of Anomalies H and also a 200m x 100m, moderately conductive -30mev anomaly is present immediately north of Anomaly K.

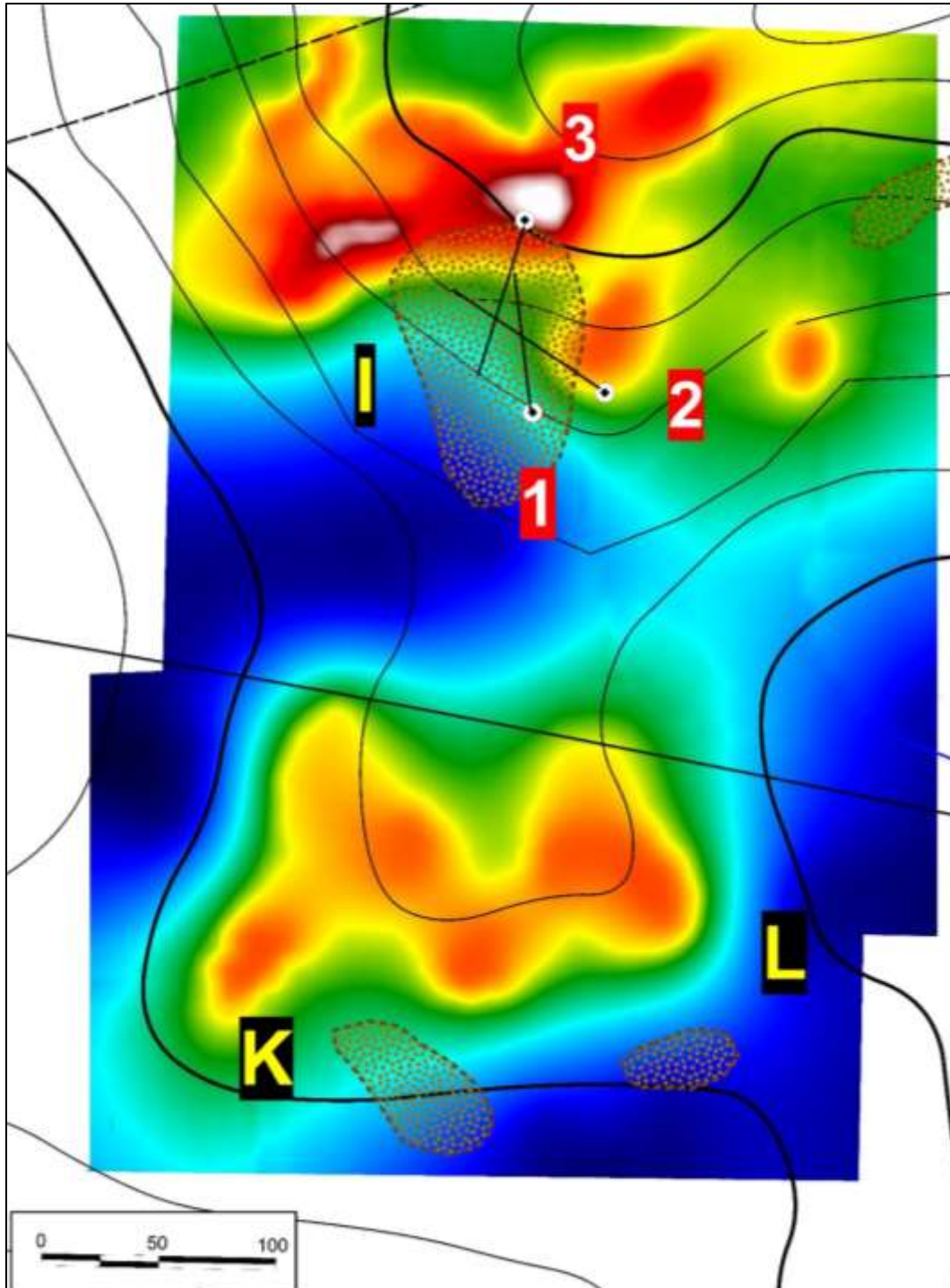


Figure 28. Colour Conductivity Plot of the IP dipole-dipole geophysical survey grid, conducted over Soil Geochemical Anomalies I, K and L. The drill hole locations (JD-1, JD-2 & JD-3) are indicated and the mapped outcrops of breccias outlined in brown. The map indicates the elongate linear ENE trending -60mev conductivity anomaly at Anomaly I would not have been tested by the drilling.

## 9.7 DRILLING PROGRAM

### Drilling

KIER (1982) drilled 12 diamond core holes (No's JD-1, JD-2... to JD-12) for a total of 1,524m of BQ core, as tabulated below). The drill hole locations are presented on the Figure below.

Hole JD-10 was a vertical hole, the other holes were drilled at various dip angles.

The drill holes were sited to mainly test the breccia outcrops at 5 of the 16 soil geochemical anomalies, including:

- ❖ **Anomaly B** (holes JD-10, 11 & 12),
- ❖ **Anomaly C** (hole JD-9),
- ❖ **Anomaly E** (holes JD-5, 6, 7 & 8),
- ❖ **Anomaly G** (hole JD-4),
- ❖ **Anomaly I** (holes JD-1, 2 & 3)

Soil geochemical anomalies A, D, F, H, J, K, L, M, N, O and P were not drill tested.

**Table 5. Drill Hole Collar Survey Data, Jangheung Cu-Zn-Pb Project.**

Anomaly	Hole ID	Easting	Northing	RL (masl)	Azimuth (°)	Dip (°)	EOH (m)
<b>I</b>	<b>JD-1</b>	316349	3838050	359	000	-58	<b>120</b>
	<b>JD-2</b>	316375	3838057	401	210	-60	<b>130</b>
	<b>JD-3</b>	316345	3838118	368	300	-64	<b>130</b>
<b>G</b>	<b>JD-4</b>	316387	3838322	385	135	-60	<b>120</b>
<b>E</b>	<b>JD-5</b>	316566	3838548	459	285	-70	<b>100</b>
	<b>JD-6</b>	316517	3838527	475	074	-70	<b>100</b>
	<b>JD-7</b>	316504	3838564	497	045	-60	<b>135</b>
	<b>JD-8</b>	316538	3838559	485	192	-60	<b>78</b>
<b>C</b>	<b>JD-9</b>	316468	3838737	476	055	-65	<b>100</b>
<b>B</b>	<b>JD-10</b>	315904	3838854	218	000	-90	<b>158</b>
	<b>JD-11</b>	315919	3838884	211	315	-60	<b>150</b>
	<b>JD-12</b>	315913	3838836	223	315	-60	<b>203</b>
<b>TOTALS</b>							<b>1,524</b>

KIER (1982) used a simplistic columnar visual log to record and display the geology encountered in each drill hole. These columnar visual logs and the cross sections for each drill hole are presented in the figures below.

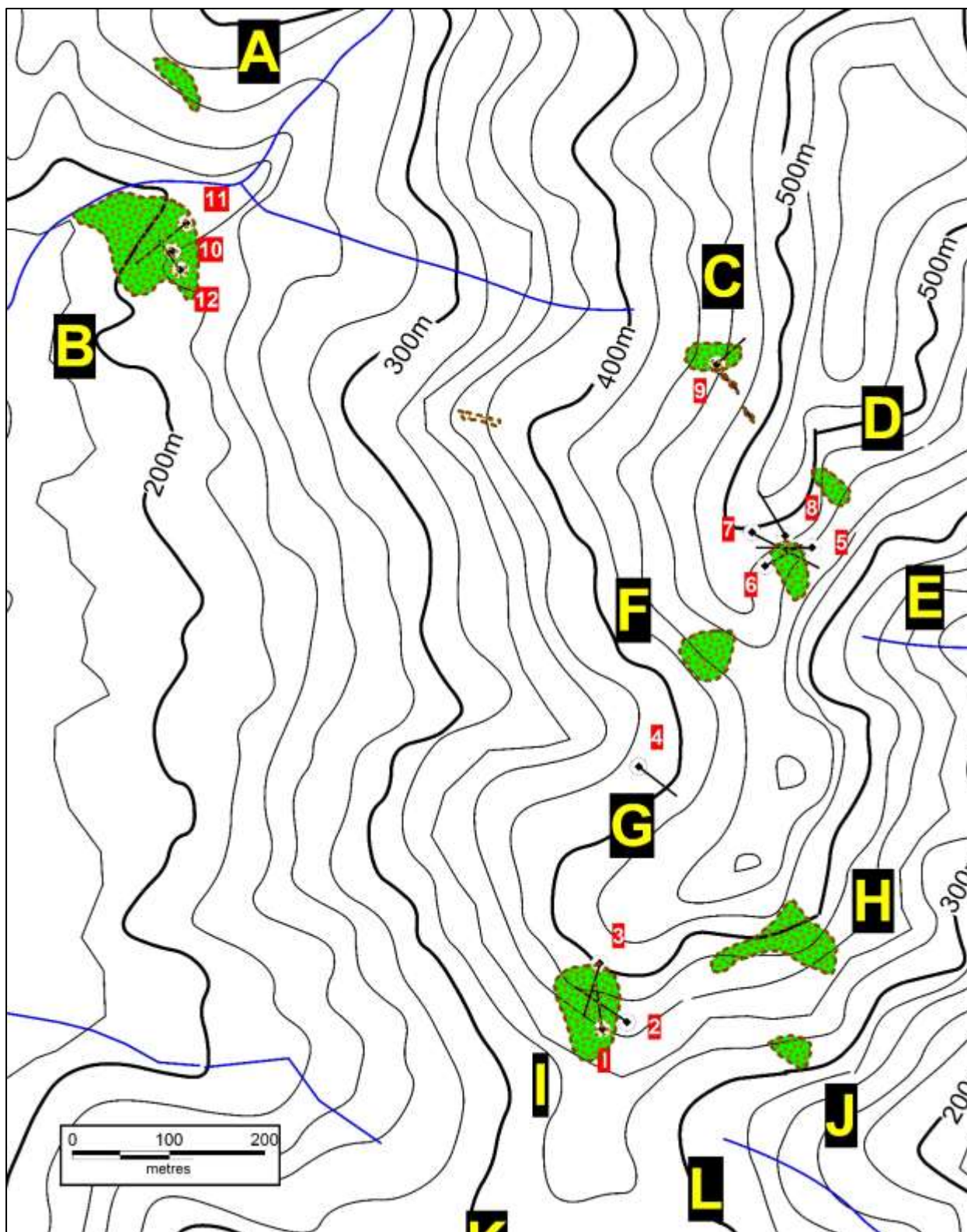


Figure 29. Drill Hole Location Map, Jangheung project. The drillhole numbers are highlighted in red (Prefix JD omitted). The mapped breccia outcrops are shown in green with brown dots. The Soil Geochemical Anomalies are labelled A-P.

Drill results indicate Anomalies B and I are Zn-enriched breccias, whilst Anomaly E is Cu-enriched.

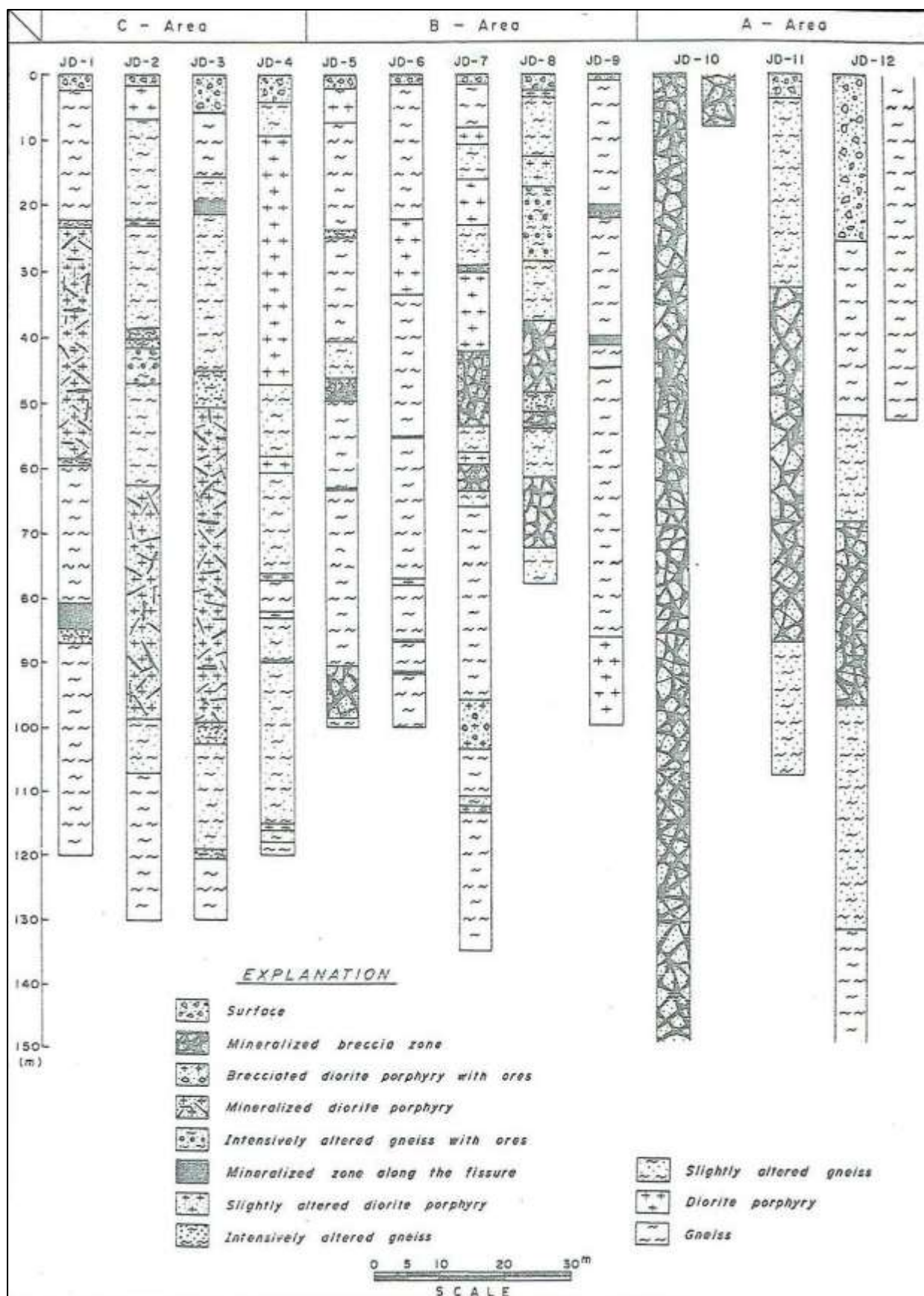


Figure 30. Drill Hole Columnar Visual Geological Logs (KIER, 1982). These visual logs were used to generate the digital drill logs presented in Appendix I.

## Sampling

The key features of the historical sampling and assaying methodologies employed by KIER on the drill program conducted at Jangheung were:

- Sampling and assaying of the small diameter AX (23.8mm diameter) and BQ (36.5mm diameter) core size used by the KMPC was sporadic and incomplete in nature. The narrow core diameter is impossible to split and the whole core was consumed in the sampling process.
- Samples were analyzed at the KMPC “in house” laboratory in Seoul.
- Only Cu, Pb and Zn were analyzed.
- Ag was not analyzed, but rock chip geochemistry indicates Ag is present in significant grades.
- Au was not assayed.
- No QAQC Quality Control measures for the sampling methodology or geochemical analyses were adopted by the KMPC. There was no check assaying using standards, blanks or duplicates.

It is not known if any of the BQ drill core was retained for visual reference purposes. A core library is maintained by KIGAMM in its Daejeon office and it is possible some of the drill core from Jangheung has been retained. If so, non-destructive analysis of the drill core using a NITON hand portable XRF analyzer is recommended, along with re-logging of the drill holes.

The BQ drill core was analyzed only for Cu, Pb and Zn and sampling intervals were variable and incomplete, with only obvious mineralized zones selected for sampling and assay (see Table below). Unfortunately, Ag or Au was not analyzed.

## Assay Results

Significant mineralized intersections of >0.40% Cu, >3% Pb and >2.0% Zn were reported from 3 of the 5 tested Anomalous Zones, as summarized in Table 6 below and in more detail in Table 7.

Some lateral geochemical zonation may possibly be evident in the drill results, with Anomalies B and I being Zn-enriched and Anomaly E is Cu-enriched.

**Table 6. Significant Mineralized Drill Intersections, Jangheung Cu-Zn-Pb Project.**

Anomaly	Hole ID	From (m)	To (m)	Intersection (m)	CuEq (%)	Cu (%)	Pb (%)	Zn (%)
<b>I</b>	JD-1	23.0	28.6	<b>5.6</b>	<b>4.10</b>	0.16	2.85	<b>7.40</b>
<b>E</b>	JD-7	16.0	24.0	<b>8.0</b>	<b>5.32</b>	<b>1.27</b>	<b>6.03</b>	<b>4.80</b>
<b>E</b>	JD-7	52.5	61.5	<b>9.0</b>	<b>2.42</b>	<b>1.10</b>	1.27	<b>2.20</b>
<b>E</b>	JD-8	51.0	52.3	1.3	<b>5.48</b>	<b>1.73</b>	<b>3.48</b>	<b>6.35</b>
<b>B</b>	JD-10	0.0	146.2	<b>146.2</b>	<b>2.45</b>	<b>0.44</b>	0.26	<b>4.87</b>
<b>B</b>	JD-11	33.0	102.0	<b>69.0</b>	<b>1.71</b>	0.21	0.09	<b>3.73</b>
<b>B</b>	JD-12	57.0	58.7	1.7	<b>10.93</b>	<b>9.33</b>	0.45	<b>3.65</b>
<b>B</b>	JD-12	70.6	105.0	<b>34.4</b>	<b>1.71</b>	0.28	0.19	<b>3.47</b>

### NOTES:

- ❖ CuEq was calculated using metal prices of Cu = US\$2.18/lb, Pb = US\$0.78/lb & Zn = US\$0.86/lb.
- ❖ Intersections of >5.0m and >1.0% CuEq are highlighted in dark red text.

Table 7. Drill Hole Database (KIER, 1982).

## Anomaly G

Drillhole ID	From (m)	To (m)	Interval (m)	Lithology	Cu (%)	Pb (%)	Zn (%)
JD-4	0.00	4.00	4.00	Soil & Colluvium			
	4.00	9.00	5.00	Gneiss			
	9.00	47.00	38.00	<b>Diorite porphyry</b>			
	47.00	52.60	5.60	<b>Diorite porphyry</b>			
	52.60	53.00	0.40	<b>Diorite porphyry</b>			
	53.00	58.00	5.00	Gneiss			
	58.00	60.50	2.50	<b>Diorite porphyry</b>			
	60.50	64.30	3.80	Gneiss			
	64.30	64.70	0.40	<b>Diorite porphyry</b>			
	64.70	74.70	10.00	Gneiss			
	74.70	75.00	0.30	<b>Diorite porphyry</b>			
	75.00	76.20	1.20	Gneiss			
	76.20	77.20	1.00	<b>Diorite porphyry</b>			
	77.20	81.90	4.70	Gneiss			
	81.90	82.90	1.00	<b>Diorite porphyry</b>			
	82.90	89.30	6.40	Gneiss			
	89.30	89.60	<b>0.30</b>	<b>FAULT</b>	<b>0.04%</b>	<b>0.62%</b>	<b>1.74%</b>
	89.60	115.10	25.50	Gneiss			
115.10	115.90	0.80	<b>Diorite porphyry</b>				
115.90	117.00	1.10	Gneiss				
117.00	120.00	3.00	Gneiss				

Table 7. Drill Hole Database (KIER, 1982).

## Anomaly I

Drillhole ID	From (m)	To (m)	Interval (m)	Lithology	Cu (%)	Pb (%)	Zn (%)
JD-1	0.00	2.00	2.00	Soil & Colluvium			
	2.00	22.00	20.00	Gneiss			
	22.00	23.00	1.00	Gneiss			
	23.00	28.60	5.60	Diorite porphyry	0.16%	2.85%	7.40%
	28.60	31.20	2.60	Diorite porphyry	0.03%	0.49%	0.75%
	31.20	34.60	3.40	Diorite porphyry	0.06%	0.20%	0.30%
	34.60	39.80	5.20	Diorite porphyry	0.03%	0.20%	0.30%
	39.80	55.60	15.80	Diorite porphyry	0.05%	0.92%	1.07%
	55.60	56.60	1.00	Diorite porphyry	0.02%	0.20%	0.20%
	56.60	58.20	1.60	Diorite porphyry	0.05%	1.42%	2.24%
	58.20	60.00	1.80	Gneiss			
	60.00	80.50	20.50	Gneiss			
	80.50	80.90	0.40	Sulphide vein	0.07%	2.09%	1.44%
	80.90	84.50	3.60	Sulphide vein	0.12%	4.51%	6.50%
	84.50	87.00	2.50	Gneiss			
87.00	120.00	33.00	Gneiss				
JD-2	0.00	1.50	1.50	Soil & Colluvium			
	1.50	6.50	5.00	Diorite porphyry			
	6.50	22.00	15.50	Gneiss			
	22.00	23.00	1.00	Diorite porphyry			
	23.00	38.00	15.00	Gneiss			
	38.00	42.20	4.20	Gneiss	0.15%	2.12%	4.20%
	42.20	42.80	0.60	Gneiss	0.13%	2.27%	5.16%
	42.80	64.40	21.60	Gneiss			
	64.40	68.20	3.80	Diorite porphyry	0.07%	2.09%	3.72%
	68.20	76.40	8.20	Diorite porphyry	0.02%	0.31%	0.85%
	76.40	82.50	6.10	Diorite porphyry	0.06%	0.20%	0.42%
	82.50	98.50	16.00	Diorite porphyry	0.08%	0.84%	0.98%
	98.50	107.00	8.50	Gneiss			
107.00	130.00	23.00	Gneiss				
JD-3	0.00	5.50	5.50	Soil & Colluvium			
	5.50	16.00	10.50	Gneiss			
	16.00	19.00	3.00	Gneiss			
	19.00	21.00	2.00	Sulphide vein	0.21%	2.72%	5.54%
	21.00	45.00	24.00	Gneiss			
	45.00	50.50	5.50	Gneiss			
	50.50	54.50	4.00	Diorite porphyry	0.06%	1.02%	2.45%
	54.50	94.00	39.50	Diorite porphyry			
	94.00	99.00	5.00	Diorite porphyry	0.03%	0.82%	1.31%
	99.00	102.00	3.00	Gneiss			
	102.00	119.50	17.50	Gneiss			
	119.50	120.50	1.00	Gneiss			
120.50	130.00	9.50	Gneiss				

NOTES: Intercepts of >5.0m width and Assays of >0.4% Cu, >2.0% Pb & >2.0% Zn are highlighted in red.

Table 7. Drill Hole Database (KIER, 1982).

## Anomaly E

Drillhole ID	From (m)	To (m)	Interval (m)	Lithology	Cu (%)	Pb (%)	Zn (%)
JD-5	0.00	7.00	7.00	Soil & Colluvium			
	7.00	10.00	3.00	<b>Diorite porphyry</b>			
	10.00	23.50	13.50	Gneiss			
	23.50	24.50	1.00	Gneiss			
	24.50	40.00	15.50	Gneiss			
	40.00	43.00	3.00	Gneiss			
	43.00	50.00	<b>7.00</b>	<b>BRECCIA</b>	<b>0.16%</b>	<b>2.70%</b>	<b>1.70%</b>
	49.50	63.00	13.50	Gneiss			
	63.00	63.10	0.10	<b>FAULT</b>			
	63.10	90.50	27.40	Gneiss			
	90.50	98.50	8.00	<b>BRECCIA</b>			
	98.50	100.00	1.50	Gneiss			
JD-6	0.00	1.50	1.50	Soil & Colluvium			
	1.50	22.00	20.50	Gneiss			
	22.00	33.40	11.40	<b>Diorite porphyry</b>			
	33.40	55.00	21.60	Gneiss			
	55.00	55.20	0.20	<b>FAULT</b>			
	55.20	76.00	20.80	Gneiss			
	76.00	77.00	1.00	<b>Diorite porphyry</b>			
	77.00	81.60	4.60	Gneiss			
	81.60	82.00	<b>0.40</b>	<b>FAULT</b>	<b>0.02%</b>	<b>0.08%</b>	<b>1.50%</b>
	82.00	86.80	4.80	<b>FAULT</b>			
	86.80	93.00	6.20	Gneiss			
	93.00	93.40	<b>0.40</b>	<b>FAULT</b>	<b>0.02%</b>	<b>1.00%</b>	<b>0.90%</b>
93.40	100.00	6.60	Gneiss				
JD-7	0.00	1.00	1.00	Soil & Colluvium			
	1.00	8.00	7.00	Gneiss			
	8.00	10.00	2.00	<b>Diorite porphyry</b>			
	10.00	16.00	6.00	Gneiss			
	16.00	24.00	<b>8.00</b>	<b>Diorite porphyry</b>	<b>1.27%</b>	<b>6.03%</b>	<b>4.80%</b>
	24.00	29.00	5.00	Gneiss			
	29.00	30.00	1.00	<b>Sulphide vein</b>			
	30.00	42.00	12.00	<b>Diorite porphyry</b>			
	42.00	52.50	<b>10.50</b>	<b>BRECCIA</b>	<b>0.13%</b>	<b>2.21%</b>	<b>2.05%</b>
	52.50	61.50	<b>9.00</b>	<b>BRECCIA</b>	<b>1.10%</b>	<b>1.27%</b>	<b>2.20%</b>
	63.50	66.00	2.50	Gneiss			
	66.00	74.00	8.00	Gneiss			
	74.00	74.20	<b>0.20</b>	Gneiss	<b>0.01%</b>	<b>0.60%</b>	<b>0.60%</b>
	74.20	99.00	24.80	Gneiss			
	99.00	100.00	<b>1.00</b>	Gneiss	<b>0.02%</b>	<b>0.60%</b>	<b>0.72%</b>
100.00	112.70	12.70	Gneiss				
112.70	115.70	<b>3.00</b>	Gneiss	<b>0.02%</b>	<b>0.21%</b>	<b>0.61%</b>	

**NOTES:** Intercepts of >5.0m width and Assays of >0.4% Cu, >2.0% Pb & >2.0% Zn are highlighted in red.

Table 7. Drill Hole Database (KIER, 1982).

## Anomaly E (Continued)

Drillhole ID	From (m)	To (m)	Interval (m)	Lithology	Cu (%)	Pb (%)	Zn (%)
JD-8	0.00	2.00	2.00	Soil & Colluvium			
	2.00	3.00	1.00	<b>Diorite porphyry</b>			
	3.00	12.00	9.00	Gneiss			
	12.00	17.20	5.20	<b>Diorite porphyry</b>			
	17.20	27.00	9.80	Gneiss			
	27.00	28.60	<b>1.60</b>	Gneiss	<b>0.13%</b>	<b>2.21%</b>	<b>2.05%</b>
	28.60	32.00	3.40	Gneiss			
	32.00	35.00	<b>3.00</b>	Gneiss	<b>0.10%</b>	<b>1.27%</b>	<b>1.34%</b>
	35.00	36.70	1.70	Gneiss			
	36.70	39.10	<b>2.40</b>	<b>BRECCIA</b>	<b>0.15%</b>	<b>1.15%</b>	<b>1.40%</b>
	39.10	48.70	<b>9.60</b>	<b>BRECCIA</b>	<b>0.16%</b>	<b>1.14%</b>	<b>1.42%</b>
	48.50	51.00	2.50	Gneiss			
	51.00	52.30	<b>1.30</b>	<b>BRECCIA</b>	<b>1.73%</b>	<b>3.48%</b>	<b>6.35%</b>
	52.30	63.00	10.70	Gneiss			
	63.00	76.50	<b>13.50</b>	<b>BRECCIA</b>	<b>0.10%</b>	<b>0.40%</b>	<b>2.50%</b>
76.50	78.00	1.50	Gneiss				

**NOTES:** Intercepts of >5.0m width and Assays of >0.4% Cu, >2.0% Pb & >2.0% Zn are highlighted in red.

Table 7. Drill Hole Database (KIER, 1982).

## Anomaly C

Drillhole ID	From (m)	To (m)	Interval (m)	Lithology	Cu (%)	Pb (%)	Zn (%)
JD-9	0.00	1.00	1.00	Soil & Colluvium			
	1.00	18.80	17.80	Gneiss			
	18.80	19.50	<b>0.70</b>	Gneiss	<b>0.10%</b>	<b>0.75%</b>	<b>1.75%</b>
	20.10	20.90	0.80	<b>Sulphide vein</b>			
	20.90	22.00	1.10	Gneiss			
	22.00	26.00	4.00	Gneiss			
	26.00	26.20	<b>0.20</b>	Gneiss	<b>0.05%</b>	<b>0.10%</b>	<b>0.30%</b>
	26.20	40.00	13.80	Gneiss			
	40.00	41.30	<b>1.30</b>	<b>Sulphide vein</b>	<b>0.27%</b>	<b>1.60%</b>	<b>2.90%</b>
	41.10	44.00	2.90	Gneiss			
	44.00	44.10	0.10	<b>FAULT</b>			
	44.10	57.80	13.70	Gneiss			
	57.80	58.20	<b>0.40</b>	Gneiss	<b>0.10%</b>	<b>0.20%</b>	<b>0.50%</b>
	58.20	86.50	28.30	Gneiss			
	86.50	100.00	13.50	<b>Diorite porphyry</b>			

**NOTES:** Intercepts of >5.0m width and Assays of >0.4% Cu, >2.0% Pb & >2.0% Zn are highlighted in red.

Table 7. Drill Hole Database (KIER, 1982).

## Anomaly B

Drillhole ID	From (m)	To (m)	Interval (m)	Lithology	Cu (%)	Pb (%)	Zn (%)
JD-10	0.00	13.20	13.20	BRECCIA	0.10%	0.44%	3.30%
	13.20	25.50	12.30	BRECCIA	0.13%	0.60%	2.40%
	25.50	39.50	14.00	BRECCIA	0.30%	0.21%	6.05%
	39.50	52.00	12.50	BRECCIA	0.60%	0.11%	6.00%
	52.00	67.00	15.00	BRECCIA	0.30%	0.15%	5.50%
	67.00	80.50	13.50	BRECCIA	0.40%	0.10%	4.20%
	80.50	92.70	12.20	BRECCIA	0.80%	0.40%	7.10%
	92.70	106.50	13.80	BRECCIA	0.30%	0.10%	5.21%
	106.50	120.00	13.50	BRECCIA	0.25%	0.10%	3.60%
	120.00	138.00	18.00	BRECCIA	1.13%	0.44%	5.73%
	138.00	146.20	8.20	BRECCIA	0.26%	0.10%	3.70%
	146.20	150.00	3.80	BRECCIA			
	150.00	151.70	1.70	BRECCIA	0.40%	0.10%	6.30%
151.70	158.00	6.30	BRECCIA				
JD-11	0.00	3.50	3.50	Soil & Colluvium			
	3.50	33.00	29.50	Gneiss			
	33.00	47.00	14.00	BRECCIA	0.02%	0.05%	4.80%
	47.00	59.90	12.90	BRECCIA	0.23%	0.10%	2.95%
	59.90	72.00	12.10	BRECCIA	0.26%	0.10%	3.26%
	72.00	84.70	12.70	BRECCIA	0.30%	0.10%	3.70%
	84.70	102.00	17.30	Gneiss	0.24%	0.10%	3.81%
	102.00	142.00	40.00	Gneiss			
	142.00	143.00	1.00	Gneiss	0.02%	0.10%	1.10%
143.00	150.00	7.00	Gneiss				
JD-12	0.00	25.00	25.00	Soil & Colluvium			
	25.00	34.00	9.00	Gneiss			
	34.00	34.20	0.20	Gneiss	0.11%	0.05%	3.75%
	34.20	57.00	22.80	Gneiss			
	57.00	58.70	1.70	Gneiss	9.33%	0.45%	3.65%
	58.70	70.60	11.90	Gneiss			
	70.60	78.70	8.10	BRECCIA	0.45%	0.34%	4.20%
	78.70	80.20	1.50	BRECCIA			
	80.20	92.20	12.00	BRECCIA	0.22%	0.10%	3.81%
	92.20	105.00	12.80	Gneiss	0.25%	0.20%	3.10%
	105.00	132.00	27.00	Gneiss			
	132.00	177.00	45.00	Gneiss			
	177.00	177.20	0.20	Gneiss	0.15%	0.11%	1.05%
	177.20	181.10	3.90	Gneiss			
181.10	182.30	1.20	Gneiss	0.20%	0.10%	2.90%	
182.30	203.00	20.70	Gneiss				

**NOTES:** Intercepts of >5.0m width and Assays of >0.4% Cu, >2.0% Pb & >2.0% Zn are highlighted in red.

## 10.0 CONCEPTUAL EXPLORATION MODEL

### Magmatic-Hydrothermal Breccia Pipe Models

Magmatic-hydrothermal breccia-pipe hosted Cu-W mineralization has been identified at several deposits on the Korean peninsula, including at the Ilkwang (Fletcher, 1977), Dalseong (Heo et al, 2002), and the Donghae mines (Kim, 1987) within the Cretaceous Gyeongsang Basin. Sennitt (2010) has previously evaluated these tourmaline breccia-pipe hosted tungsten-copper-cobalt deposits and considers the mineralization and style of brecciation to be closely analogous to the breccia pipe-hosted deposits found in Chile, Mexico and Peru. The Jangheung prospect lies outside the Gyeongsang Basin and is of a different Cu-Pb-Zn mineralization style.

Breccia pipes consist of a vertical cylindrical- or conical-shaped pipe-chimney filled with blocks and clasts, which are surrounded by a vertical sheeted vein fracture system. Several theories have been put forward to explain the formation of magmatic hydrothermal breccia pipes, as discussed in the following models.

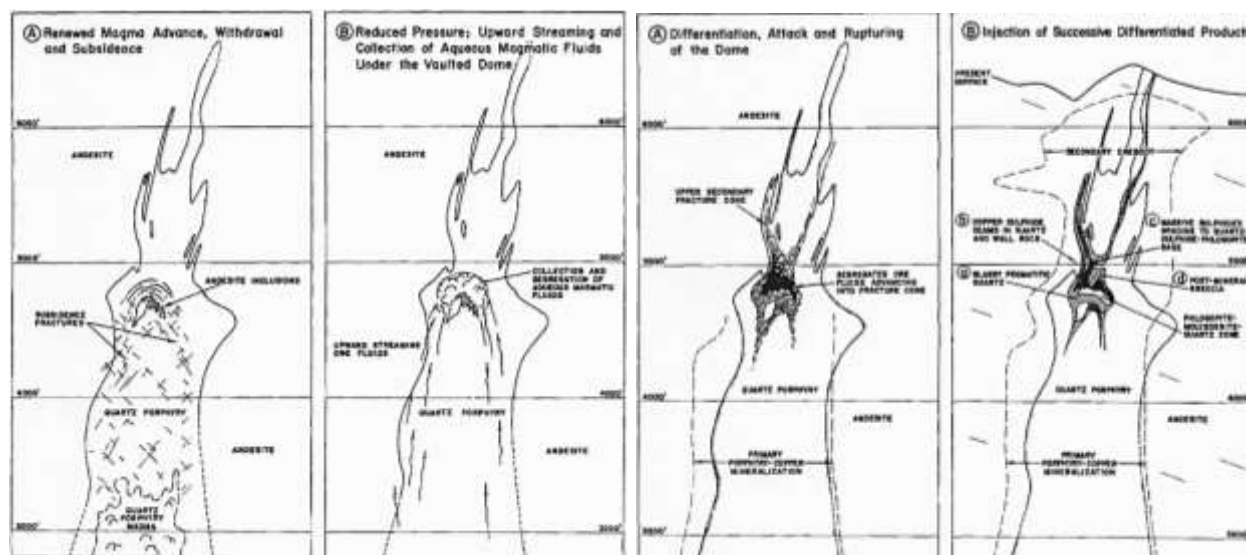
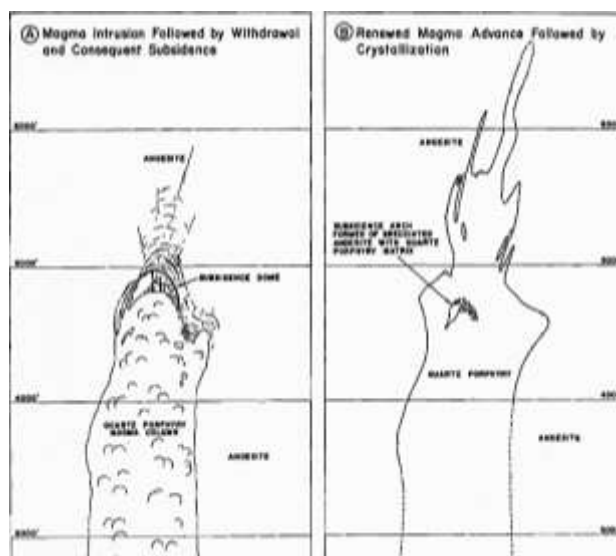
#### Magma Retraction & Subsidence Breccia Pipe Model (Perry, 1961)

Perry (1961) studied the physical geological characteristics of the Cu-mineralized breccia pipes found in the Cananea district (Mexico), concluding that they formed from aqueous magmatic fluids that concentrated at reduced pressures near the tops of subsidence columns.

In this model, a quartz porphyry plug magma is emplaced but then retracts, probably as a result of volcanic eruption elsewhere. This sudden magma loss produces a sudden reduction in pressure in the cupola, which in turn generates domical ring fracturing, subsidence and downward slumping of roof and wallrocks into a restricted breccia column.

Pegmatitic quartz representing the collection and segregation of aqueous magmatic fluids, crystallized above the cupola of the quartz porphyry plug.

Withdrawal, cooling and crystallization of the magma promoted the injection and collection of upward-streaming mineralizing fluids of silica, silicates and sulphides into the void spaces of the breccia column.



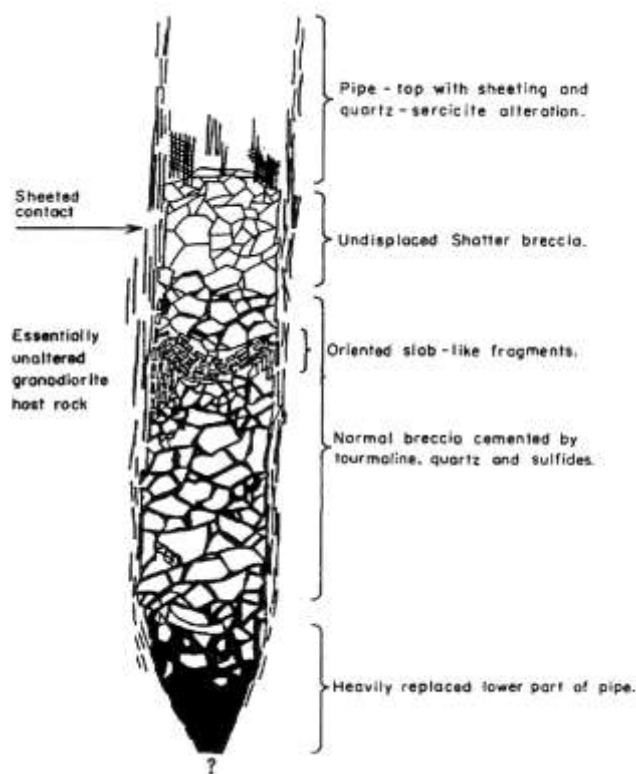
### Collapse Breccia Pipe Model (Sillitoe & Sawkins, 1971)

The tourmaline breccia pipes in Chile and Peru are located along a separate, but parallel belt to the porphyry Cu deposits of the high Andes, where they are emplaced into small, epizonal plutons of Late Cretaceous age.

Sillitoe & Sawkins, (1971) interpret tourmaline breccia pipes as post-magmatic hydrothermal collapse breccias, which formed as a result of the removal of rock by the corrosive action of hydrothermal fluids, over-pressuring, pressure quenching, CO<sub>2</sub> immiscibility and subsequent pressure reduction and gravitational collapse of the breccia. Continued upward passage of hydrothermal fluids through these uncemented breccia columns, results in the development of the replacement and open space-filling stages of mineralization.

The typical paragenetic sequence of these tourmaline breccia pipes can be summarized (Sillitoe & Sawkins, 1971) as:

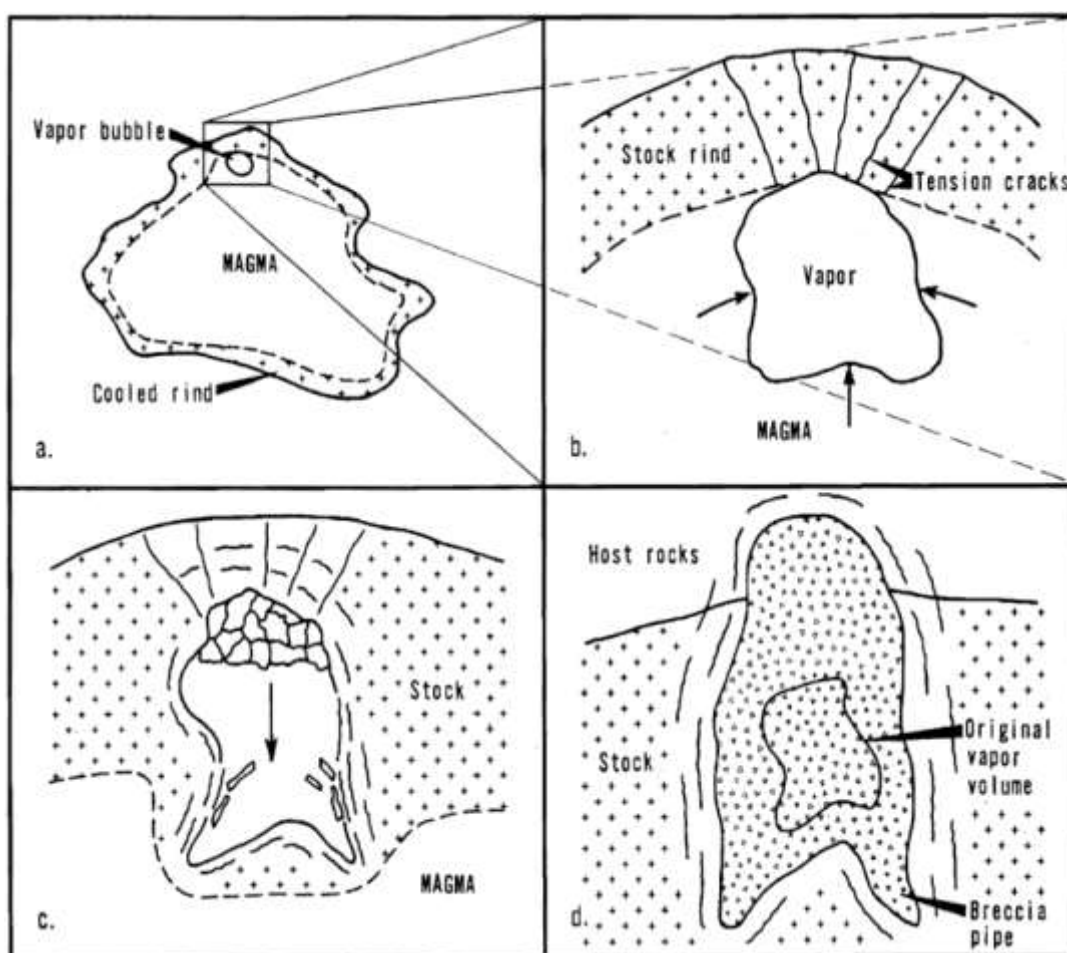
- ❖ Early replacement of feldspars altered to sericite and quartz, accompanied by some fracturing attributable to insitu chemical brecciation.
- ❖ Decompressive shock collapse breccia event, with platy, tabular clasts, often curved indicating decompression at the pipe margin and subsequent collapse.
- ❖ Early open space-filling by intense black tourmalinization ("schorl") accompanied by specularite and open-space filling granular quartz-sericite.
- ❖ Open space-filling mineralization stage. Early scheelite-arsenopyrite, then chalcopyrite-pyrite with native gold and molybdenite, followed by galena-sphalerite.
- ❖ Late-stage deposition of anhydrite-barite (Ca & Ba sulphates) and carbonates (dolomite-siderite-ankerite) as crystalline vugh-fillings and veinlets.
- ❖ Post-pipe magmatic and mineralization activity, comprising dykes and small bosses of porphyritic andesite, typically carrying rosettes of tourmaline.



**Magmatic Breccia Pipe Model (Norton & Cathles, 1977)**

Norton and Cathles (1977) propose the breccia void formed from the exsolution of magmatic water from the magma during emplacement of a stock/pluton, as depicted and summarized below.

- Magmatic water exsolves as a vapor bubble as a result of decreasing solubility within a melt, but is trapped beneath a cooling, crystallizing outer rind.
- The bubble becomes large enough and the cooling outer rind brittle enough for the bubble to break through and be released along tensional sheet cracks/fractures.
- Drop in hydrostatic pressure results in collapse of the sheet cavity by sheet fracturing.
- The pipe continues to grow until the void is filled and supported by breccia clasts.



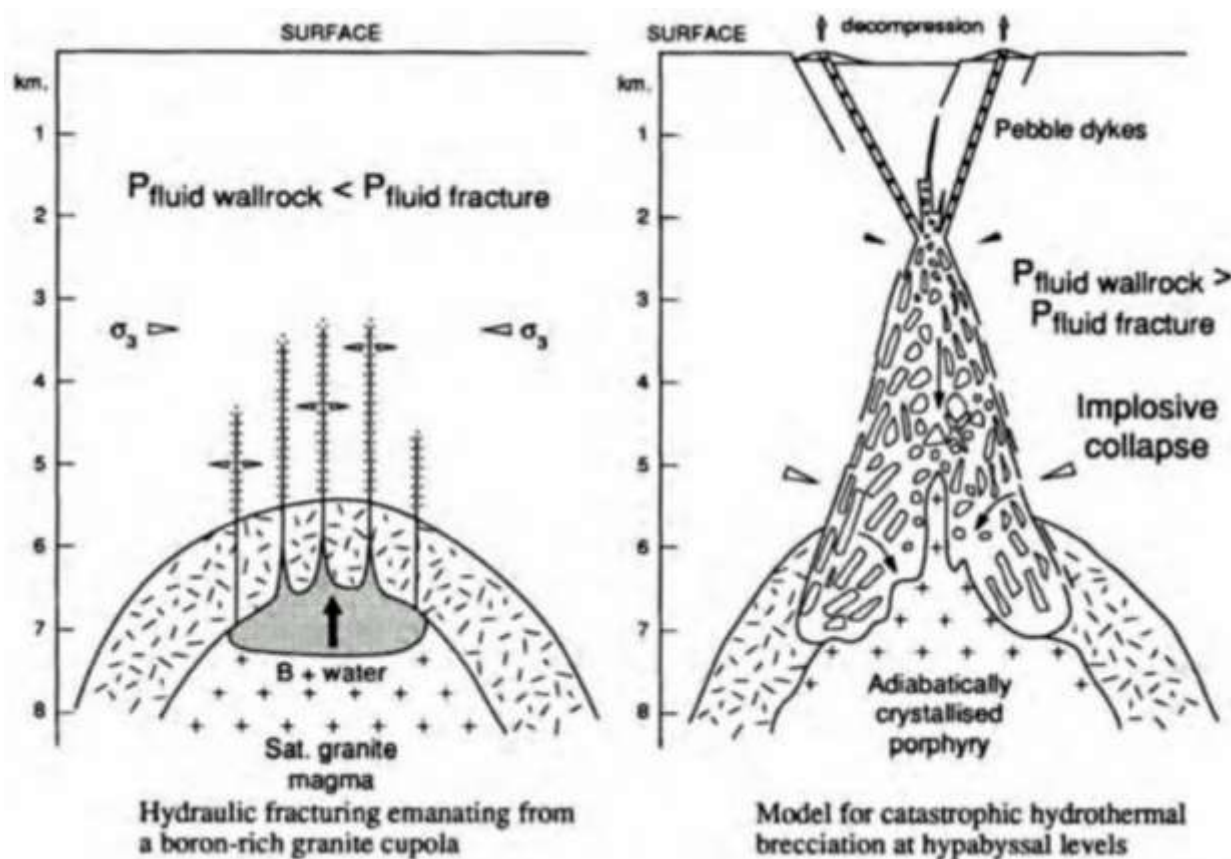
### Hyperbyssal Breccia Pipe Model (Halls, 1994)

Halls (1994) proposed a geological Model for the formation of a hyperbyssal hydrothermal breccia pipe, as depicted below.

The breccia pipe is developed as an inverted cone/carrot-shaped body interpreted as sitting above an inferred 'blind' porphyry intrusion at depth. As the granite magma rises, boron-rich fluids and volatiles accumulate in the cupola.

Fluid pressures build up in the overlying rocks as the intrusion rises, resulting in hydraulic fracturing "ring fractures" around the pipe, which then propagate and then penetrate upwards. When fluid pressures in the wallrocks exceed the fluid pressures in the overlying fractures, sudden decompression occurs.

Implosive collapse then follows the decompression event, along with subsequent adiabatic crystallization (due to heat loss) of the underlying porphyry intrusion.



### Magmatic-Hydrothermal Breccia Pipe Model (Sillitoe, 2010)

Sillitoe (2010) has subsequently revised his earlier geological model for the evolution of a magmatic-hydrothermal breccia pipe, as depicted.

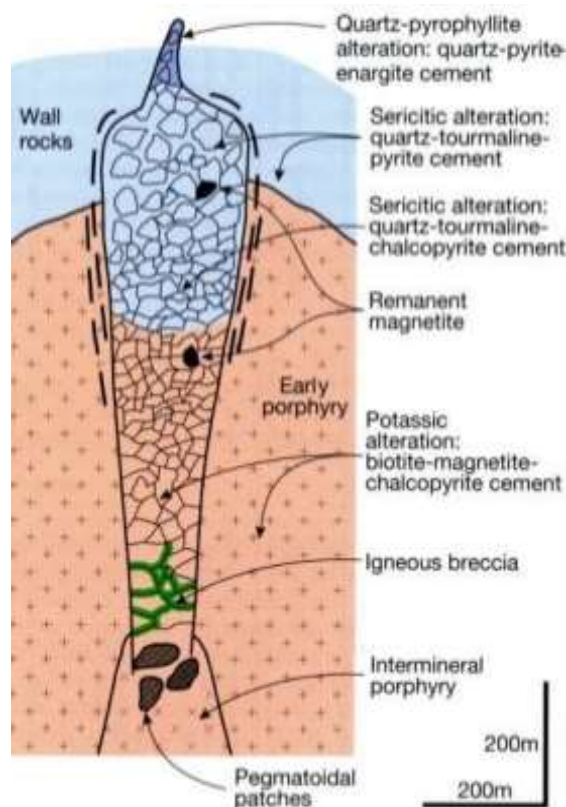
The breccia pipe is produced by over-pressured magmatic fluids to form a steep-dipping, cone-shaped pipe body, developed above a late-stage porphyry intrusion, that was emplaced into an early granodiorite intrusion.

The breccia pipe is normally blind to the surface and does not vent. They are characterized by the absence of tuffaceous material.

The breccia pipes are regarded as inter-mineral. Potassic alteration consisting of secondary biotite and magnetite may be present as an early stage. Potassic alteration typically predates the mineralizing event and may be present in clasts within the breccia.

Sericitic (phyllitic) alteration is better developed in the upper levels of the breccia pipe and surrounding country rock. The alteration is accompanied by quartz-tourmaline-pyrite cementation of the breccia.

Quartz-pyrophyllite alteration is developed as apophyses/bosses above the pipe. Quartz-enargite-pyrite cement can be present in this zone.



Igneous matrices are more common in the pipe at depth nearer the magmatic source, grading downwards into "igneous breccia" and then porphyry intrusion with pegmatoid.

### Intrusion-Related Breccia Pipe Model (Kirwin et al, 2018 & Kirwin, 2021)

Kirwin et al (2018) postulate copper-bearing tourmaline pipes form a distinct class of intrusion-related breccias, derived from fractionated granitic to granodioritic magmas. These intrusion-related Cu-tourmaline pipes are considered to develop at deep crustal levels (4-8km depth). Intrusion-related pipes tend to increase in size with depth displaying an "inverted cone" or "carrot" shaped morphology and can have vertical dimensions exceeding 1km.

Decompressive shock textures, "shingle breccias" and "UST" unidirectional solidification textures are commonly developed in the upper levels of intrusion-related pipes. Pegmatoid quartz is present at the base of the pipe. These features provide supporting evidence for deep crustal level emplacement.

Complex multi-element sulphosalt metal assemblages (Cu, Mo, Au, Ag, As, Bi, W, Pb and Zn deposited during a single event) characterize the intrusion-related pipes, which also tend to occur in clusters of multiple pipes. The highest metal concentrations are normally found near the inside margins of the intrusion-related pipes, particularly where there is intense development of shingle breccias.

The breccias are polymictic, with sericite and silica-altered wallrock clasts set in a tourmaline and sulfide-rich matrix. Breccia contacts with the surrounding country wallrocks are sharp and there is a well-defined halo away from the contact, characterized by sheeted quartz-sericite-sulfide veining.

In contrast, the copper-bearing pipes associated with porphyry copper deposits form at shallower depths (1-4km) and tend to be large, flaring upwards due to lower lithostatic pressures exerted by the wallrocks at shallower-level. A much simpler Cu-Mo association is also recognized in porphyry Cu environments.



### Common Features of Breccia Pipes

Of particular significance for exploration programs are the recognition of the common features observed in tourmaline breccia pipes associated with intrusion-related Cu deposits, which include:

- ❖ Breccia pipes tend to display an elongate vertical axis with a height to width ratio of >3:1. The pipe vertical extent can extend down to 2,000m depth. The elongate axis corresponds to the dominant structural trend.
- ❖ The breccia pipes tend to occur in “clusters” within a relatively small area. This offers multiple exploration targets. The density of pipes in a “cluster” should theoretically increase where conditions are more favorable for enhanced groundwater flow.
- ❖ There may be some linear structural control on localization of pipe, and this is probably the result of an existing major fault structure/predisposed line of weakness tapping an underlying magma cupola.
- ❖ In a global sense, numerous breccia pipes are found in the Andean volcanic and porphyry copper belt of Arizona, Mexico, Peru and Chile.
- ❖ Vertical sheeted veins and fractures (infilled by quartz/tourmaline) form a ring-shape above and along the margins of the breccia pipe.
- ❖ Breccia pipes terminate at higher levels and do not vent to the surface.
- ❖ Steep, inward-dipping tabular/slab-like “shingle” clasts are found along pipe contact margins (rip effect). The platy and tabular clasts are often curved, indicating a “decompression shock event” occurs at the pipe margin and subsequent collapse/downward settling of the suprajacent column.
- ❖ Horizontal slab-like clasts tend to be preferentially found in the upper roof of the breccia pipe contact zone.
- ❖ Breccia clasts are porous and apparently corroded. The scarcity of rock flour and the angularity of most clasts/fragments suggests fragment attrition or abrasion during collapse plays a minor role. The angular nature of clasts indicates the host rocks were solidified or nearly so at the time of brecciation. The presence of rounded fragments is considered to be due to spalling off of the softer, hydrothermally altered rims during collapse.
- ❖ Vugs and voids are usually well-developed within the breccia column, but are particularly evident in the upper portions of the pipe.
- ❖ Hydrothermal deposition of quartz, tourmaline and sulphides (usually complex polymetallic mineralogy with sulphosalts) occurred as a single paragenetic event immediately after the decompression shock “event”, during the subsequent collapse and settling of clasts within the pipe column.
- ❖ Brecciation tends to decrease in intensity with depth.
- ❖ Porphyry-matrix igneous breccia is commonly transitional between overlying open-space breccia and underlying porphyry intrusion.
- ❖ The upper-most parts of breccia pipes are characterized by oval-circular areas of quartz-sericite alteration. These are likely to produce recessive circular topographic depressions in the near-surface erosional/weathering environment, with the core of the pipe usually more prominent.
- ❖ Breccia pipes have a close affinity to quartz porphyry plugs and are commonly hosted within small epizonal granodiorite or quartz monzonite stock intrusions.
- ❖ Late stage, post-pipe magmatic activity consists of andesite porphyry and pebble dykes.

### Mineralization Zonation

Sillitoe and Sawkins (1971) recognized that the magmatic-hydrothermal breccia pipes exhibit similar mineral species and paragenetic sequence. Sulphide mineralization infills open spaces within the breccia pipe as cement and replacement of matrix and clasts.

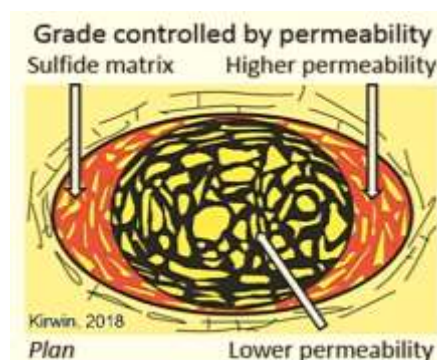
Fluid inclusion and mineralogic studies by Carlson and Sawkins (1980), Heo et al (2002), Skewes et al (2003) and Yang and Bodnar (2004) all indicate the initial hyper-saline, boiling or non-boiling hydrothermal mineralizing fluids were magmatic-derived, exsolving from an underlying cooling, crystallizing porphyry phase, under relatively high (>1 kbar) lithostatic pressures. Anderson et al (2009) indicate a supercritical, highly saline fluid condenses to a dilute aqueous vapor and a hypersaline brine. Progressive influx by cooler, low-salinity meteoric fluids follow,

precipitating sulphates and carbonates. The fluid inclusion, mineralogic and stratigraphic evidence indicates that the breccia pipes typically formed at paleo-depths of 1.4 to 3.6 km.

Mineralization typically consists of 3 paragenetic stages:

- ❖ Early-stage scheelite-arsenopyrite, consistent with a high-temperature regime.
- ❖ Middle-stage deposition of chalcopyrite-pyrite with native gold and molybdenite.
- ❖ Late-stage galena-sphalerite, consistent with a lower temperature regime.

Sulphide content is mainly controlled by permeability and tends to increase at the pipe margins and upper levels. Sulphide grain size also tends to decrease in size with depth, corresponding to the lower porosity-permeability encountered within the deeper levels of the pipe.



A vertical geochemical mineralization zonation pattern is evident within the Cu-mineralized intrusion-related breccia pipe at the Mammoth mine in Arizona (Anderson et al, 2009), including:

- ❖ Upper Ore zone, sulphide mineralization consists of pyrite-chalcopyrite as coarse-grained blebs infilling open spaces, accompanied by minor bornite-molybdenite-tennantite-scheelite-galena-sphalerite.
- ❖ Carbonate Zone (central zone), pyrite-chalcopyrite occur with trace bornite-molybdenite.
- ❖ Lower Zone, mineralization comprises disseminated chalcopyrite-bornite-molybdenite with trace pyrite-galena-sphalerite-chalcocite. The hydrothermal fluids probably exsolved from an underlying porphyry intrusive phase into the base of the breccia pipe.

#### Alteration Zonation

Breccia pipes will have higher permeability relative to surrounding rocks and initially the pipe will be filled with magmatic water and vapor, resulting in erratic alteration-mineralization. Later fluid flow through the pipe can produce a more extensive alteration zoning-reaction front away from the pipe because of increased porosity and permeability.

Early replacement stage alteration consists of feldspars altering to sericite and quartz, accompanied by some fracturing attributable to insitu chemical brecciation by Sillitoe and Sawkins (1971).

Early open space-filling stage is distinguished by intense black Fe-rich tourmaline (schorl), comprising euhedral black prisms, radiating acicular crystals (rosettes), or bundles of olive-green fibers. Platy specularite and lesser magnetite are commonly associated with the tourmaline. Specularite tends to replace mafic minerals and early chlorite (Skewes et al, 2003). Kirwin (2021) indicates hornfels alteration is commonly developed above the breccia pipe.

Late-stage deposition of carbonates (dolomite, siderite, ankerite and calcite) as crystalline vugh-fillings and veinlets is common. A late generation of euhedral pyrite may accompany dolomite.

A vertical alteration zonation pattern was recognized by Anderson et al (2009) within the intrusion-related breccia pipe at the Mammoth Cu mine (Arizona). The *Upper Ore Zone* is dominated by quartz, with subordinate calcite-dolomite and minor apatite. The *Carbonate Zone* (central-middle zone) is dominated by quartz and carbonate minerals, comprising dolomite, ankerite and calcite, along with minor chlorite, anhydrite and specularite. The *Lower Zone* is characterized by lavender-coloured anhydrite and specularite but minor quartz, sericite and ankerite. Anhydrite and specularite contents tend to increase with depth. Quartz crystal size and clast alteration intensity decreases with depth, suggesting magmatic hydrothermal fluid-wallrock reactivity also decreases with depth. Kirwin (2021) observes that anhydrite-barite (Ca & Ba sulphates) is more common in the larger, upward-flaring pipes associated with porphyry Cu deposits.

### Geophysical Characteristics of Breccia Pipes

The Jangheung base metal breccia pipe ore bodies at Anomalies B, E and F have small ovoid-shaped plan dimensions of ~40m diameter (but with significant vertical depth extents). The breccia pipes therefore have a relatively discrete target “footprint”. There is also a likely linear fault structural control on pipe localization/emplacement.

The base metal mineralization contains conductive sulphides (pyrite and galena), with typical combined contents of >5% conductive sulphides, indicating EM and IP geophysical methods can be used as viable exploration methods. In addition, the hydrothermal mineralization in the breccia pipes may contain anomalous radioactive minerals (brannerite reported by Sillitoe & Sawkins, 1971), suggesting a radiometric geophysical survey could also be useful to locate mineralized pipes using the U-channel.

Given the nature of the topography at Jangheung, comprising moderately-steep slopes, relief ranging from 50m to 670m, and a dense thorny “gashin” vegetation cover, a drone UAV or helicopter-borne EM system would be more effective than a fixed-wing system. These platforms would enable relatively close-spaced lines (50m) and higher density sampling at lower flight heights (drone UAV system particularly). Case studies have shown that data from helicopter-borne surveys is as good as, if not better than ground EM data and can be used to site drill holes. Thus, a drone UAV fitted with an EM system is considered the most cost-effective means to explore for base metal breccia pipes at Jangheung, as well as detect ‘blind’ hidden deposits at depth.

A typical helicopter-borne time-domain EM system consists of a transmitter-receiver loop, that is towed approximately 30-50m below the helicopter so the loop is ~35m above the terrain. A helicopter speed of 35-45 knots provides a sampling interval of 8-10m. When compared to fixed-wing systems, helicopter TEM allows for deeper penetration, higher spatial resolution, better resistivity discrimination and ultimately the detection of more subtle anomalies at depths of >300m at low operating frequencies in the 25Hz to 30Hz range.

In most surveys a magnetometer is incorporated into the configuration between the EM loop and the helicopter, providing additional significant geophysical information.

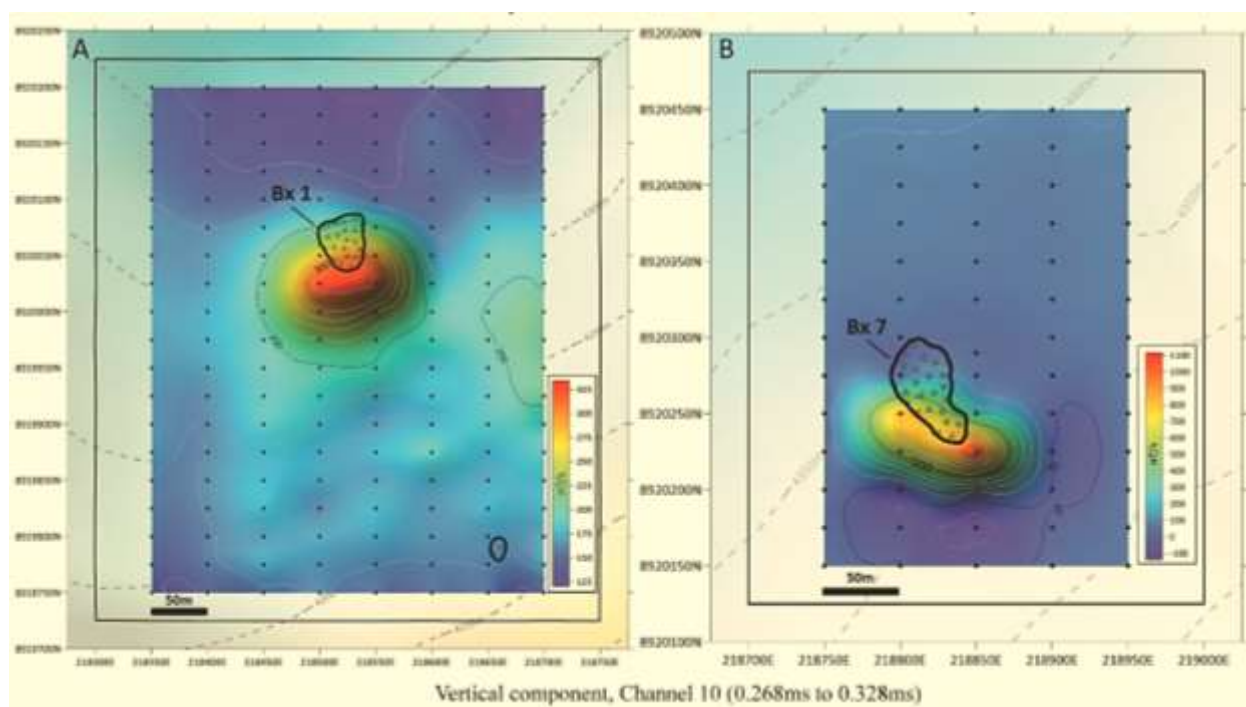


Figure 31. Examples of Time Domain EM geophysical survey used to detect conductive sulphides within breccia pipes (*Chakana Copper* company presentation, 2020). The surface trace of each breccia pipe coincides well with a conductive anomaly.

## 11.0 PROPOSED EXPLORATION PROGRAM

### Exploration Potential

Magmatic-hydrothermal breccia pipes can make attractive exploration targets, because of the following characteristics:

- ❖ Common in porphyry camps globally.
- ❖ Can be world-class deposits.
- ❖ Vertically extensive. The predictable sub-vertical geometry facilitates cost-effective drill testing.
- ❖ The pipes can form inverted cone geometry with a larger diameter at depth.
- ❖ The pipes in clusters above a granitic cupola. It is possible to develop a central mill facility fed by ores from multiple pipes.
- ❖ Typically contain relatively high grades, particularly on the pipe margins.
- ❖ Small area of the pipe has minimal surface footprint and minimizes environmental disturbance.
- ❖ The pipe's vertical geometry is particularly amenable to extraction by the *Sustainable Mining by Drilling* method. This method improves the project economics, safety, environmental and significantly lowers the project risk profile.

Several features of the base metal mineralization at Jangheung suggest good potential for a significant polymetallic deposit, including:

- ❖ Breccia pipe-hosted mineralization containing high Cu and Zn grades over significant widths occurs at **Anomalies B, E and I** and appear to be vertically-dipping inverted cone structures.
- ❖ The Cu-Pb-Zn mineralization is open at depth and along strike. Interpretation of the drill sections indicates the breccia pipes at **Anomaly B** and **Anomaly E** both have diameters of at least 40m and all appear to be vertically-dipping, with inverted cone/carrot shaped morphology.
- ❖ The diorite porphyry intersected in drill holes JD-1, JD-2 and JD-3 of **Anomaly I** and drill holes JD-7 and JD-8 of **Anomaly E** contains stockwork and disseminated sulphide mineralization, accompanied by carbonate alteration.
- ❖ Some lateral geochemical zonation may be evident in the drill results, with **Anomalies B and I** being Zn-dominant and **Anomaly E** being Cu-dominant. The high-grade Cu mineralization is located on the margins of the pipes.
- ❖ The mineralized diorite porphyry recognized at **Anomaly E and I** is a potentially larger Exploration Target than the breccia pipes.
- ❖ The breccia pipes at Jangheung appear to occur in clusters above a diorite porphyry cupola.
- ❖ The presence of at least 16 soil geochemical anomalies suggests additional 'blind' mineralized pipes and structures may remain undetected in the Jangheung area.
- ❖ Only 5 of the 16 breccia pipe outcrops with soil geochemical anomalies have been drill-tested to limited depth (< 100m). Numerous unexplored breccia pipes remain to be tested.
- ❖ The regional foliation trend is moderate dip to the NW, suggesting more preserved breccia pipes are possible in this direction

Interpretation of satellite imagery of the Jangheung project area has identified several recessive circular features that potentially represent sericite alteration zones above or around large breccia pipe targets for future exploration.

The individual breccia, geochemical and geophysical Exploration Targets identified by KIER (1982) are summarized in the following sections.

### Anomaly A

Anomaly A has a 60m x 10m breccia outcrop orientated NW, with a coincidental 80m x 50m weak Cu-Pb soil geochemical anomaly. Anomaly A was not drill tested by KIER.

Anomaly A lies 120m to the north of Anomaly B. The Pb soil geochemistry suggests Anomaly A may potentially be linked at depth with Anomaly B. Anomaly A is regarded as a priority Exploration Target. Additional geophysical surveys and drill testing is warranted in this area.

### Anomaly B

Anomaly B displays a 150m x 150m strong Cu-Pb-Zn soil anomaly. It has an elliptical-shaped breccia outcrop with 150m diameter at surface, perhaps with some WNW structural control. It was drill tested by KIER (1982) with holes JD-10, JD-11 and JD-12. The drilling confirmed the outcrop at Anomaly B is a breccia pipe with an inverted cone, carrot-shaped morphology.

Excellent results were recorded from the 3 drillholes at Anomaly B, including 146.2m @ 2.45% CuEq. These results suggest Anomaly B has an Exploration Target of 3Mt size grading 1-2.5% CuEq.

Anomaly B is the largest breccia pipe mapped at Jangheung. It is a high-priority Exploration Target and additional geophysical surveys and drill testing is warranted.

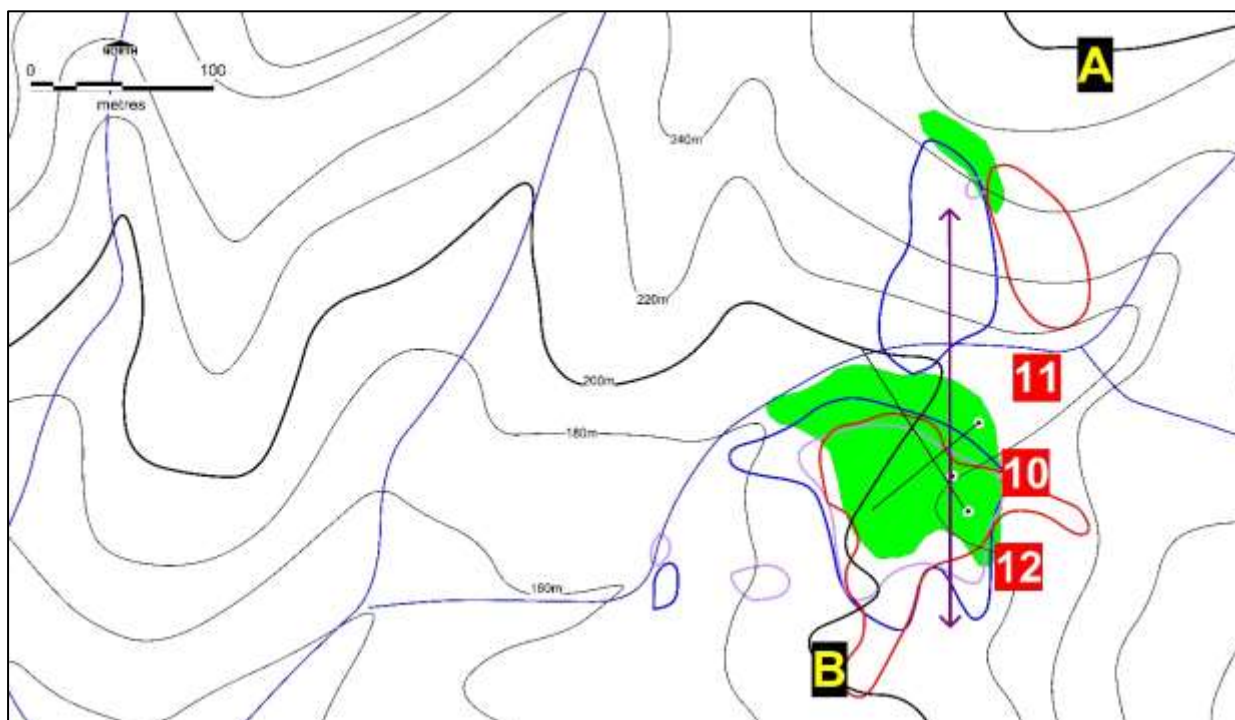


Figure 32a Drill Plan Anomaly B. The soil geochemical anomalies are shown (Cu = red line, Pb = blue line & Zn = grey line), along with breccia pipe outcrops in green. The Drill Section is shown as the purple arrowed line.

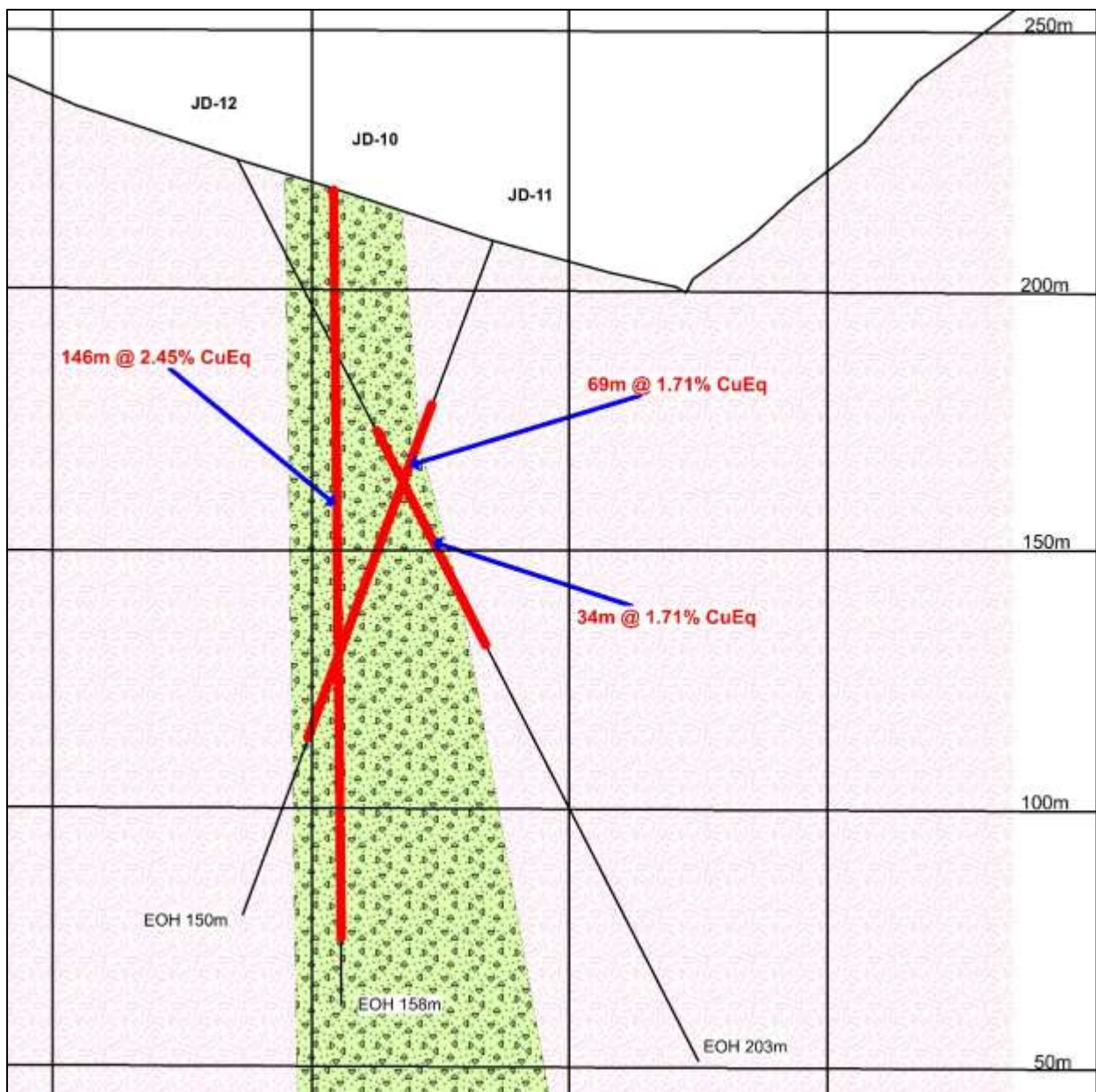


Figure 32b. Anomaly B - Drill Hole Section (Looking West).

**Anomaly C**

Anomaly C has a small 60m x 30m breccia outcrop orientated EW. There is a coincidental Cu-Pb-Zn soil anomaly of 50m x 50m area. The breccia lies on the margin of mapped diorite porphyry intrusion.

Anomaly C was tested by a single drill hole JD-9, which intersected several narrow sulphide veins. The hole terminated in diorite porphyry, but no samples-assays were reported from this zone.

Anomaly C lies about 200m NW of Anomaly D. A mafic dyke was mapped striking NW-SE suggesting there is some underlying structural control and possible connection with Anomaly D.

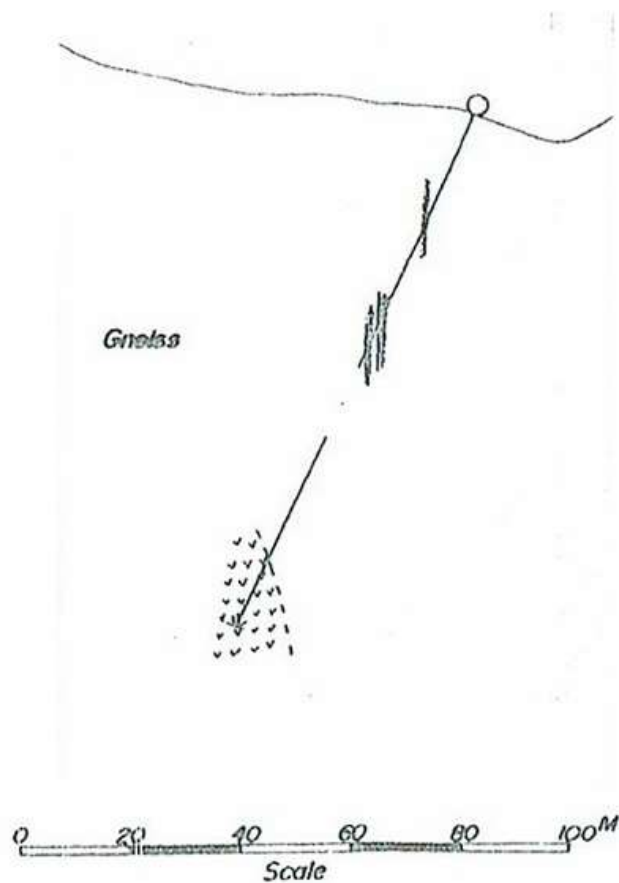


Figure 32c. Drill Hole JD-9, Anomaly C (KIER, 1982).

### Anomaly D

Anomaly D has a 25m x 25m breccia outcrop and a coincidental 50m x 10m weak Cu-Pb soil anomaly. A mafic dyke was mapped about 100m to the NE of Anomaly D, striking NW-SE, suggesting a possible structural connection. Anomaly D was not drill tested by KIER.

### Anomaly E

Anomaly E exhibits an elongate very strong Cu-Pb-Zn geochemical anomaly over a 200m x 150m area. A small 75m x 50m breccia outcrop is coincidental with this geochemical anomaly, which is also connected to Anomaly F. Some "leakage" anomaly extensions of 200m x 25m suggest there is evidence for some underlying WNW structural control. The soil anomaly extends easterly away from the drilling, possibly suggesting mineralization may continue down slope towards the east.

Anomaly E was tested by drill holes JD-5, JD-6, JD-7 and JD-8, with good intercepts reported in all drill holes except JD-6. The copper assays are particularly noteworthy and indicate the Anomaly E breccia pipe is Cu-enriched compared to the other more zinc-dominant pipes. Also of particular significance, mineralized diorite porphyry was intersected on the margin of the breccia pipe.

A 5m deep prospecting pit was excavated at Anomaly E and a bulk sample of high-grade breccia ore material collected for metallurgical testwork described in a later section (KIER, 1982). This bulk sample assayed 143g/t Ag, 5.43% Pb, 4.30% Zn, 1.12% Cu, 1.68% Mn. Au was assayed but not detected.

Anomaly E is probably linked to Anomaly F indicating there is potential for a much larger area of mineralization at depth. Anomaly E is regarded as the highest ranked priority target. Additional geophysical surveys and further drill testing is warranted in this area.

### Anomaly F

Anomaly F has a 60m x 50m breccia outcrop, with coincidental strong Cu-Pb-Zn soil geochemical anomaly that is connected to Anomaly E. Anomaly F was not drill-tested by KIER.

Anomaly F is probably connected to Anomaly E and so is a priority Exploration Target. Geophysical surveys and drill testing is warranted in this area.

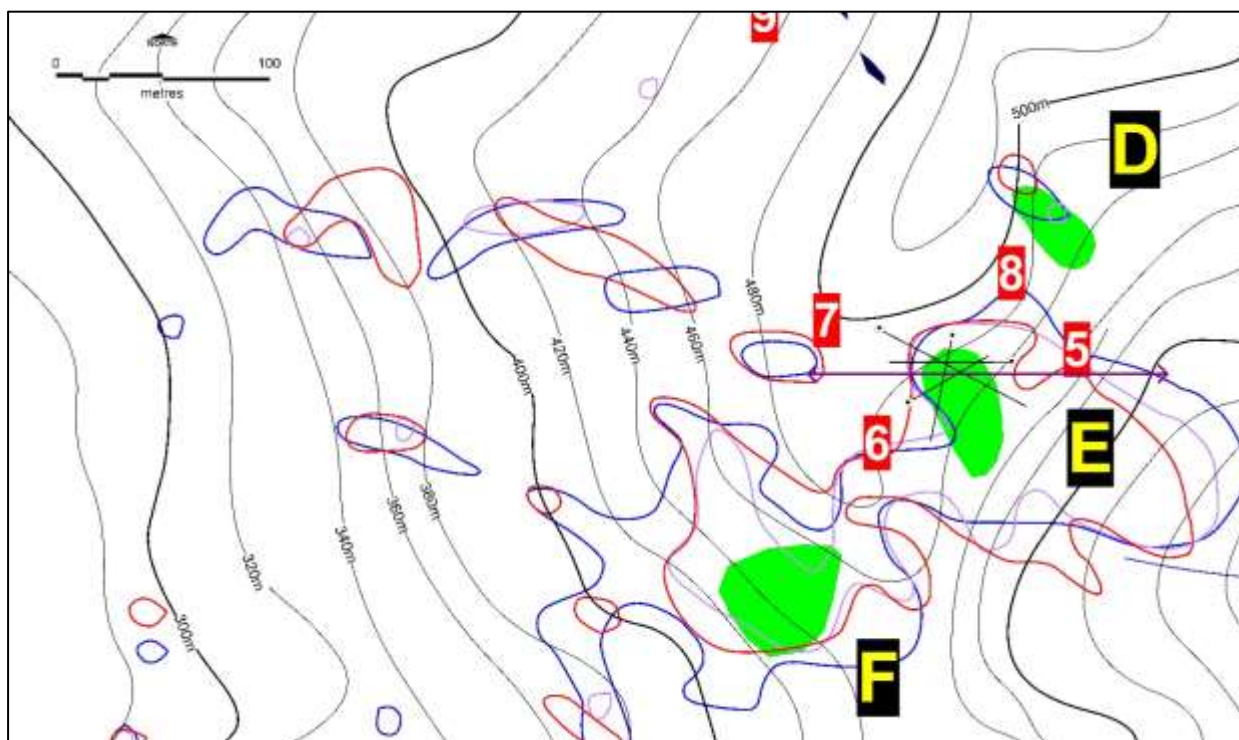


Figure 32d Drill Plan Anomaly E. The soil geochemical anomalies are shown (Cu = red line, Pb = blue line & Zn = grey line), along with breccia pipe outcrops in green. The Drill Section is shown as the purple arrowed line.

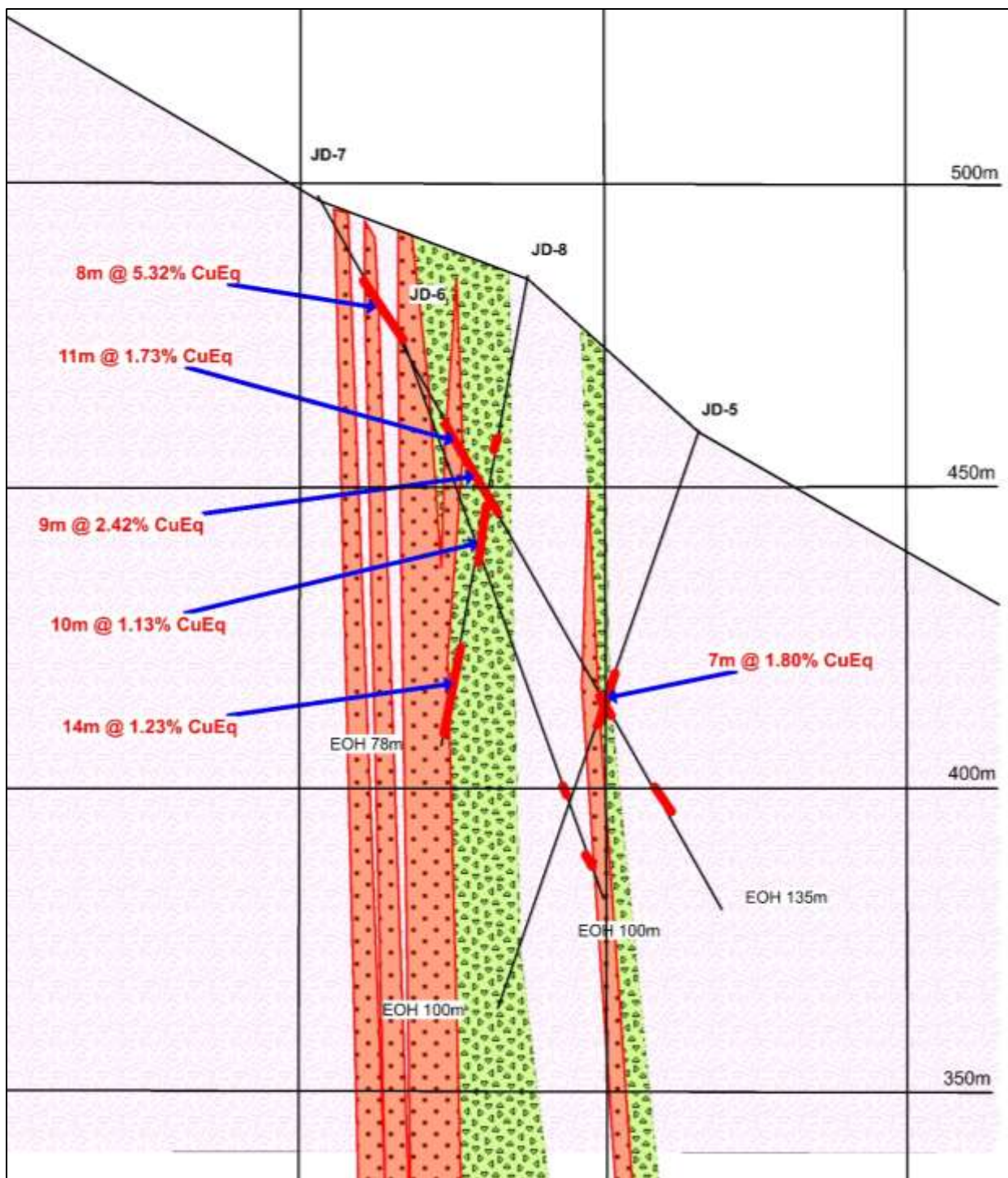


Figure 32e. Anomaly E - Drill Hole Section (Looking North). A diorite porphyry has intruded granite gneiss with a strongly-mineralized breccia pipe developed on its margins/contact zones.

**Anomaly G**

Anomaly G consists of a small 50m x 25m weak Pb soil geochemical anomaly. It has a coincidental weak VLF-EM anomaly. There is no breccia outcrop mapped.

Anomaly G was tested by drill hole JD-4. Only 1 sample-assay of a narrow fault was taken. Diorite porphyry was intersected frequently in the hole, but was not sampled-assayed.

It is not known why this Anomaly was selected for drill testing by KIER in preference over better geological, geochemical and geophysical targets.

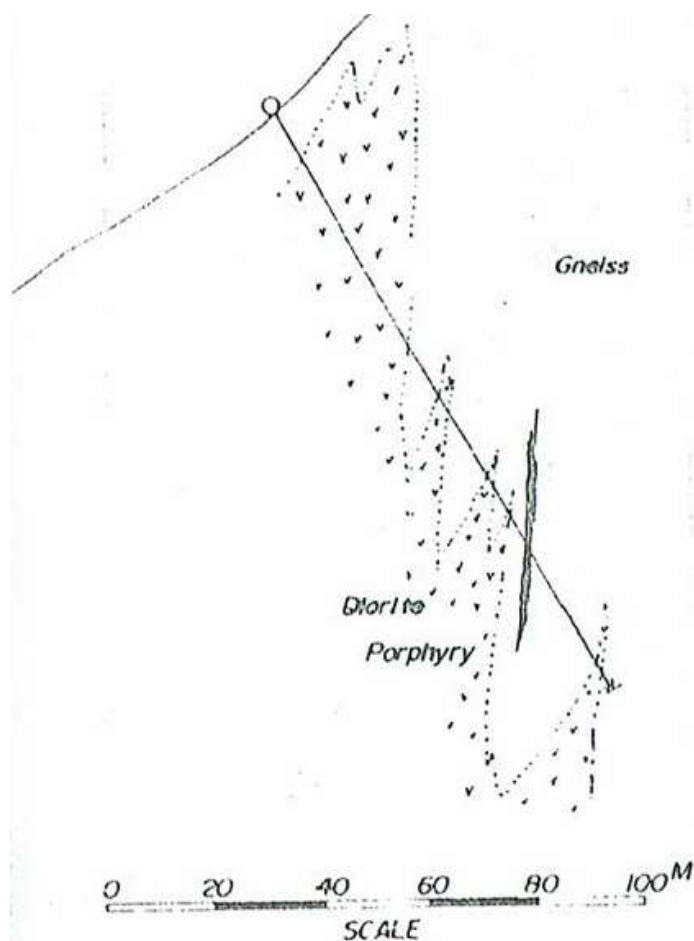


Figure 32fb. Drill Hole JD-4, Anomaly G (KIER, 1982).

### Anomaly H

Anomaly H has a 150m x 100m breccia outcrop that exhibits some ENE structural control (possible underlying connection to Anomaly I, located about 200m to WSW). A 150m x 100m area of weak Cu-Pb-Zn soil geochemical anomalism is coincidental with the breccia outcrop. Anomaly H also has a coincidental strong EW trending VLF-EM anomaly. Anomaly H was not drill tested by KIER.

Anomaly H has a relatively large outcrop size and is regarded as a priority Exploration Target. Further geophysical surveys and drill testing is warranted in this area.

### Anomaly I

Anomaly I consists of a 100m x 100m breccia outcrop and a coincidental 100m x 100m area of very strong Cu-Pb-Zn soil geochemical anomalism. The breccia outcrop was tested by drill holes JD-1, JD-2 and JD-3. Thick Zn-dominant mineralization was intercepted in all holes, associated with stockworks and disseminations within a diorite porphyry intrusion (best result of 6m @ 4.10% CuEq).

A strong ENE trending VLF-EM anomaly lies immediately north of the breccia, but this feature was not drill tested. In addition, a NNE trending magnetic low feature lies immediately west of the breccia and was also not drill tested.

Anomaly I is a priority Exploration Target. Geophysical surveys and further drill testing is warranted-recommended in this area.

### Anomaly J

Anomaly J has a small 30m x 20m outcrop of breccia and a coincidental small 50m x 25m weak Cu-Pb-Zn soil geochemical anomaly. Anomaly J was not drill tested.

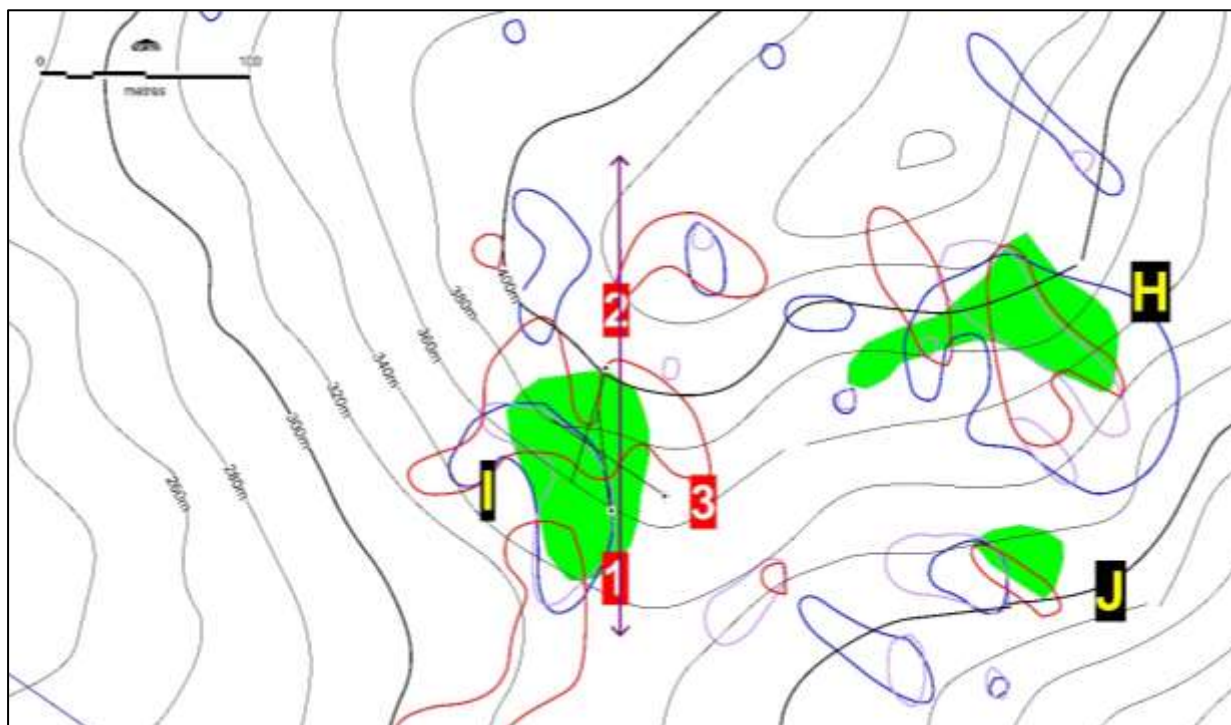


Figure 32g Drill Plan Anomaly I. The soil geochemical anomalies are shown (Cu = red line, Pb = blue line & Zn = grey line), along with breccia pipe outcrops in green. The Drill Section is shown as the purple arrowed line.

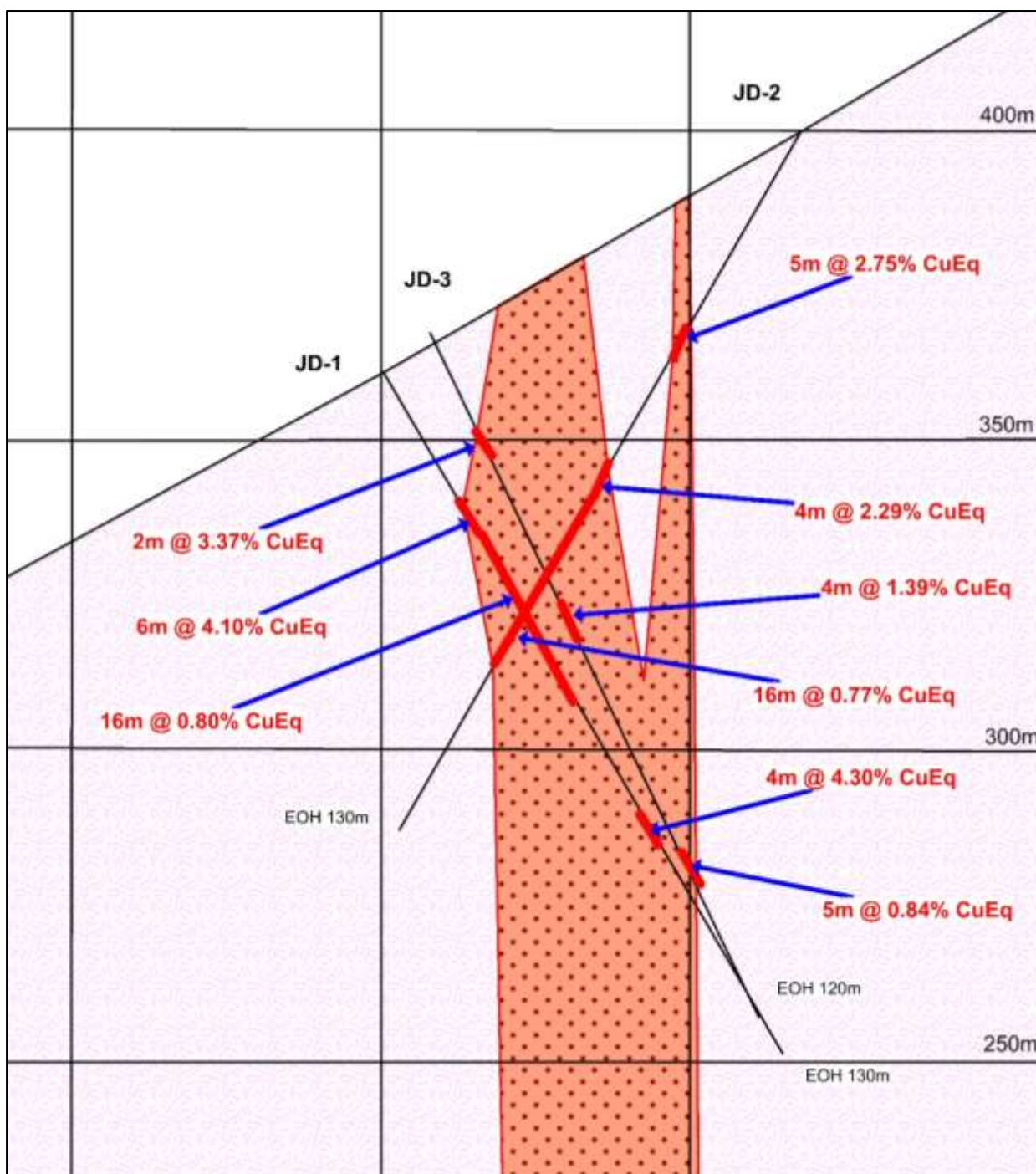


Figure 32h Anomaly I - Drill Hole Sections (Looking West). Stockwork and disseminated mineralization is associated with a carbonate altered diorite porphyry intrusion.

### Anomalies K, L & M

Small outcrops of breccia are mapped at Anomaly K (60m x 25m), about 100m to the east at Anomaly L (30m x 15m) and 100m south at Anomaly M (15m x 15m). These breccia outcrops have coincidental weak Pb-Zn soil geochemical anomalies of 50m x 25m size. A strong EW trending VLF-EM anomaly appears to connect Anomalies K & L. Anomalies K, L & M were not drill tested.

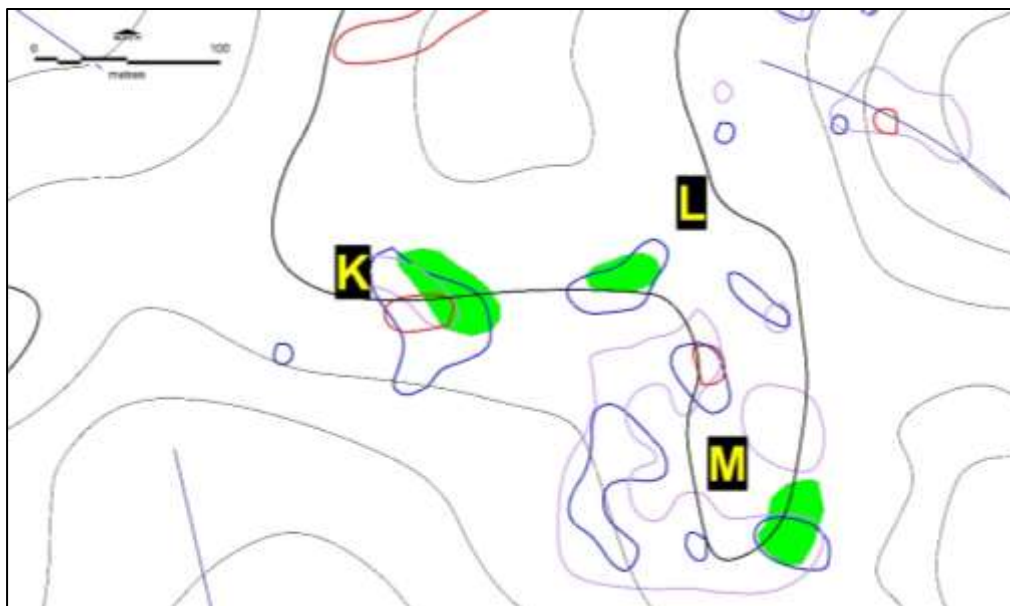


Figure 32i Anomalies K, L & M Plan. The soil geochemical anomalies are shown (Cu = red line, Pb = blue line & Zn = grey line), along with breccia pipe outcrop in green.

### Anomaly N

Anomaly N is a small isolated breccia outcrop (60m x 20m) with a coincidental 100m x 50m Cu-Pb-Zn soil anomaly. Anomaly N was not drill tested.

### Anomalies O & P

Small breccia outcrops are mapped at Anomaly O (20m x 15m) and Anomaly P (40m x 15m) which could be connected by an underlying NW structure. Both outcrops display coincidental 75m x 50m weak Pb-Zn soil geochemical anomalies. Anomalies O and P were not drill tested.

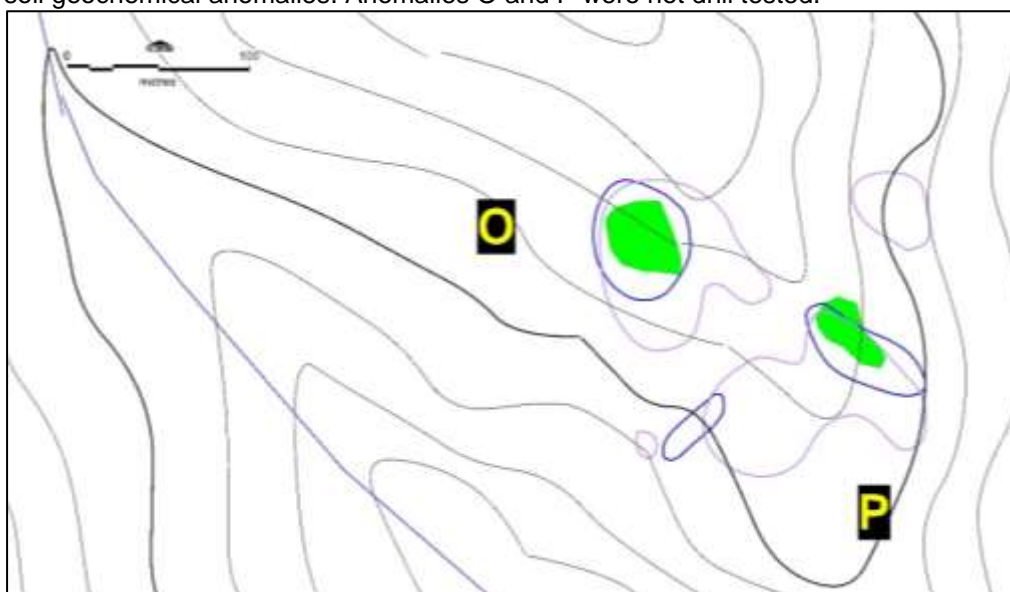


Figure 32j Anomalies O & P Plan. The soil geochemical anomalies are shown (Cu = red line, Pb = blue line & Zn = grey line), along with breccia pipe outcrop in green.

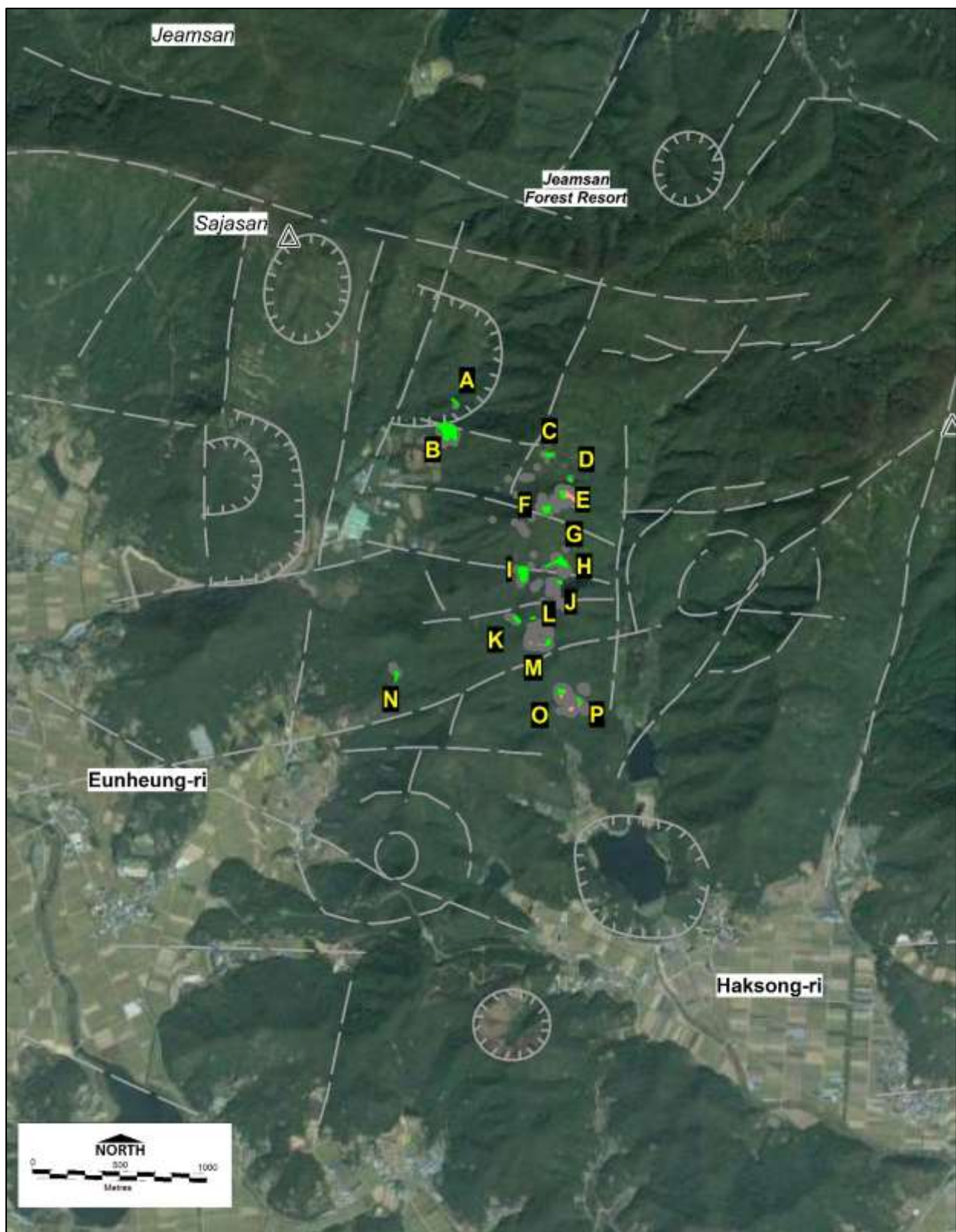


Figure 33. SPOT Satellite Image Jangheung Cu-Ag-Zn-Pb Project. (SK Energy & Centre National d'Etude Spatiales, 2014) downloaded from Google Earth. Interpretation of the imagery has identified several recessive circular features that potentially represent sericite alteration zones above or around large breccia pipe targets for future exploration.

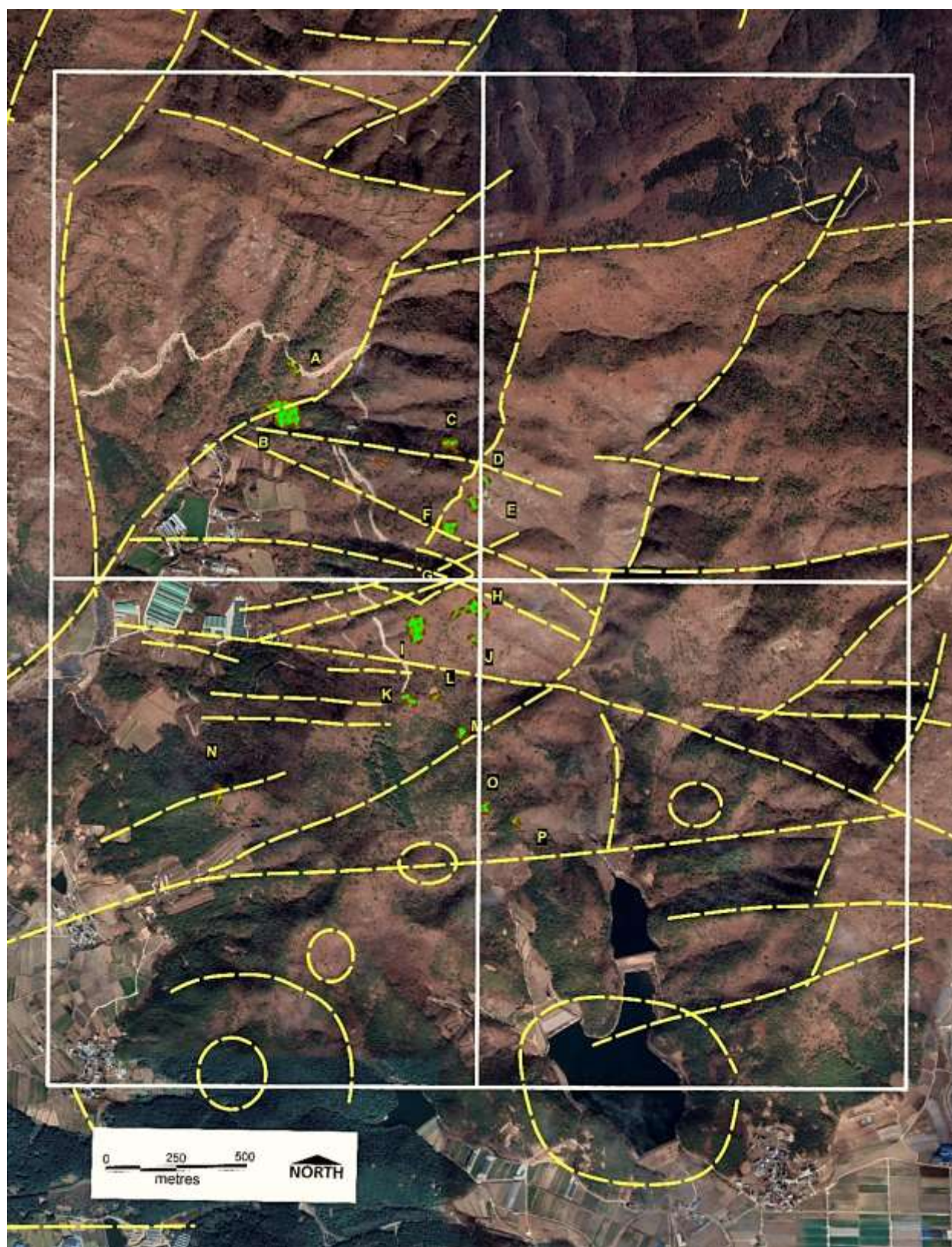


Figure 34. Satellite Image of Jangheung Cu-Ag-Zn-Pb Project showing interpreted structures (Maxar Technologies, CNES, Airbus, 13/02/2021).

## Exploration Program

### Objectives

A staged exploration program is proposed to evaluate the Exploration Targets identified in this report. The primary objective of this exploration program is to locate and test Exploration Targets for an initial Phase I drill program.

Should this Phase I drill program intercept significant mineralization to warrant further evaluation, additional work would probably involve follow-up resource definition drilling, resource estimate, followed by detailed metallurgical, engineering and economic studies.

### Recommended Initial Exploration Program

The following Exploration Program is recommended for the Jangheung project:

1. Geological mapping & sampling at 1:5,000 scale of the Jangheung project.
2. 1:5,000 scale digital topographic data purchased for use as a base map.
3. Worldview 3 satellite image acquisition. Band ratioing may be useful in identifying clay alteration.
4. Close-spaced (50m line spacing) drone UAV Magnetometer and VLF-EM geophysical survey.
5. Soil geochemical surveys over Exploration Targets.
6. Drill targets identified after review of above survey results.
7. Access tracks re-established, geologically mapped and sampled.
8. Phase 1 Drilling Program (10 holes x 200m = 2,000m HQT).

### Recommended Exploration Budget

The cost structure for exploration programs in South Korea is based on unit costs established from >28-years operational experience. The recommended Exploration Budget for the Jangheung project is presented in the Table below (No contingency has been provided for in this budget estimate).

**Table 8. Recommended Exploration Budget.**

COST CODE	Unit Cost (US\$)	Quantity Units	AMOUNT (US\$)
Geological Mapping & Sampling (days)	\$1000	20 days	20,000
UAV Drone geophysical survey (Line km)	\$450	170 km	77,000
Consultant Geophysicist Data Processing & Interpretation	\$2000	5 days	10,000
Soil Geochemical Surveys (days)	\$40	800 samples	32,000
Rock chip sampling (samples)	\$60	100 samples	6,000
Satellite Imagery base map & DEM (US\$/image)	\$10,000	1	10,000
Excavator Hire-Site Preparation (\$/hr)	\$200	140 hrs	28,000
Site Access Fee/Security Bond (\$/site)	\$2,000	10 sites	20,000
Drilling HQT & Devicore BBT + DeviGyro hire (\$/m)	\$150	2000m	300,000
Laboratory Geochemical Analysis (US\$/sample)	\$60	2000 samples	120,000
Landman-Logistics (\$/day)	\$200	10 days	2,000
Field Assistant (\$/day)	\$200	100 days	20,000
Geological Consultant & CP (\$/day)	\$1000	40 days	40,000
Junior Geologist (\$/day)	\$200	50 days	10,000
Airline Travel (International Return)	\$5000	2	10,000
Vehicle Fuel (\$/day)	\$20	100 days	2,000
Hotel Meals & Accommodation (\$/pp)	\$80	71 days	6,000
Site Office - Field Depot Rent (\$/month)	\$1000	12 months	12,000
<b>TOTAL=</b>			<b>\$725,000</b>

### Drone UAV Magnetometer & Electro-Magnetic Survey

A close-spaced, drone UAV combined Magnetometer and Electro-Magnetic (EM) geophysical survey is recommended over the Jangheung project area, covering the known breccia pipe outcrops.

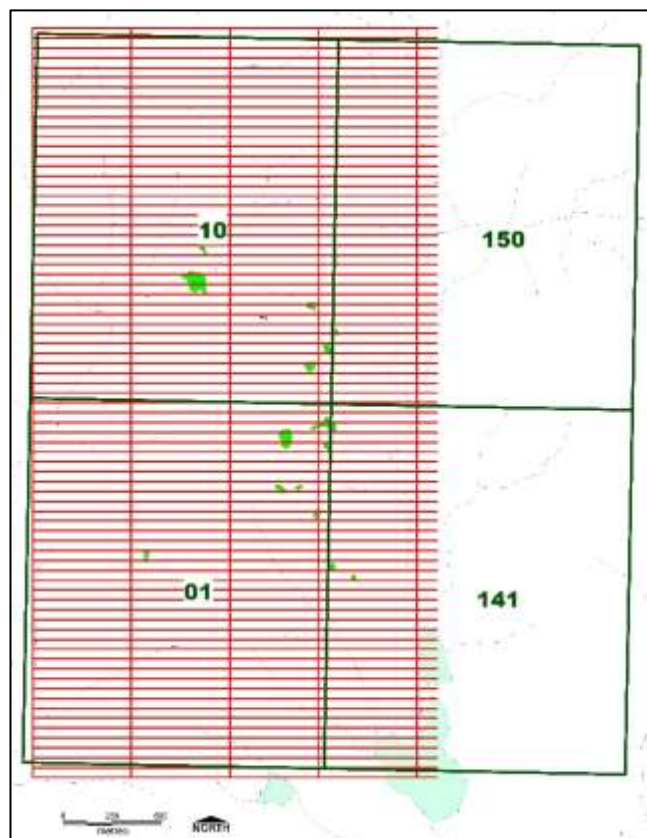
The presence of varying amounts of conductive sulphides (such as pyrrhotite and pyrite) associated with chalcopyrite-galena-sphalerite mineralization within breccia pipes of 40m diameter, suggests that EM could be used as a viable exploration tool. The hilly terrain and moderately steep forested slopes, with relief ranging from 100m to 750m and a relatively discrete target “footprint” is a challenge for safe helicopter, fixed-wing operations and ground surveys.

The EM system consists of a transmitter/receiver loop that is towed below the airship such that the loop is a nominal 35m above the terrain. This system allows for deeper penetration, higher spatial resolution, better resistivity discrimination and ultimately the detection of more subtle anomalies. A depth penetration of 300m is possible with this system. A magnetometer is incorporated in the configuration, providing additional significant geophysical information.

Case studies have shown that data from helicopter-borne surveys is as good as, if not better than ground EM data and can be used to site drill holes.

Using a line spacing of 50m, with east-west orientated flight lines over a 2000m x 3800m area, a total of 77 flight lines are required. A further 5 tie lines orientated north-south should be used to help correct the survey. The total line km is estimated as 173 Line km. The key parameters of the survey are tabulated below.

Survey Direction	Length (m)	No of Lines	Line Metres
East-West Grid Survey Lines	2,000	77	154,000
North-South Tie Lines	3,800	5	19,000
<b>TOTAL Line Metres =</b>			<b>173,000</b>



KIGAM have developed a specially-designed airship, fitted with magnetometer and electro-magnetic instruments which could be chartered to undertake the survey. The airship is a remotely controlled drone navigated by GPS control system and ground operator. The KIGAM airship offers numerous advantages over helicopter or fixed-wing systems, including a much slower speed to provide greater sampling density, high accuracy, better resolution, good terrain-following capability, very safe, as well as much lower operating cost.



The KIGAM airship drone and proposed Survey Grid.

### Drone UAV Magnetometer & Electro-Magnetic Survey

GEM Systems supplies a new lightweight VLF “towed bird” designed for low-altitude c-drone UAV geophysical mapping surveys. The GSM-90AVU(B) is a Very Low Frequency (VLF) Electromagnetic Method (EM) survey instrument which maps electromagnetic resistivity in the ground and is suitable for mineral or water exploration, bedrock mapping, fault detection for earthquake research, locating underground pipelines, or other near subsurface surveying tasks. The unit passively picks up the continuous broadcasts from time signal or military naval transmitters around the world at frequencies below 30kHz with two sensors (each tuned to a different transmitter), measuring vertical deviations due to the ground conditions below the sensors. In the case of South Korea, the useful transmitter stations are at Northwest Cape Australia (NWC; 22.3KHz) and Ebina, Japan (NDT; 17.4KHz). In areas where transmitter coverage is poor, a local transmitter can be used.

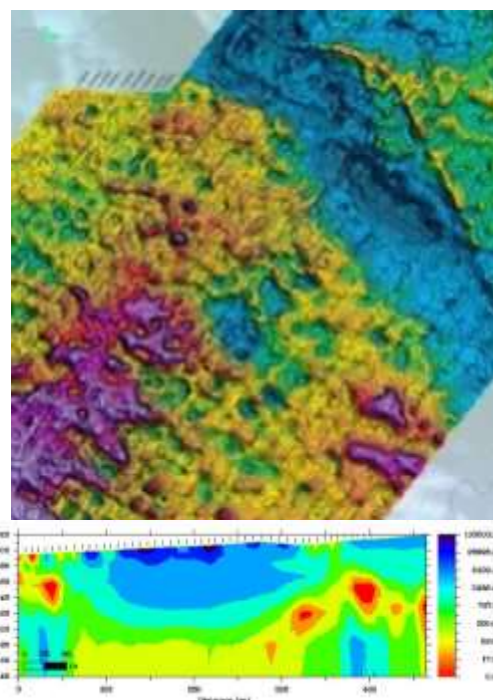
The rugged VLF-EM bird is designed to be towed from any VTOL (Vertical Takeoff and Landing) c-drone which can lift the 6kg load, for example the *DJI Wind4/Wind8*, *DJI Matrice 600 Pro* models, the *Freefly Alta-8*, the *Vulcan Black Widow*, or the *Versadrones Heavy Lift Octocopter*. The flight path is planned and prepared in advance with an autopilot such as *Pix4D*, running back and forth along predefined GPS waypoints. The c-drone UAV solution provides precise data cost-effectively compared to ground or aircraft-based measurement.



Flying at low altitude (30m) with the bird on a 10m tow line, at a minimum speed of 10m/s to minimize drag, a c-drone UAV can cover ground 6-10 times faster than a walking operator, in all types of terrain, be flown at night, in poor visibility conditions, and over dangerous topography.

The unit transmits XYZ format data over a radio link to a ground base station, comprising a collapsible radio mast, and optimized Panasonic Toughbook (running *GEMDAS* and *GEMLink+*, GEM’s bespoke software for data acquisition and file transfer, respectively). *Emtomo’s VLF2DMF* software is used to convert the multifrequency source data to graphic images.

The GSM-90AVU(B)’s 1.3Ah onboard lithium battery will outlast the flight time of most large c-drones; the battery can be swapped out if necessary. The bird’s length is 1.5m. Operating temperature range is -40°C to +50°C. GEM provide client-customized system (bird, radio antenna, ground control station) with a three-year warranty.



### Soil Geochemical Surveys

Close-spaced soil geochemistry surveys (10m sample site spacing) are recommended over targets generated by the VLF EM geophysical survey. These surveys will help define surface geochemical patterns for Cu, Pb, Zn and Ag. The elements As, Bi, Mo can be used as indicators to help target drill holes.

### Phase 1 Drilling Program

An initial Phase 1 Drilling Program is proposed, with a minimum recommended program comprising 10 diamond drill holes for 2,000 metres of HQ core (average 200m hole depth), with at least 3 Exploration Targets tested by 3-4 holes each. Holes should be angled at 50-70° to maximize penetration across the breccia pipes.

HQ Triple Tube diamond core is recommended to maximize recovery of massive sulphide minerals (minimizes disturbance to core, limiting losses of sulphides to water flows). HQ core permits a large representative sample to be recovered, maximizing the potential for geological information, geochemical sampling, geotechnical data and metallurgical sample size. The drill core should be orientated, as this maximizes geological and geotechnical data on vein, fracture, joint and bedding orientations (suitable tools include *Reflex ACT III* or *DeviCore BBT*. Downhole survey using a *DeviGyro* to provide an accurate down hole survey. A Competent Person should be appointed for the Project to supervise the drilling program.

### Logging Methods & Sequence

Processing of drill core should involve the following sequence:

- Core Orientation & Markup into metre intervals
- Core recovery determined
- Core Tray Photography
- Specific Gravity determinations
- Logging
- RQD determined
- Structural orientation readings (bedding, foliation, veins, fractures, joints)
- Geotechnical data for use in engineering.
- Geophysical measurements (magnetic susceptibility, gamma counts).
- Sampling (1/4 core for assay, 1/4 core for metallurgy, 1/2 core visual reference)
- Collar surveying using a DGPS

### QA/QC Protocols

QA/QC procedures should be adopted and include blanks (quartz chips) and suitable standards (certified reference materials) regularly inserted every 20 samples.

### Laboratory Analytical Methods

The closest ISO accredited and certified laboratories to South Korea are located in Brisbane or Vancouver (operated by *ALS Global*, *Actlabs* and *SGS*). The target metals are Ag, Cu, Pb, Zn plus Au, Co, Bi, In, Mn, Mo, Sb and Te. Recommended ALS Laboratory analytical methods are:

1. QAR-01. Quarantine & Customs Fee. \$0.50/sample.
2. LOG-22. Receival and Log each Sample. \$0.80/sample.
3. CRU-21. Dry and Crush each Sample. \$1.15/sample.
4. PUL-31. Pulverize 250g each Sample. \$6.10/sample.
5. Au-AA26. Au analysis by 50g Fire assay and AAS analysis. \$14.05/sample.
6. ME-MS61 Multi-Element Package (48 elements), 4 acid digest and ICP-AES. \$40.85/sample.
7. RTN-21. Return of Pulp & Coarse Reject samples to client.
8. BAT-01. Administration Fee. \$34.00/Batch

ME-MS61 includes the elements Ag, Al, As, Ba, Be, Bi, Ca, Cd, Ce, Co, Cr, Cs, Cu, Fe, Ga, Ge, Hf, In, K, La, Li, Mg, Mn, Mo, Na, Nb, Ni, P, Pb, Rb, Re, S, Sb, Sc, Se, Sn, Sr, Ta, Te, Th, Ti, Tl, U, V, W, Y, Zn & Zr. For very high sulfide content, an oxidizing fusion method may be required to completely digest the matrix.

### Alteration Mineralogy

The Hyperspectral Mineralogy of a rock sample can be determined with method **HYP-PKG**, using the dried coarse rejects from the drill core samples. It is a cost-effective method using a combined package of **TerraSpec® 4HR scanning** and **aiSIRIS™** spectral interpretation software. Mineral assemblages and spectral parameters are provided in EXCEL spreadsheet format. Cost is <\$14.50/sample.

### Drill Rigs

The typical *Hanjin DNB-16D* rubber track-mounted diamond drill rig is illustrated in the photograph below. The key features of the Korean drilling rig are:

- ❖ Track-mounted, enables the rig to shift by itself to next site and fit onto tight pads, minimizing environmental disturbance.
- ❖ Capable of drilling HQ diameter core to 300m depth and NQ to 500m depth.
- ❖ Capable of drilling angled holes between 45-90° dip.
- ❖ Drill crew comprises a driller and offsider and is independent of the exploration team.
- ❖ Korean drilling standard work practice is a single 12-hour shift per day, 6 days a week, with 1 day a week (Sunday) for maintenance and crew rest.
- ❖ The rig typically drills a conservative 25m per shift, depending on local ground conditions. An average of 600 metres can be expected to be completed each month.



### Logistics Considerations

#### Landowner Access Clearance

Negotiation with the surface right landowners is required to enable site access for drilling operations. A cost of \$2,000 per drill hole should be provided for in the budget for private landowners. Government land operated by the Korean Forestry Service requires a “security bond” to be lodged prior to activities, which is refunded after rehabilitation of the site is completed. The *Security Bond* is calculated on the basis of land area to be disturbed.

#### Access & Site Preparation

The hilly terrain, soil and talus scree cover, together with thick secondary regrowth vegetation and poor outcrop make access and geological mapping difficult within the project area. Existing forestry tracks and access to each anomaly should be re-opened with a small excavator and exposures geologically mapped in detail.

A small excavator is required to prepared drill sites and access tracks for the drill rigs. A relatively flat area of about 10m x 20m is required for a safe working environment at each site. The track mounted drill rig is highly maneuverable and can fit onto tighter drill pads, requiring only minimal site preparation.



#### Fuel Supply

A local *SK Energy* fuel service station is located in Jangheung. Most service stations operate their own small fuel bowser trucks for delivering diesel fuel direct to customers (see photograph), enabling the drill rigs and other equipment to be refueled directly on site.

#### Water Supply

A small water tank is normally used by the drillers to provide ready-use water supply to the drill rig. Depending on local site conditions, a water pump can be used to pump from creeks with sufficient water, or a small water tanker is hired for the duration of the program, to continuously cart water to the 2 drill rigs from nearby dam or perennial river-creek sources.

### Accommodation

The town of Jangheung is situated 7km (20 minutes drive) from the Project area. Good quality hotel-motel style accommodation is available in Jangheung and even closer at Sumumpo Beach. Internet is usually available in the motel room. Numerous restaurants in Jangheung offer a wide variety for breakfast and dinner meals, but are limited at Sumumpo.

### Support Vehicle

A second-hand *KIA Motors Bongo* or a *KIA Ceres 4WD* trayback light truck is recommended for purchase to be used as a support vehicle for drilling operations.

The vehicle can be used for personnel transport from Hotel to site and depot, core collection and bulk equipment carriage (1-tonne capacity). In its 4WD version, with agricultural tyres fitted, the *Bongo* or *Ceres* is an ideal support vehicle, highly manoeuvrable and able to climb steep hills.



### Site Office & Field Depot

A site office is required for geological supervision, storing field equipment, logging drill core, core processing, sample collection and sample dispatch. Sturdy tables are required to rest the core on for logging in an open air setting. Integrated with the site office, a field depot is required to store drill core and field consumables. Both the office and depot need to be secure weatherproof facilities and provide a comfortable working environment. Electrical power is required for the core saw, as well as tap water supply for lubrication/cooling of the saw blade. Ideally, the depot should be away from residences because of the noise generated by the core saw.

The core trays and consumables can be stockpiled at the depot and collected as required. Upon completion of the drill program, steel welded storage racks for the split core trays can be made up and are best placed on a concrete slab for stability. Upon completion of the drilling program, the 4WD vehicle can be stored within a lock up garage at the site depot.



### Supervision & Labour

A Korean junior geologist should be employed to assist the drilling program. This geologist will supervise sample dispatch, logging, excavator site preparation, organizing rig logistics and act as interpreter. This geologist can communicate effectively with the CP ex-pat consulting geologist and liaise with the driller and field assistant team.

A landowner liaison officer should be employed to negotiate access and liaise with the local community. Ideally this person should be familiar with drill rig logistics. One or two Field Assistants should be sourced from the local community to assist with the exploration program with sampling and general labour duties.

## 12.0 METALLURGY

Petrological studies by KIER (1982) indicated the following characteristics of the mineralization at Jangheung:

- ❖ Sphalerite is the dominant mineral species, with grains ranging in size from 2.85mm down to 20µm.
- ❖ Sphalerite grains commonly contain 10µm sized inclusions of chalcopyrite, pyrite and covellite.
- ❖ Galena and chalcopyrite grains are commonly intergrown with sphalerite.
- ❖ Galena grains range in size from 150-300µm.
- ❖ Chalcopyrite grains range in size from 10-350µm.
- ❖ Covellite is observed as grains up to 1.6mm size, but also commonly occurs as minute 10µm sized exsolution inclusions and spots within individual sphalerite grains.
- ❖ Screen sizing distribution tests using Tyler Mesh sieves indicated 39% of Zn, 40% of Cu and 50% of Pb is <75µm in size.

The complex carbonate and oxidized ores in the supergene zone are usually difficult to recover using conventional flotation processes. The ores at Jangheung were initially investigated by Hwang and Yang (1977) and further metallurgical studies undertaken by KIGAM's *Mineral Processing Division* in Daejeon. A bulk sample was collected from a 5m deep prospecting pit excavated at **Anomaly E** (original Area B), which assayed:

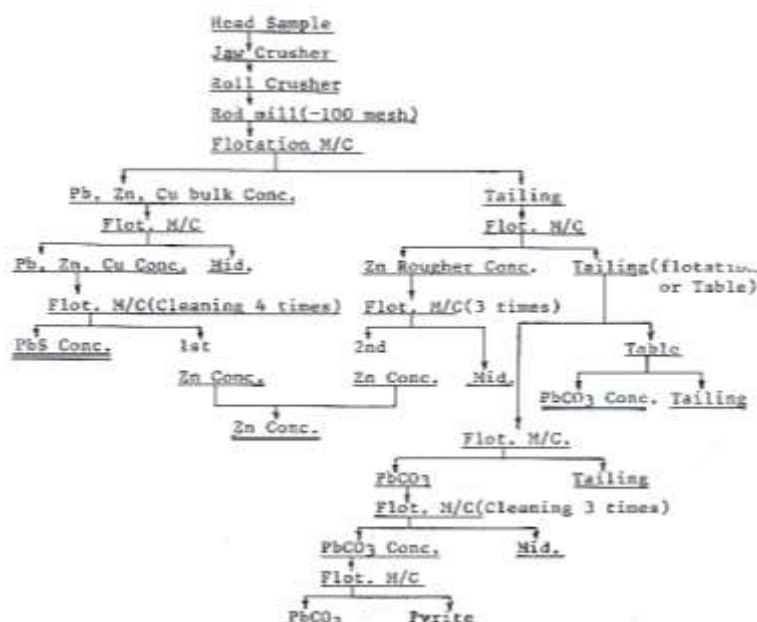
- ❖ 143g/t Ag, 5.43% Pb, 4.30% Zn, 1.12% Cu, 1.68% Mn. Au was not detected.

The metallurgical studies evaluated a variety of 'modifier', 'collector' and 'frother' agents, commonly used at that time in the conventional flotation process.

The metallurgical program testwork flowsheet is shown at right.

The testwork indicated the most suitable "collector" reagent was KEX (ethyl xanthate). Modifying the pH varied the recoveries of Cu, Pb and Zn, with the best recoveries obtained using the "modifiers" NaCN and Na<sub>2</sub>CO<sub>3</sub>. Pine oil was found to be the best "frother" agent.

In conjunction with the flotation testwork, gravity concentration using tabling was also employed to recover a cerussite (lead carbonate) concentrate.



Three mineral concentrate products were ultimately produced:

- A. A Zinc flotation concentrate grading 45.0% Zn, 7.2% Pb & 3.50% Cu.
- B. A Lead flotation concentrate grading 62.4% Pb, 4.4% Zn, 3.8% Cu & 1170g/t Ag.
- C. A Lead carbonate tabled gravity concentrate grading 67.0% Pb, 1.99% Zn & 0.73% Cu.

Metallurgical studies will be required to determine the optimum flowsheet for Jangheung. It is expected that modern processing technologies will result in better recoveries and higher quality products.

## 13.0 CONCEPTUAL MINING & MILLING OPERATION

### Conceptual Mining Operation – Sustainable Mining by Drilling

*Korean Metals* envisages mining the vertical breccia pipes using a combination of Tracked RC and Tracked Pile Top RCD drill rigs, both of which are manufactured in South Korea.

A tracked RC drill rig (Hanjin DNB-16Multi-Purpose drill rig) is used to drill an initial vertical RC hole through the mineralized breccia pipe. Geological logging and continuous sampling of the RC drill cuttings can be used as grade control.

The initial RC hole acts as a pilot hole for a “stinger” attachment fitted to the wide-diameter drill bit of the *Buma CE* Pile Top RCD. The pilot hole guides the stinger and hence the Bottom Hole Assembly Drill Bit, as well acting as a “hole-opener” initiation of rock breakage for the Drill Bit as Pile Top RCD drilling proceeds.

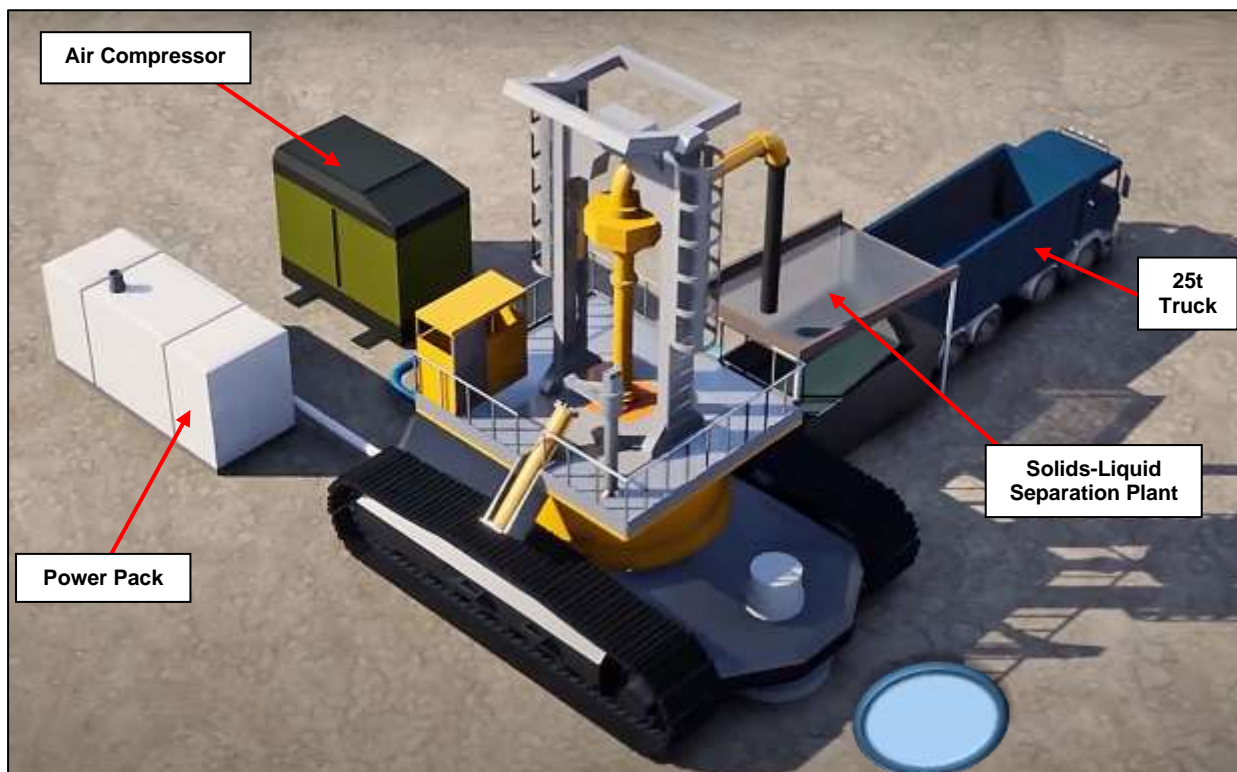


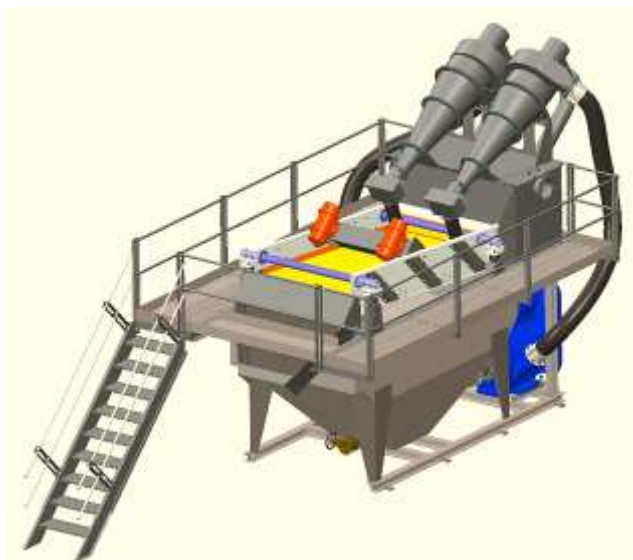
Figure 35. Conceptual Pile Top RCD mining operation, showing the main equipment components on site.

### Conceptual Beneficiation Plant

In the Sustainable Mining with Drilling operation, the lifted Drill Cuttings can be used as “Run of Mine” Ore feed for the Mill.

The Drill Cuttings can be pumped directly to a nearby Mill or beneficiated at/near the drill sites using various technologies, including hydrocyclones, vibrating screens, centrifugal screws, dense media separation, or jigs. Water recycling using these solids-liquids separation technologies helps minimize water losses (estimated to be <10%).

The Drill Cuttings can be potentially beneficiated on site by 1mm screening. A combination of **Dense Media Separation** (“DMS”) to treat the +1mm size material (Sepro Systems Condor) and **Jigs** (Gekko IPJ) for the -1mm size fraction could potentially beneficiate the ore by recovering denser sulphides, gravity concentrates and rejecting the lighter waste rock material. The gravity concentrates could be further processed using a high-centrifugal force concentrator (Falcon or Knelson) to recover gravity silver.



In the case of a satellite mining operation, the Drill Cuttings could be processed by Modular Mobile Plant, or de-watered, stockpiled and then loaded and carted to a Mill by 25t truck.

In all cases, the lighter waste rock is returned as backfill down the Pile Top RCD Hole and the process water is recovered and recycled for re-use in the drilling process.

### Geochemical Analysis of Pile Top ECD Cuttings in “Real Time”

Real-time XRF analysers can be fitted to the Drill Cuttings stream from the Pile Top RCDs to determine ROM grade of Au, Cu, Pb, Zn and Ag.

This on-line analysis can assist with grade control, by potentially identifying streams of high-grade, low-grade or waste Drill Cuttings as they are lifted and collected on the surface.



### Conceptual Milling Process – Continuous Vat Leach

*Innovat Mineral Process Solutions Limited* is the owner of the Continuous Vat Leaching (CVL) process (invented by Dan Mackie), also referred to as an “*Ecovat*”. The Innovat CVL is a “Turn Key” plant that consists of ROM feed hoppers and belt conveyors, two large rectangular tank/vats, freshwater tank, reagent tank, head tank, bucket wheel excavator, discharge hopper, a series of wash-filter screens, and a discharge conveyor, as depicted in the oblique schematic diagrams below.

Ore is crushed to an optimum size of -6mm (1/4”) and continuously fed to the large rectangular vats as a piped “Slurry Stream” or as “Dry Ore” fed by belt conveyor (fitted with a weightometer). If dry ore is fed, it is slurried by solution injected into the bottom of the vat. This solution fluidizes and mixes the slurry by means of periodic pulses of liquid from the bottom of the vat. A result of the fluidization process is liquifaction and results in rapid leaching of the ore. The fluidization process may occur up to 20 times per hour, with flows peaking at 30,000 litres/hour/m<sup>2</sup>, considerably greater than conventional vats or heap leach pads. These sharp injections of fluid accelerate dissolution of the gold and copper due to the dynamic contact between the leach solution and solid ore particles.

In the bottom of the tank is a French drain for solution removal for processing. The **Wash Solution** and part of the French drain liquid are pumped to a **Head Tank** set at a height approximately double the depth of the ore bed. Hydrostatic pressure generated is used to inject solution into the ore bed. The Ecovat is typically pre-set to “dump” solution for 10 seconds every four minutes.

At the end of the Vat opposite the feed is a slowly revolving **Bucket Wheel Excavator** (fitted with inlet ports and compartments), which continuously removes material from the vat. The bucket wheel creates a void in the ore bed and by constantly adding and removing ore, creates a tendency to re-establish a level surface which gradually moves towards the discharge wheel.

The slow rotation speed of the Bucket Wheel Excavator (0.2 rev/min), allows the slurry to drain back into the vat during removal. The liquid drains back into the treatment section, while the solids are discharged, via a hopper, onto a belt conveyor (at 5-15% moisture content, depending upon ore characteristics). The solids are moved through a series of wash and detoxification filter screen sections to systematically and selectively remove toxic materials (depending upon ore characteristics) and decant and recover glycine by solid-liquid separation.

Process water is removed, reclaimed and recycled for re-use by *Innovats* novel **Paste Thickener**. The *Innovat* Paste Thickener utilizes a peripheral feed arrangement, which distributes the solids laden in solution to the outer edges of the thickener. Clear solution is allowed to rise and is either drawn back into the feed pipes as a diluting agent, or overflowed into a launder where it can be distributed further. The thickeners rake-less design has no moving parts, resulting in low power consumption and maintenance.

The paste eliminates the need for a tailings dam. The detoxified paste is environmentally safe and can be disposed of as a “dry stack”, or mixed with cement and pumped directly as paste backfill into the Pile Top RCD void, open pit or underground workings.

The advantages of the CVL plant include:

- Commercially viable treatment of low-grade Cu-Au ores.
- Easy to operate. Monitoring of a CVL plant is estimated at 4 workers, with minimal training required.
- Low capital and operating costs. Plant simplicity with low-cost materials for construction.
- Recovery of metals speed is rapid, about 24 hours.
- Fully detoxified, neutralized dry tailings are available for immediate disposal as backfill. Tailings dams are not required.
- Leach solutions are contained. Minimal environmental risk of leakage or accidental discharge.
- Recovery and recycling of glycine lixiviant (estimated at <5% losses).
- Recovery and recycling of process water (85-90% recovery of water).
- Can be used in dry, wet, cold or environmentally sensitive locations.
- Low environmental footprint of the CVL plant.

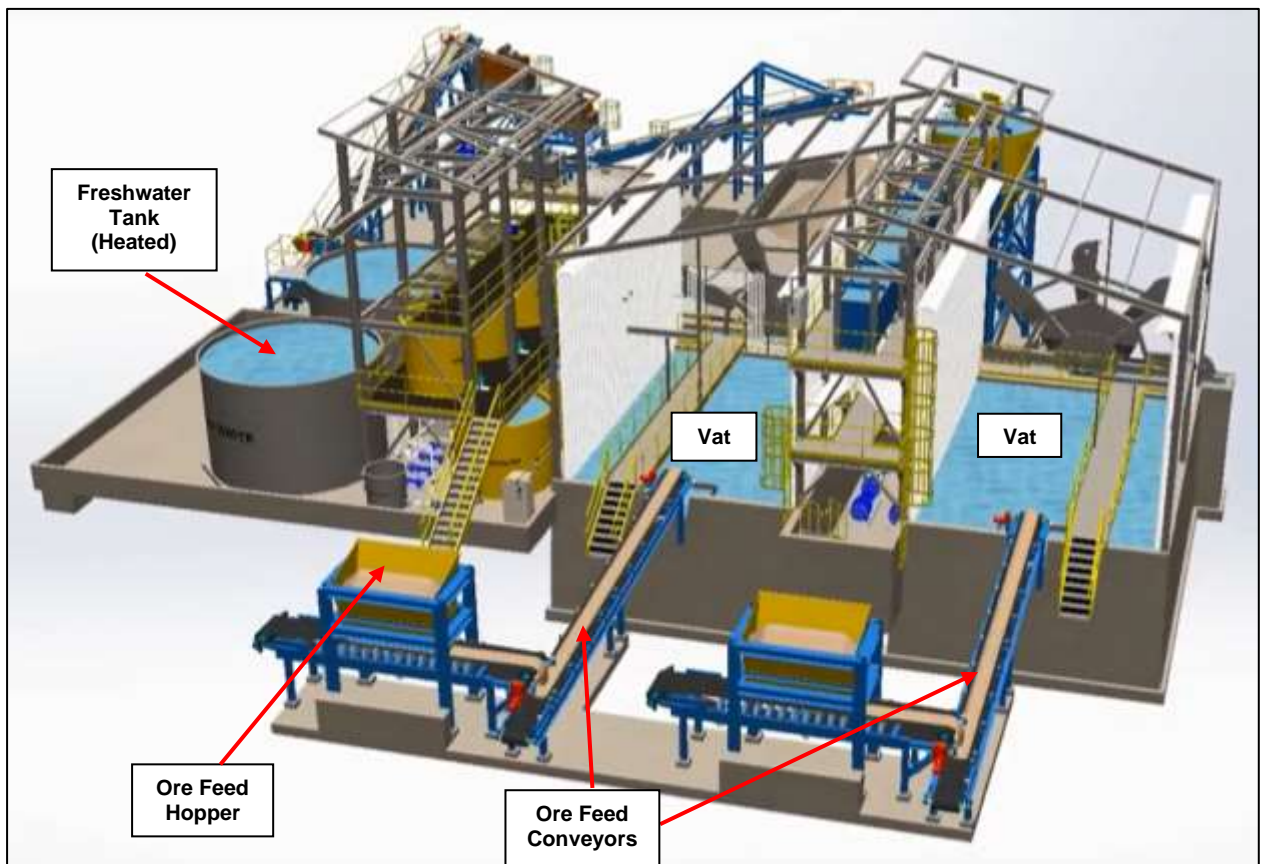
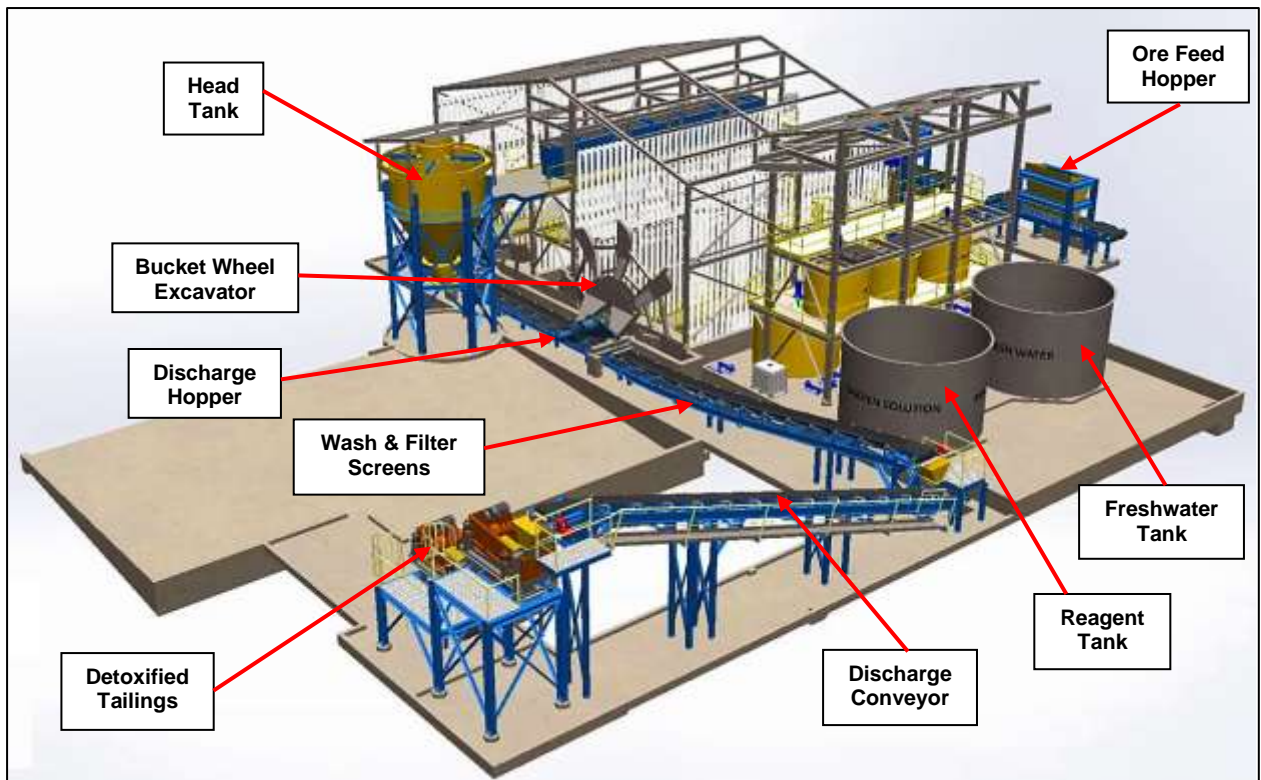


Figure 36. Oblique front and rear views of the schematic layout of a Continuous Vat Leach “Turn-Key Plant” (Innovat Ltd).

### Glycine Lixiviant

Glycine ( $\text{NH}_2\text{CH}_2\text{COOH}$ ) is a low-cost, non-toxic, stable, environmentally benign amino acid/reagent that can be recovered and reused. Sodium Glycinate ( $\text{C}_2\text{H}_4\text{NNaO}_2$ ) is readily available commercially in bulk industrial quantities and at low cost (about US\$1.75/kg). It is commonly used as a food additive, is biodegradeable and non-toxic to most living organisms.

### The GlyLeach™ Process

*Mining & Process Solutions Pty Ltd* (“MPS”) holds the global licence to the **GlyLeach™**, a glycine leaching process developed by *Curtin University’s Western Australian School of Mines*. GlyLeach™ is an environmentally benign hydrometallurgical process that is capable of leaching base and precious metal oxide, mixed oxide and sulphide ores.

Glycine is selective on which metals it leaches, as shown in the periodic table excerpt below.

25 <b>Mn</b> Manganese 54.9	26 <b>Fe</b> Iron 55.9	27 <b>Co</b> Cobalt 58.9	28 <b>Ni</b> Nickel 58.7	29 <b>Cu</b> Copper 63.5	30 <b>Zn</b> Zinc 65.4	31 <b>Ga</b> Gallium 69.7	32 <b>Ge</b> Germanium 72.6	33 <b>As</b> Arsenic 74.9	34 <b>Se</b> Selenium 79.0
	44 <b>Ru</b> Ruthenium 101.0	45 <b>Rh</b> Rhodium 102.9	46 <b>Pd</b> Palladium 106.4	47 <b>Ag</b> Silver 107.9	48 <b>Cd</b> Cadmium 112.4	49 <b>In</b> Indium 114.8	50 <b>Sn</b> Tin 118.7	51 <b>Sb</b> Antimony 121.8	52 <b>Te</b> Tellurium 127.6
	76 <b>Os</b> Osmium 190.2	77 <b>Ir</b> Iridium 192.2	78 <b>Pt</b> Platinum 195.1	79 <b>Au</b> Gold 197.0	80 <b>Hg</b> Mercury 200.6	81 <b>Tl</b> Thallium 204.4	82 <b>Pb</b> Lead 207.2	83 <b>Bi</b> Bismuth 209.0	

● Glycine Solubility Unknown   
 ● Known Glycine Leachable   
 ● Unknown Subject to Experiment  
● Known Glycine Insoluble   
 ● Known Glycine Leachable Limited Test work   
● Known Amphoteric Anions

### Leaching characteristics of various metals at pH values between 9-12 using Sodium Glycinate as a solvent.

Alkaline glycine can be used as the predominant lixiviant/solvent under alkaline conditions of pH 9-12 to leach and dissolve most copper oxide and copper sulphide ore minerals, concentrates, tailings, slags and mattes (Oraby & Eksteen, 2014).

Glycine leaching of chalcopyrite concentrates is enhanced using a combination of mildly-elevated temperature (50-60°C), ultrafine grinding and alkaline pre-oxidation. Solar cells can be mounted on the Mill Plant roof and a solar-heating system installed to heat the water and glycine, backed up by gas-powered heating system during winter. Using lagged tanks to retain heat, vat leaching offers the ability to control the leach temperature and minimize heat loss. A side benefit is the heated water will not freeze in pipes during winter. Glycine leaching of gold-copper ores is strongly catalyzed by the addition of small amounts of cyanide (used as rate accelerant), resulting in higher leach rates, significantly reduced cyanide consumption and eliminating detoxification requirements (Eksteen et al, 2017).

Glycine is retained in the aqueous solution and can be easily recovered after the metals recovery stage using solid-liquid separation and can be recycled for reuse again. Flow sheet test work and modelling to date has shown that <5% Glycine loss can be expected, indicating low reagent consumption costs.

Sulphides are converted to sulfates and can be removed as jarosite and gypsum for disposal or sale as fertilizer.

After removal of glycine, the process water is recovered for recycling using a hydrocyclone, producing a relatively dry tailings (5-10 wt% moisture content) suitable for “dry stack” storage/stockpiling.

The use of glycine under mildly alkaline conditions enables simple, standard, readily-available, low-cost equipment with low-cost standard construction materials.

**Metal Recovery**

Gold and silver can be recovered directly from the Pregnant Leach Solution (“PLS”) by adsorption onto activated carbon (Oraby & Eksteen, 2015).

Copper can be easily recovered by adding sulphur dioxide or sodium hydrosulphide (NaSH) to produce a pure, coarse-grained covellite precipitate (high-grade Cu concentrate). Copper metal can be recovered using the SX-EW method if project economics permit.

Lead and zinc can potentially be recovered from the PLS. After leaching, arsenic is collected from a bleed stream during the recycle stage and can be treated by As-fixing methods.

**Metallurgical Testing of Ores**

*Innovat MPS Limited* has a clearly defined series of metallurgical tests designed to test the efficacy of the Innovat CVL leaching technology to a mineral deposit. Independent metallurgical test facilities are available at Lakefield, Ontario, Reno, Nevada and Perth, Western Australia. Treatment of ore is site-specific and is determined by a series of metallurgical tests. The bench-scale metallurgical testing of ores for their amenability to vat leaching is similar to that for heap leaching and includes:

1. Sighter Tests to determine if the chemistry and mineralogy of the ore is amenable to leaching.
2. Bottle-roll tests of finely-ground material to determine:
  - a. Ultimate recovery of gold.
  - b. Any preg-robbing characteristics of the ore.
3. Pulsed Column Leaching tests to determine:
  - a. Gold recovery.
  - b. Preg-robbing characteristics of ore.
  - c. Size of feed material.
  - d. Solution strength.
  - e. Agglomeration requirements.
  - f. Time duration of leach.
4. Flow rates, applicability of soaking cycles, and direction of flow to determine the optimum set of conditions.

**Pre-Feasibility Study/Structured Cost Analysis of Project**

A pre-feasibility study and structured cost analysis of the project can be undertaken by *Innovat MPS Limited* is *RMD Stem*. The results from this study can be used to move to the next stage of bankable feasibility study.

**Engineering, Procurement, Construction Management**

Working in co-ordination with *Innovat MPS Limited* is *Dan Mackie & Associates* (“DMA”), a full-service Engineering, Procurement, Construction Management (“EPCM”) company. DMA focusses on CVL plant and process design covering metallurgical, economic and technical feasibility studies, detailed engineering, plant construction, commissioning and operations.

DMA expertise covers the total process cycle, including crushing, grinding, leaching, concentration, pressure, extraction and tailings management to maximize economic return to each project. DMA also has expertise relating to regulatory and financial requirements relating to development of mineral projects.

Design of peripheral plant works around the CVL plant would be undertaken by an engineering group (Korean companies such as *POSCO Engineering* can undertake this role).

*Innovat MPS* can finance the CVL plant (terms and conditions apply) with repayment from production.

## 14.0 REFERENCES

- Anderson, E.D., Atkinson, W.W., Marsh, T. & Iriondo, A., 2009. Geology and geochemistry of the Mammoth breccia pipe, Copper Creek mining district, southeastern Arizona: evidence for a magmatic-hydrothermal origin, *Miner Deposita*, 44, 151-170.
- Baker, E.M., Kirwin, D.J. & Taylor, R.G., 1986. Hydrothermal Breccia Pipes, *Economic Geology Research Unit Contribution 12*, James Cook Uni. North Qld., 45pp.
- Blenkensop, T. & Duckworth, R., 2007. Breccias, *Abstracts Volume Breccia Symposium June 2007*, EGRU, James Cook Uni. North Qld., 29pp.
- Cha, M.S. & Yun, S.H., 1988. Cretaceous volcanic cauldrons and ring complexes in Korea, *Jour. Geol. Soc. Korea*, 24, 67-86.
- Choi, S.G., Pak, S.J., Kim, S.W., Kim, C.S., & Oh, C.W., 2006. Mesozoic Gold-Silver Mineralization in South Korea: Metallogenic Provinces Re-estimated to the Geodynamic setting, *Econ. Environ. Geol.*, 39, 5, 567-581.
- Chough, S.K., Kwon, S.T., Ree, J.H., & Choi, D.K., 2000. Tectonic and sedimentary evolution of the Korean peninsula: a review and new view, *Earth Science Reviews*, 52, 175-235.
- Eksteen, J.J., Oraby, E.A., Tanda, B.C., Tauetsile, P.J., Bezuidenhout, G.A., Newton, T., Trask, F., & Bryan, I., 2017. Progress in the Process Development of the Alkaline Glycine Based Technologies for Gold-Copper Ores and Concentrates, Proc. ALTA 2017 Conference, Perth.
- ESCAP, 1987. *Atlas of Mineral Resources of the ESCAP Region, Volume 3, Republic of Korea*, Explanatory Brochure, United Nations Economic and Social Commission for Asia and the Pacific, 51pp.
- Fletcher, C.J.N., 1977. The geology, mineralization, and alteration of Ilkwang mine, Republic of Korea. A Cu-W-bearing tourmaline breccia pipe, *Econ. Geol.*, 72, 753-768.
- Halls, C., 1994. Energy and mechanism in the magmatic-hydrothermal evolution of the Cornubian batholith: a review, In: Seltmann, R., Kaempf, H., & Moeller, P. (eds), *Metallogeny of collisional orogens*, Czech Geol. Surv., Prague, 274-294.
- Heo, C.H., Yun, S.T., & So, C.S., 2002. Breccia pipe Cu-W mineralization of the Dalseong mine, Korea: Mineralogical and geochemical studies, *Jour. Inst. Korea Mining Geol.*, 39, 1-10.
- Hwang, D.H., Kim, M.S., Oh, M.S. & Park, N.Y., 1990. Study on geology and mineralization for metallic mineral deposits in Korea, *Korea Inst. Energy & Resources*, Rept. No. KR-90-2A.
- Hwang, S.K. & Yang, J.I., 1982. Feasibility study of oxidized lead-zinc-copper ore by heating flotation from Jun Hung mine, in Annual Report on Geoscience and Mineral resources 1977, *Korea Institute of Geoscience and Mineral Resources*, 2, 275-282.
- Innovat, 2013. Continuous Vat Leaching, Innovat Mineral Process Solutions Limited.
- KIER, 1982. Geochemical and geophysical exploration of Pb-Zn breccia pipe deposits conducted in the Jangheung area, *Korea Institute of Energy & Resources*, Bulletin 29.
- KIGAM, 2001. Geochemical Atlas of Korea (1:700,000), Series 1-7, *Korea Institute of Geoscience and Mineral Resources*.
- KIGAM, 2008. Magnetic Anomaly Maps of Korea, (*Korean Institute of Geoscience and Mineral Resources*).
- Kim, J.D., 1987. Geology and Ore Deposits of the Donghae Mine, Goseong Area, *Jour. Korean Inst. Mining Geol.*, 20, 4, 213-221.
- Kim, J.M., Cheong, C.K., Lee, S.R., Cho, M.S., & Yi, K.W., 2008. In-situ U-Pb titanite age of the Chuncheon Amphibolite: Evidence for Triassic regional metamorphism in central Gyeonggi massif, South Korea, and its tectonic implication, *Geosciences Jour.*, 12, 4, 309-316.
- Kim, S.E. & Hwang, D.H., 1983. *Metallogenesis in Korea – Explanatory Text for the Metallogenic Map of Korea*, Kor. Inst. Energy Resources, 16-23.

- Kirwin, D.J., Kelley, D., Azevedo, F. & Wolfe, R., 2018. Characteristics of intrusion-related copper-bearing tourmaline breccia pipes, *Conference Abstract, Metals, Minerals and Society, Econ.Geol.*, Keystone, Colorado, USA.
- \_\_\_\_\_, Tourmaline breccia pipes associated with intrusion-related copper deposits, examples from Latin America, *AIG Brisbane Technical Talk* (10 August 2021).
- Lee, D.S., 1987. *Geology of Korea*, Geol. Soc. Korea, Kyohak-Sa, 514pp.
- MPS, 2016. CVL Economics, *Mining and Mineral Processing Solutions Pty Ltd.*
- Norton, D.L. & Cathles, L.M., 1973. Breccia Pipes – Products of Exsolved Vapor from Magmas, *Econ. Geol.*, 68, 540-546.
- Oraby, E.A. & Eksteen, J.J., 2014. The selective leaching of copper from a gold-copper concentrate in glycine solutions, *Hydrometallurgy*, 150, 14-19.
- \_\_\_\_\_, 2015. The leaching and carbon-based adsorption behaviour of gold and silver and their alloys in alkaline glycine-peroxide solutions, *Hydrometallurgy*, 152, 199-203.
- Park, Y.S., & Kim, J.K., 2011. Geochemical characteristics on geological groups of stream sediment in the Boseong-Hwasun area, Korea, *Jour. Korean Earth Science Soc.*, 32, 7, 707-718.
- Perry, V.D., 1961. The significance of mineralized breccia pipes, *Min. Eng.*, 113, 4, 367-376.
- Reedman, A J & Um, S H, 1975. The Geology of Korea, *Korea Inst Energy & Res*, Seoul, 139 pp.
- Sennitt, C.M., 2010. Tourmaline Breccia Pipe-Hosted Tungsten-Copper Mineralization, Gyeongsang Basin, South Korea, *Unpubl. Co Rept. (Senlac Geological Services Pty Ltd)*.
- Sillitoe, R.H. & Sawkins, F.J., 1971. Geologic, mineralogic and fluid inclusion studies relating to the origin of copper-bearing tourmaline pipes, Chile, *Econ. Geol.*, 66, 1028-1041.
- Sillitoe, R.H., 2010. Porphyry Copper Systems, *Econ. Geol.*, 105, 3-41.
- Skewes, M.A., Holmgren, C. & Stern, C.R., 2003. The Donoso copper-rich, tourmaline-bearing breccia pipe in central Chile: petrologic, fluid inclusion and stable isotope evidence for an origin from magmatic fluids, *Mineralium Deposita*, 38, 2-21.
- Song, Y.S., Lee, H.S., Park, K.H., Fitzsimons, I.C.W., & Cawood, P.A., 2015. Recognition of the Phanerozoic “Young granite gneiss” in the central Yeongnam massif, *Geosciences Journal*, 19, 1, 1-16.
- Soo, M.W., Park, S.M., Choi, S.G., & Ryu, I.C., 2005. Geochemical Study of the Cretaceous Granitic Rock in Southwestern Part of the Korean Peninsula, *Econ. Environ. Geol.*, 38, 2, 113-127.
- Spadafora, M.J., & Kirwin, D.J., 1988. Report on a visit to assess the potential for precious metal exploration and mining business opportunities in the Republic of Korea, *Consultants Rept. (Paragon Resources NL)*.
- \_\_\_\_\_, 1994. A report on a visit to assess the exploration potential and opportunities for precious metal and porphyry copper mineralization, *Internal Co Rept., Indochina Goldfields Ltd.*
- Tamas, C.B & Milesi, J.P, 2003. Hydrothermal breccia pipe structures – General Features and Genetic Criteria, *Studia Universitatis Babeş-Bolyai, Geologia*, XLVIII, 1, 55-66.
- Taylor, R.G., 2000. Ore Textures: Recognition and Interpretation, Broken Rocks Breccia 1, *EGRU, James Cook Uni. North Qld.*, 52pp.
- Taylor, R.G., 2003. Ore Textures: Recognition and Interpretation, Broken Rocks Breccia 2, *EGRU, James Cook Uni. North Qld.*, 52pp.